Metal-Mediated and Metal-Catalyzed Reactions Under Mechanochemical Conditions

Andrea Porcheddu, Evelina Colacino, Lidia de Luca, Francesco Delogu

ACS Catalysis

ACS AUTHORCHOICE

pubs.acs.org/acscatalysis Review

Metal-Mediated and Metal-Catalyzed Reactions Under Mechanochemical Conditions

Andrea Porcheddu,* Evelina Colacino, Lidia De Luca, and Francesco Delogu

Cite This: *ACS Catal.* 2020, 10, 8344–8394 Read Online

ABSTRACT: The extraordinary impact of metal-based complexes on synthetic methods is still recognized nowadays, and attempts are currently undertaken to further extend the use of metal-assisted chemistry to environmentally friendly processes within the strongly invoked green chemistry paradigm. In recent years, mechanochemistry seems to provide attractive responses with processing methods having origins lost in the mists of time. Focusing on the panorama of organic synthesis, this Review highlights some recently developed metal-assisted mechanochemical reactions to introduce the reader into the fascinating, quite unexplored world of mechanochemistry.

KEYWORDS: *mechanochemistry, green chemistry, no-solvent reactions, ball-mill, C−H bond activation, C−C bond formation, TEMPO-assisted oxidations, transition-metal catalysis*

1. INTRODUCTION

Since time immemorial, man has pondered the nature, the origins, and the properties of matter, spontaneously compelled to understand its secrets and manipulate it at will. Starting from knowledge inherited from the early, obscure days lost in the mists of time, the slow, albeit inexorable, succession of discoveries and findings gradually formed a single thread unfolding across ages. Eventually materializing into a unique combination of spiritual elevation and skilled craftsmanship, shards of erudition were wisely handed down from masters to pupils. Not surprisingly, metals and their *spirits* lay at the heart of the arcane.

There are straightforward reasons behind the relevance of metals for ancient scholars and philosophers. Metals have had the terrible and majestic power of overthrowing fortunes, literally determining the rise, decline, and fall of ancient peoples and empires. Initially, it was the consequence of achievements in physical metallurgy, which resulted in improved mechanical properties of metal artifacts. The brute force of more efficient weapons has decided the destinies of ancient civilizations, and the resistance of engineering constructions has made their grandness. Then, something else was added: something related to a more elevated need for human beings, something on soul and matter. Basic tenets belonged to separated levels of knowledge that were combined into complex, elusive disciplines for initiates. Alchemy is, probably, the most popular example.

The dream of transmutation thrust alchemists into their Icarian flight overages. Closer to high spirituality, wrongly accused of heresy, doomed to face Inquisition, alchemists have left an invaluable legacy.[1] Undeniably, their aspiration to obtain the *philosopher's stone* to control chemical transformations and transmute metals has changed the life of humankind. Chemical sciences are deeply indebted to the first, scattered studies carried out by the most brilliant minds of antiquity and the Middle Ages and to the yet unexplored *corpus* of knowledge that has been accumulated. Metals were a primary subject, and metals catalyzed the development of scientific thought.

The extraordinary influence of metals on chemistry can be even better appreciated today because their revolutionary potential in activating and driving otherwise unfeasible reactions has been consistently explored.[2] Emphasis has gradually shifted from elemental metals and metal alloys to be used in heterogeneous catalytic processes to more complicated chemical species with metal cations at the center of a mostly distorted geometric arrangement of ligands. These

Received: January 9, 2020
Revised: May 24, 2020
Published: May 27, 2020

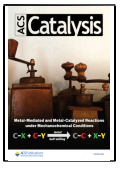

https://dx.doi.org/10.1021/acscatal.0c00142
ACS Catal. 2020, 10, 8344–8394

metal complexes share with metal solids one of the most remarkable and useful chemical properties, namely the capability of facilitating alternative reaction pathways with lower activation energies, thus enabling the reduction of reaction temperatures.[3] Study in the field has been ceaseless, and many organic reactions initially catalyzed by expensive metal complexes containing Rh, Ir, and similar noble and rare metals can be currently carried out using abundant and cheaper elements such as Fe, Cu, Mn, and Ni.[4]

The 12 principles of green chemistry have given further thrust to the fundamental and applied research on the subject. Indeed, even chemical processes catalyzed by metals extensively use organic solvents.[5] This is no longer compatible with the formidable challenges that chemistry is called upon to meet in the attempt of reversing climate changes and playing a pivotal role in the design, planning, and organization of sustainable development.[6] In this regard, the solvent conundrum is crucial.

In a typical chemical process, the solvent constitutes nearly 90% of the total reactive system, thus raising serious concerns about its impact on public health and the environment.[7] Moreover, solvent preparation requires cumbersome synthetic steps, with further negative effects on its sustainability due to energy consumption and waste generation.[8] Although green solvents prepared from biomasses are attracting significant interest from both academia and industry with their promise of reducing CO_2 gaseous emissions, high costs and technical issues still prevent their use on a large scale.

A possible way out of this problem is performing metal-catalyzed reactions under solvent-free conditions, according to the green chemistry motto that the best solvent is *no solvent*. Unfortunately, the thermal activation of highly concentrated reactive systems often leads to the formation of too many byproducts, which imposes solvent-based purification inconsistent with the target initially set.[9] Thus, alternative strategies likely to scale-up from laboratory to industrial production are, at present, actively sought.

In this respect, methodologies based on the mechanical activation of solids, possibly in the presence of catalytic amounts of liquid, are currently attracting considerable interest.[10]

2. MECHANOCHEMISTRY FOR SOLVENTLESS REACTIONS

Mechanochemistry is the branch of chemistry that investigates the chemical transformations activated by the application of anisotropic mechanical stresses to solids.[11] Its apparently simple practices are deeply rooted in the dark ages related to the origins of man. Our ancestors soon learned how to hammer, crush, rub, and grind metals, minerals, wood, herbs, and several other solid and granular substances to obtain shards and powders as well as blends and mixtures. Compressing, shearing, and folding operations underlying the undisputable success of mortars and pestles over the centuries still offer, with their simplicity, valuable processing solutions at the cutting edge of advanced research in materials science and inorganic and organic synthesis.

2.1. The Devices. Although the ancient device for milling continues to find use in chemical laboratories and pharmacy, scholars and scientists interested in mechanochemistry no longer pound the particulates in a mortar with the pestle. Starting from the beginning of the 19th century, more efficient grinding equipment became available to research in the field of mineral crushing and rubber processing. Today, chemical compounds are mostly processed in ball mills.[12]

The most widely used, commercially available ball mills fit into one of the three main classes that can be distinguished in terms of compressive and shear forces exerted by milling tools on the processed powder.[13]

Low compressive and high shear forces characterize planetary and attritor ball mills. In a planetary ball mill (Figure 1), the cylindrical jars spin around their main axis while

Figure 1. Fritsch-pulverisette 5, a planetary ball mill.

rotating eccentrically about the sun wheel axis. The device reproduces the motion of spinning earth moving along its orbit around the Sun. Accordingly, two centrifugal forces combine inside the vessels, allowing the milling balls to exhibit a disordered dynamic involving powders in frictional and impulsive processes.

Most popular planetary ball mills are released by Fritsch GmbH[14] and Retsch GmbH.[15] They offer several solutions in terms of processing conditions and materials utilized to fabricated jars and balls, allowing capacities roughly between 10 and 500 mL and rotational speeds up to 1100 rpm. Attritor ball mills with vertical geometry consist of a rotating shaft equipped with impellers placed inside a cylindrical container filled with small balls and powder. The shaft rotation induces the vigorous stirring of balls and powders. Szegvari attritors such as those released by Union Process and the Simoloyer released by Zoz GmbH can allow very intensive mechanical processing of large powder charges.[16]

In contrast with the planetary and attritor ball mills, shaker ball mills are characterized by high compressive and low shear forces. Jars undergo a simple back-and-forth oscillation combined with some lateral swing (Figure 2). Impact modes prevail on attrition ones, and the balls are subject to a relatively ordered dynamics, particularly under processing conditions allowing quasi-one-dimensional confinement.

Typical examples of shaker ball mills are the devices introduced on the market by Retsch GmbH and, more recently, by InSolido[17] Technologies and Form-Tech Scientific.[18] These ball mills allow processing sample volumes between 1 and 50 mL, and the milling frequency can be between approximately between 3 and 36 Hz. Larger samples can be processed using the Super Misuni ball mill, fabricated by Nissin Giken Co. Ltd.[19]

The more complicated three-dimensional swing of its milling vial characterizes the SPEX Mixer/Mill 8000 (Figure 3).[20] The

https://dx.doi.org/10.1021/acscatal.0c00142
ACS Catal. 2020, 10, 8344−8394

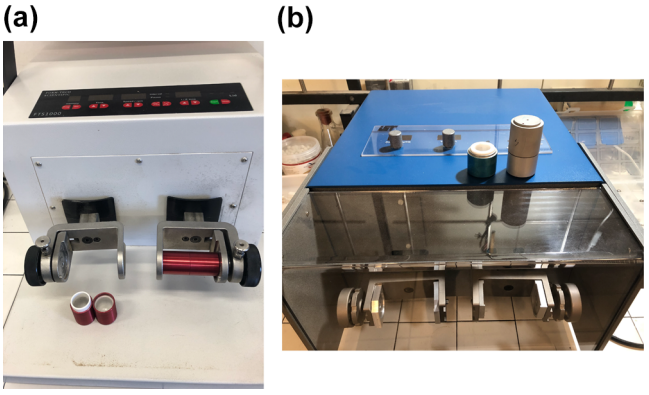

Figure 2. Form-Tech Scientific (left, panel a) and InSolido Technologies (right, panel b) ball mills.

Figure 3. SPEX Mixer/Mill 8000 ball mill.

vial is swung along a complex three-dimensional trajectory stemming from the combination of the partial reactor rotation with a synchronous back-and-forth oscillation on the vertical place.

In principle, the intensity and the efficiency of the mechanical treatment in impulsive and attrition modes can be suitably adjusted in every ball mill by varying the processing parameters. The most important ones include the materials composing jars and balls, the number and size of milling balls, the milling frequency, the ball impact energy, and the amount of powder charge.[21] Because of the complex ball and powder dynamics, these parameters are often intertwined, and detailed characterization of the milling dynamics is needed to untangle their effects.

This no longer holds for ball mills characterized by low compressive and low shear forces. Within this class fall, the classical rotary ball mills often referred to as pebble ball mills.[22] These devices have horizontal geometry. A horizontal drum partially filled with relatively small balls and powder rotates around its axis. As the drum rotates, the balls experience centrifugal forces that, initially, push them against the drum wall and, then, make them drop due to gravity.[23] Other ball mills provide alternative solutions to industrial needs.[24]

While the devices mentioned so far are utilized in common research practice, other possible solutions are used or have been developed for the mechanical activation in the absence of balls. Typical examples are rod and pan mills. The former consists of a cylindrical reactor containing vertical rods as milling tools. Powders undergo a frictional dynamic comparable with that of low-energy attritors. In pan mills, a moving pan rolls over a stationary pan allowing the processed material to experience shear stresses due to the weight of the moving pan.

Finally, it is worth mentioning the opportunities offered by screw extrusion. It is a mechanical process based on the forced flow of two or more substances through a die or an orifice to produce semifinished or finished composite materials. Typically used to produce thermoplastic products, it has been recently successfully used to scale-up mechanochemical transformations.[25]

2.2. Fundamentals. In a mechanically activated process, chemical reactions are initiated by the transfer of mechanical energy from the grinding media to solids.[26] Whenever an impact occurs between two balls or between a ball and the reactor wall, the impacting surfaces trap a fraction of the powder charge, and powder particles undergo dynamic compaction at relatively high rates. Initially, the increasing confinement reduces their movements until a disordered close packing is attained. Then, mechanical stresses arise at the points of contact between particles, eventually forming force chains characterized by geometries and intensities at different times.[27]

It is the nature of powders and the particle size to determine the mechanical response of the packed particles in connection with the intensity of local mechanical loading. For instance, a brittle fracture immediately occurs when local mechanical stresses overcome hardness in the case of brittle metals such as Mo and W.[11] In contrast, plastic deformation and related cold-welding processes predominate, initially, in the case of ductile metals such as Al and Cu.[11] Indeed, the continuous generation of lattice defects caused by plastic deformation induces the gradual hardening and stiffening of the metal, eventually favoring fracture.[11]

Quite different, at least on a quantitative basis, is the mechanical behavior of molecular crystals. Much softer than metals and minerals, they can easily undergo plastic deformation even at small mechanical loadings. Therefore, it is reasonable to expect extensive grinding and blending processes accompanied by considerable codeformation in the case of mixtures, eventually leading to the formation of extended interface areas and mixing on the molecular scale.

The complex interplay of factors characterizing the mechanical activation of solids is complicated further by the fact that mechanochemical transformations are not limited solely to solids but can also involve liquid reagents. These can be adsorbed onto inert materials such as NaCl, PEG, and silica gel and can act as process control agents or auxiliary phases.[28] It has been shown that the solvent can contribute significantly to enhance the reaction rate. It can be added to the solid mixture in micromolar quantities or, in any case, in amounts comparable with those of reagents, which allows performing liquid-assisted grinding (LAG).[29] This allows overcoming all the tedious issues related to the incomplete solubility and/or conversion observed in reactions that occur in a single liquid phase under homogeneous conditions.

The evidence that chemical transformations can be driven by mechanical work done on granular solids, or particulates wet with minimal amounts of liquids, challenge beliefs deeply rooted in culture. Aristotle's famous claim *no corpora nisi fluida* has lost, somehow, its strength. Similarly, empirical observations traditionally considered to be true have run into evident paradoxes, although they are still invoked.[30]

https://dx.doi.org/10.1021/acscatal.0c00142
ACS Catal. 2020, 10, 8344−8394

Admittedly, mechanochemistry exhibits unique features and can have a revolutionary impact on well-established practices related to the fabrication of novel materials and the production of fine chemicals. It has been already shown that the mechanical processing of powders has unprecedented ease to form nanostructured and amorphous metals that cannot be obtained by conventional metallurgical methods based on high-temperature treatments.[11] Along the same line, chemical processes triggered by mechanical activation can lead to a broad spectrum of molecules inaccessible by traditional solution routes.[31] Within this context, chemical knowledge accumulated in centuries of careful investigation is seemingly unable to provide a satisfactory explanation of experimental findings. While its validity is not questioned, a revisitation of its theoretical framework is needed to suit the incontrovertible evidence that mechanochemical processes require a new way of thinking chemistry.

2.3. Similarities and Differences between Thermochemistry and Mechanochemistry. Experience gained so far shows that, undeniably, mechanochemistry has a uniqueness profile.[32] There are so many differences in terms of kinetic and thermodynamic scenarios between the classical chemical reactivity in liquid solution and the chemical behavior in mechanically activated powders that the validity of even the most elementary common assumptions is questioned. It is precisely here that formidable challenges to the correct understanding of mechanochemical transformations originate.

To clear the field of ambiguous interpretations, it should be clarified first that there exist two broad classes of chemical transformations initiated by the application of mechanical forces. On the one hand, local mechanical stresses can directly involve chemical bonds. This is the case of mechanochemistry mediated by bond breakage and formation in single molecules[33] and polymers[34] as well as in ionic crystals[35] and metals.[11] On the other hand, mechanical activation can result in the intimate mixing of molecular species without the breakage of chemical bonds.[36] In this second case, molecular crystals are severely codeformed, and the individual molecules are displaced from their original position and exposed to different chemical surroundings. Chemical transformation can still occur because of the intimate contact between the different chemical species, but no direct activation of covalent systems can be ascribed to mechanical forces.

In this work, we restrict our analysis to this latter class of mechanochemical transformations. Although it may appear less general, it is, by far, the most relevant and influential case for the present burgeoning of the field. It is also best suited for pointing out similarities and differences between solution thermochemistry and mechanochemistry.

First and foremost, the mechanochemical transformations that fall into this class involve two distinct elementary processes, namely the intimate mixing of the chemical species in the solid-state and the chemical reaction between their functional groups. Concerning the chemical reactivity of functional groups in itself, there is, in principle, no difference with common reactions in a liquid solution. The functional groups have to be brought into contact, and we can expect that they exhibit their usual chemistry to a first approximation. Additional factors related to the effects of mechanical stresses on molecular configurations, and, thus, on functional groups, can be easily hypothesized. Nevertheless, in the absence of direct activation of covalent systems, they can also be expected to be less critical. Therefore, differences between thermochemical reactions in a liquid solution and mechanochemical processes in the solid-state can be primarily ascribed to the way the chemical species are brought into intimate contact.

In this respect, the contrast between thermochemical and mechanochemical scenarios emerges in all its strength. In liquid solution, reactants come into contact after several diffusive steps mediated by the solvent and governed by thermal motion.[37] Similarly, concentration in the liquid phase and persistence of solvent cages determine the frequency of reactive events together with the activation energy and the steric contributions of the molecules involved in the formation of the activated complex.[34] In the solid-state, particularly at low homologous temperatures, diffusion is remarkably slower, and it ceases to have the crucial role typically played in the liquid and gaseous phases. Chemical species belonging to different solid particles can come into contact only at the interfaces between the particles.[38] Thus, it is the codeformation of solid reactants that underlies mechanochemical transformations and controls their rates.[12]

The physics of codeformation marks the peculiarity of mechanically activated processes. Local mechanical stresses beyond the yield strength determine the plastic deformation of molecular crystals,[39] which results in the generation of interfaces that allow the molecules on the opposite sides of the interface to face each other. The more "*bulk modulus*" the solid phases, the larger the interface area that can be obtained by codeformation. Similarly, the smaller the particle size, the larger the interface area that can be generated during dynamic compaction events.

Codeformation is assisted by other processes. Any difference in density between the molecular crystals can give rise to so-called Kelvin−Helmholtz instabilities,[40] which determine the roughening of interfaces and a further increase of the contact area between the different chemical species. Finally, shearing effects at interfaces can induce the fine mixing of chemical species because of local vorticity related to turbulent plastic flows.[41]

The evidence mentioned above clearly indicates that the volume density of contacts between different chemical species at interfaces can be extremely high. Depending on the mechanical properties of the solid phases, the extension of interface area and the diffuse character of interfaces can result in a frequency of potentially reactive events unusually high compared with the one typical of liquid solution phases.

This is not all. The initial rearrangement of loose powders makes neighboring particles slide against each other. Irrespective of the particle size and shape, sliding gives rise to frictional processes involving the points of contact between the particles. Mechanical energy is dissipated by plastic deformation in the bulk solid closer to the real contact area and, especially, in a few atomic layers below the sliding surfaces.[42] The resulting frictional heating can cause a significant increase in temperature that, in turn, can affect the mechanical response of the solids.[43]

Deformation processes also involve dynamic energy storage in the deformed solids, which can lead to significant temperature changes upon energy dissipation.[44] For instance, adiabatic shear bands are associated with a dramatic increase of local temperature, and shear localization can take place because of dynamic recrystallization.[45]

The localized generation of heat, mostly concentrated in relatively small volumes that have been referred to as hot spots,[41] can be reasonably expected to give rise to transient

https://dx.doi.org/10.1021/acscatal.0c00142
ACS Catal. 2020, 10, 8344−8394

local softening and melting processes. Particularly in the case of molecular crystals, surface and subsurface regions can readily exhibit liquid-like behavior. Under mechanical loading conditions, softening facilitates the formation of roughened interfaces, and the rapid interface rearrangements can be equated to melting. The localized dissipation of mechanical energy can also result in true melting and, because of the mechanical stresses operating deformation, in the forced mixing of different chemical species in the liquid phase. In this latter case, codeformation no longer leads to a diffuse interface but rather to highly energetic regions, where reactants are mixed on the molecular scale. In principle, in these regions, reactive processes can be highly intensified compared with those taking place in a dilute liquid solution phase.

2.4. Challenges. On the basis of the general considerations reported above, it appears that chemical processes taking place under typical solution chemistry conditions and chemical transformations occurring under the effects of mechanical activation can hardly be compared. Conventional engineering approaches based on the rough comparison of reaction yields and conversion rates are neither satisfactory nor helpful. First, it is easy to make mistakes or to draw poorly meaningful conclusions in the absence of a detailed life-cycle analysis. Second, a rough comparison does not allow more-in-depth insight into the real mechanochemical conundrum.

For instance, let us focus on time. Time is a process variable to be carefully considered in the case of mechanically activated reactions, particularly when mechanical activation is carried out by ball milling. Balls spend most of their time traveling between different positions inside the vial, but it is only when impacts take place that mechanical activation occurs.[11] Also, it is only the material subjected to impacts that can undergo transformation.[11] However, impact duration is remarkably shorter compared with the time interval between consecutive impacts.[46] How can we really compare the results of mechanical activation with those obtained under thermal activation? The latter involves a homogeneous and uniform distribution of temperature over the reaction time.

Similar considerations can be made for temperature. While thermochemical reactions take place at a definite temperature, what is the real temperature at which mechanochemical transformations occur? What is the role of hot spots? What is their lifetime?

Along the same line, other questions arise in connection with the number of reactants involved in reaction during mechanical activation. While the whole volume of the liquid solution is involved in reactive events at any given time, only a small fraction of powders is engaged in the case of mechanical processing. What is such an amount?

The questions mentioned above and similar ones that can be effortlessly proposed here concerning the most diverse aspects of mechanical activation pose terrible challenges to current scientific understanding and analytical methods. Apart from a few theoretical studies and computational investigations, information regarding the microscopic processes underlying mechanochemical transformations is lacking. Much worse, it appears that the direct analysis and characterization of local processes are out of reach presently.

Under these circumstances, a systematic analysis of literature data and their critical discussion is probably the best option to gain insight into the chemical processes activated and driven by mechanical forces. Although such analysis can only result in indirect information, it can still be instrumental in addressing future research and stimulating the advancement of knowledge.

2.5. Mechanochemical Reactions Catalyzed by Metals. In this Review, we carry out a detailed analysis of the available literature on a particular class of mechanochemical transformations that, for long time, attracted little interest. This class includes the mechanochemical reactions catalyzed by metals, which are currently the subject of intense research activities.

Until a few years ago, it was believed that these reactions, with only a few exceptions, could not be replicated in a ball mill. The deleterious effects of moisture, sufficient to decompose metal complexes and any organometallic compound in general, were typically invoked to justify such expectation. However, recent literature has demonstrated that mechanochemical processes involving metal catalysts can be even more efficient than those carried out in the liquid phase both in terms of final yield and reaction duration.[47] Paradoxically, it has been suggested that the reason for the observed success is that the water content in solid organic reagents is much lower than the most anhydrous solvent commercially available.

In the following, we examine the most recent literature on metal-catalyzed mechanochemical reactions. We have selected the discussed cases among the most important in the panorama of organic synthesis with the aim of introducing the reader into this yet relatively unexplored area of investigation in mechanochemistry.

3. MECHANOCHEMISTRY FOR CLASSICAL C–C BOND-FORMING REACTIONS

3.1. Mechanochemical Assisted Suzuki–Miyaura Reaction. Suzuki–Miyaura reaction is a metal-catalyzed cross-coupling reaction, typically with palladium (0), between boronic acid derivatives and organohalides and is one of the most powerful tools for producing conjugated systems of alkenes, styrenes, or biaryl compounds (Scheme 1).[48] The reaction takes place in the presence of a base, which is crucial to promote the activation of the organoboron species and proceeds under very mild conditions.

Scheme 1. Classical Suzuki–Miyaura reaction

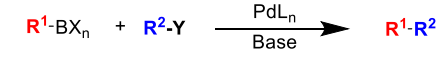

X_n = $(OH)_2$, $(OR)_2$, R_2, F_3K L_n = Ligand

Y = Cl, Br, I, OTf, *etc.*

Due to the significant simplicity, versatility, and wide availability of common boronic acids, Suzuki–Miyaura reactions have garnered substantial attention in recent years, particularly for the synthesis of intermediates for pharmaceuticals, fine chemicals, and complex natural products.[49] Nevertheless, Suzuki–Miyaura couplings are a highly topical field of study, which received, and are still undergoing, a huge amount of attention intending to develop new, more environmentally friendly reaction conditions. Working in this direction, some teams investigated the role played by solvents and investigated *solvent-free strategies* intended to maximize yields and simplify the experimental procedure.[50] Su et al. studied the effect of liquid-assisted grinding on reaction performance using mechanical Suzuki–Miyaura reaction of *p*-chloroacetophenone

https://dx.doi.org/10.1021/acscatal.0c00142
ACS Catal. 2020, 10, 8344–8394

$1a_1$ and phenylboronic acid $2b_1$ as the model reaction.[51] At first, the authors tested different kinds of ligands (dppf, dppe, dppp, dppb, PCy_3, and PPh_3), but considering the low reactivity of aryl chlorides, only bidentate ligand Davephos gave acceptable results (Scheme 2).

Scheme 2. Investigation of Ligands in the Mechanochemical Suzuki−Miyaura Reaction. Adapted with Permission from Ref 51. Copyright 2016 American Chemical Society

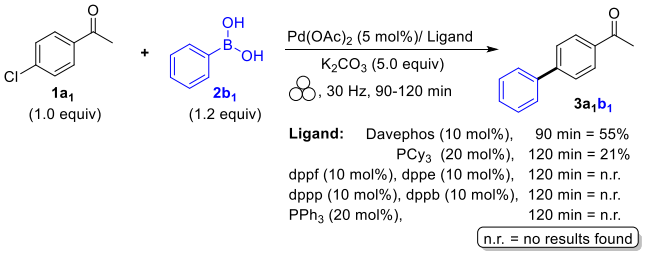

Su et al. hypothesized that the solvents commonly used in the coupling of Suzuki could play a significant role in determining the outcomes of these mechanochemical processes. Once again, the model reaction was evaluated using DMF, CH_3CN, dioxane, and THF as additives (η = 0.045 μL/mg) and DavePhos and PCy_3 as referral ligands under the previously optimized conditions (Table 1, entries 1−5). The sharp fluctuation of yields pointed out the strong dependence of the coupling reaction with solvents and phosphine ligands also in the solventless environment. Further examination of LAG additives highlighted that aprotic solvents (hexane, $CHCl_3$, CH_2Cl_2) had a moderate positive effect for both ligands, while ethyl ether gave positive result only in combination with PCy_3 (Table 1, entry 6). These fluctuating results radically changed for the better, switching to polar solvents such as protic solvents (methanol, ethanol, and H_2O), which gave the desired product in almost quantitative yields (Table 1, entries 7−9). Sterically hindered alcohols such as *i*-PrOH and *t*-BuOH turned out to be less efficient, suggesting

Table 1. Examination of LAG Additives[a]

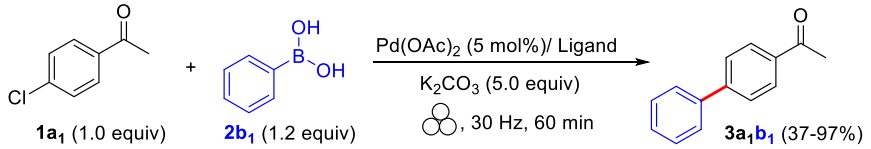

entry	solvent	Davephos (5 mol%) % yield ($3a_1b_1$)	%dev.	PCy_3·HBF_4 (10 mol%) %yield ($3a_1b_1$)	%dev.
1	neat	66	-	38	-
2	THF	87	+19	56	+18
3	dioxane	90	+23	47	+9
4	DMF	85	+18	37	-4
5	CH_3CN	60	-6	48	+10
6	Et_2O	60	-6	67	+29
7	MeOH	98	+32	97	+59
8	EtOH	99	+33	94	+56
9	H_2O	88	+21	87	+49
10	*i*-PrOH	68	+2	77	+39
11	*t*-BuOH	67	+1	42	+4

[a]Yield based on $1a_1$, average of three runs. [b]Deviation of yield from neat conditions. Adapted with permission from ref 51. Copyright 2016 American Chemical Society.

https://dx.doi.org/10.1021/acscatal.0c00142
ACS Catal. 2020, 10, 8344−8394

they take part in the catalytic cycle (Table1, entries 10−11). During the grinding process, the use of CsF and KF in place of carbonates drastically depressed the yields (71% and 70%, respectively), while alkoxides boosted the procedure instead (MeOK: 95%, MeONa: 88%). The activity of catalyst remained unchanged even after adjusting for the amount of catalyst loading of $Pd(OAc)_2/PCy_3$ from 5 to 2 mol % in the presence of methanol (η = 0.045 μL/mg).

The scope of the mechanical Suzuki−Miyaura reaction was successfully explored toward the synthesis of different 22 biaryls by coupling 13 aryl halides ($\mathbf{1a_1}$-$\mathbf{1a_{13}}$) with 9 boronic acids ($\mathbf{2b_1}$-$\mathbf{2b_9}$) in high yields, as depicted in Scheme 3. In all probability, cross-coupling reactions have been investigated in a screw-capped vessel under air, but the authors did not mention anything explicitly.

Scheme 3. Examination of Substrate Scope under High-Speed Ball-Milling Conditions. Adapted with Permission from Ref 51. Copyright 2016 American Chemical Society

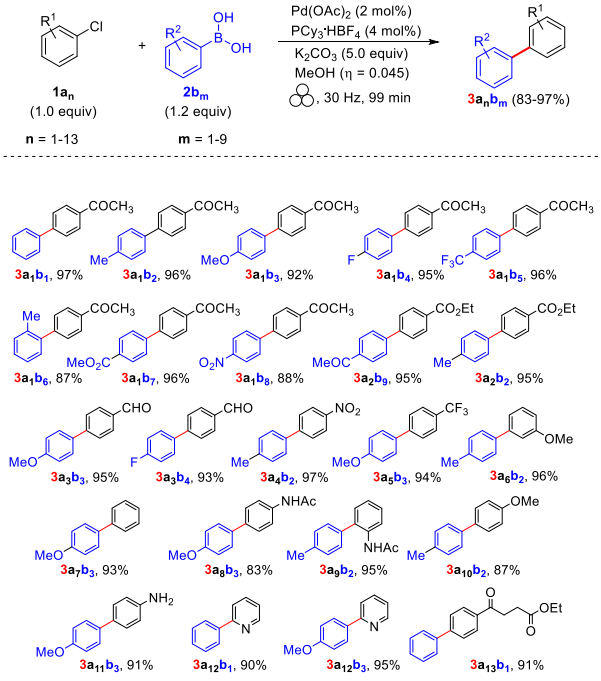

In 2017, Borchardt et al. developed a solvent-free Suzuki polycondensation procedure for the synthesis of linear and hyperbranched polyphenylenes under mechanochemical conditions (Scheme 4).[52] The reaction, which operates under an inert atmosphere (N_2 or Ar), does not require any additional ligand for the palladium catalyst. Once again, K_2CO_3 proved to be the best base to adopt for the mechanosynthesis of linear to hyperbranched polyphenylenes. Aryl bromides and iodides exhibited high reactivity in the coupling reactions leading to the formation of the titled polymers in as little as 30 min, compared with 12 to 24 h for similar results in a solution.

In 2019, Ito[53] and Ananikov,[54] starting from the considerations just discussed above, resume the study of the Suzuki reactions focusing their attention on the "*solid−solid coupling*" of aryl halides with organoboron reagents. These feature articles investigate one of the most noteworthy reactions in the panorama of organic synthesis so that they could be considered a masterpiece of scientific culture. As expected, Ito points out that the mechanochemical Suzuki−

Scheme 4. Suzuki Cross-Coupling Reaction of Different Systems Conducted in a Planetary Ball Mill. Adapted with Permission from Ref 52. Copyright 2017 The Royal Society of Chemistry

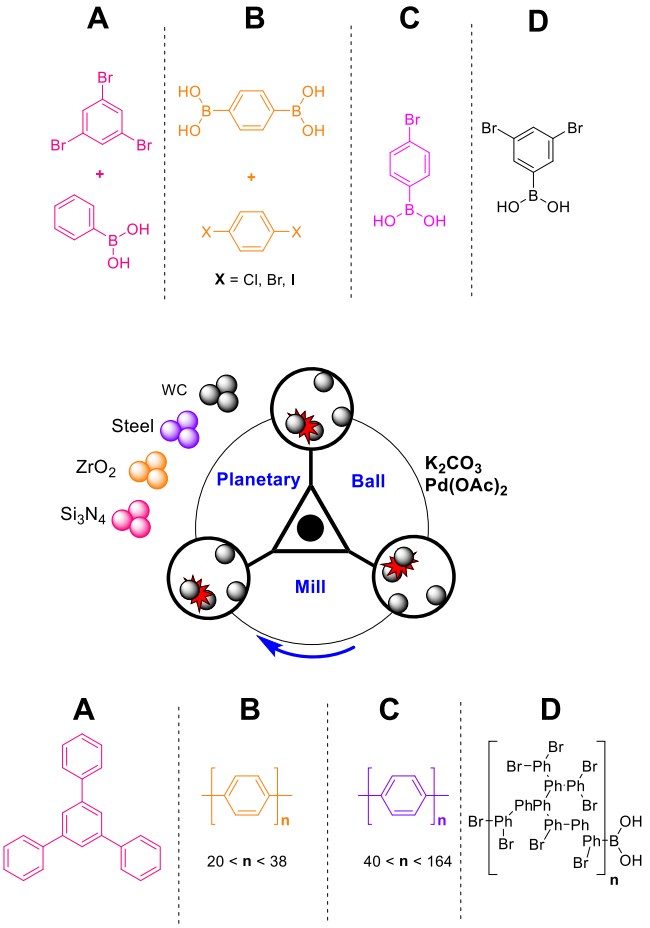

Miyaura cross-coupling reaction of liquid 1-bromobenzene ($\mathbf{1a_7}$) and solid 4-bromo-1,10-biphenyl ($\mathbf{1a_{14}}$) with 4-dimethylaminophenylboronic acid ($\mathbf{2b_{10}}$) in the presence of $Pd(OAc)_2$/DavePhos proceeded smoothly under mild conditions and gave the corresponding coupling product ($\mathbf{3a_7b_{10}}$) in excellent yield (92%; Scheme 5, pathway a). In contrast, the cross-coupling of solid 4-bromobiphenyl $\mathbf{1a_{14}}$ under the same reaction conditions resulted in only 26% of product $\mathbf{3a_{14}b_{10}}$ (Scheme 5, pathway b).

The results emphasized a very significant difference in terms of reactivity between liquids and solids substrates, probably because of the decreased mixing efficiency of solid reactants and catalyst, even under mechanochemical conditions. The performance of the mechanical Suzuki reaction improved significantly by adding a liquid additive (0.12 μL/mg of reactant). Liquid-assisted grinding (LAG) reactions dramatically accelerated in the presence of 1,5-cyclooctadiene (1,5-COD) affording the coupling product $\mathbf{3a_{14}b_{10}}$ in almost quantitative yield (97%; Table 2). Among all the ligands examined, DavePhos (4.5 mol %), in combination with $Pd(AcO)_2$ (3 mol %), led to the best results (97%), also suggesting that phosphine ligands are crucial for this solid-state cross-coupling reaction. To further explore the substrate scope of this reaction, the optimized conditions were successfully extended to a variety of structurally different solid aryl halides, including also unactivated aryl chlorides (Scheme 6). This

https://dx.doi.org/10.1021/acscatal.0c00142
ACS Catal. 2020, 10, 8344−8394

Scheme 5. Mechanochemical Suzuki–Miyaura Cross-Coupling Reactions: (a) under Neat Liquid Conditions and (b) in the Solid-State Conditions. Adapted with Permission from Ref 53. Copyright 2019 The Royal Society of Chemistry

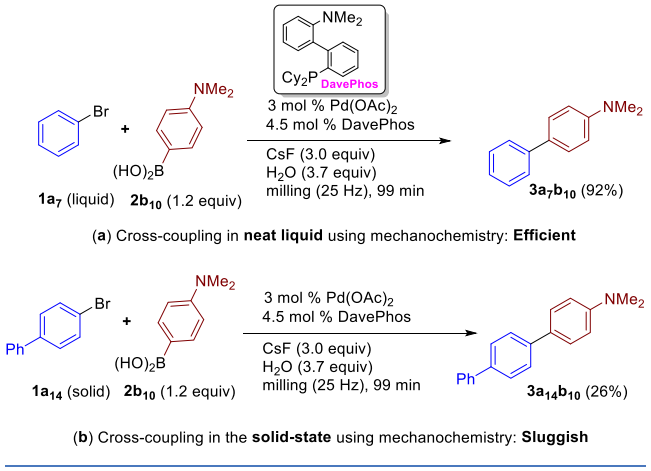

solid-state Suzuki cross-coupling reaction was particularly useful for the construction of complex molecular architectures, especially in the case of poorly soluble substrates such as large polyaromatic hydrocarbons. Unlike classical Suzuki cross-coupling in solution, the mechanochemical version of insoluble aromatic substrates did not require dry solvents, inert atmosphere, hugely expensive equipment, or special operational skills and could also be extended to large-scale. After the addition of olefin, TEM images of the crude reaction mixture clearly showed the presence of palladium nanoparticles (approximate size: 3–5 nm).

The absence of 1,5-cod led to the aggregation of palladium nanoparticles into dense particles, suggesting that olefin additives might act as dispersants. Solid-state (SS) ^{31}P NMR spectra of the crude reaction mixtures of 2-bromonaphthalene ($\mathbf{1a}_{16}$) and *p*-methoxyboronic acid ($\mathbf{2b}_{3}$) after grinding in the presence of 1,5-cod showed the absence of any known peaks corresponding to DavePhos and the formation of a new distinct signal attributable to the in situ generation of DavePhos-ligated monomeric palladium species. ESI mass spectrometry studies provided evidence of the presence of DavePhos-Pd(0)–(1,5-cod) in the crude reaction, confirming the SS ^{31}P NMR analysis. In contrast to solution-phase, where a Pd(0) complex is known to be unstable, in a Suzuki solid-state reaction mixture, the longevity of this Pd(0) specie is probably due to the low diffusion efficiency of gaseous oxygen. Another non-negligible aspect to be considered is the temperature inside the milling jar after grinding for 99 min at 25 Hz. The thermographic analysis showed that the surface had an average temperature of 35 °C, suggesting that the reaction temperature did not significantly increase under mechanochemical conditions.

According to the data collected so far, the reaction should only take place at points of impact (hotspots) where very high temperatures can be reached for a fraction of a second. How did the reagents behave during impacts? Did they melt, sublimate? Did the different phases spread over each other? Borrowing a crime term, the reaction works very well, but the investigation would not yet be finalized entirely. A recent and interesting paper by Ananikov[54] provides further valuable insights on solvent-free Suzuki–Miyaura reaction showing that solid arylboronic acids and aryl halides can also react in the absence of a solvent and any added liquids. From the literature, it is known that cost-effective metal cross-coupling reactions in solution promote leaching of the metal catalyst, which in turn contributes to the contamination of the final products, drastically reducing the catalyst turnover. Solid-state reactions could represent an innovative approach to these complex problems with both chemical and environmental implications. It is now well-established that in Suzuki protocols conducted in the presence of liquid reagents, the reaction takes place in a melt. In the literature, there are a very limited number of investigations regarding real solid-phase solvent-free Suzuki–Miyaura reactions and mechanistic understanding of these solid-state catalytic reactions are still today a challenge. In this regard, Ananikov et al. investigated a solid-phase Pd/C-catalyzed Suzuki–Miyaura reaction under conventional heating without using special equipment to identify the most critical and key parameters that influence the occurrence of these solvent-free processes.

Table 2. Mechanochemical Suzuki–Miyaura Cross-Coupling under Liquid-Assisted Grinding (LAG) Conditions. Adapted with Permission from Ref 53. Copyright 2019 The Royal Society of Chemistry

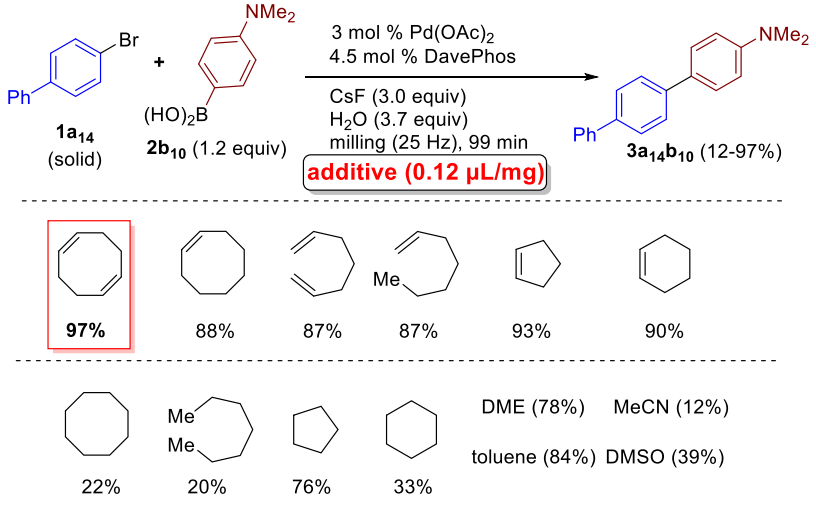

https://dx.doi.org/10.1021/acscatal.0c00142
ACS Catal. 2020, 10, 8344–8394

Scheme 6. Substrate Scope of the Olefin-Accelerated Solid-State Organoboron Cross-Coupling. Adapted with Permission from Ref 53. Copyright 2019 The Royal Society of Chemistry

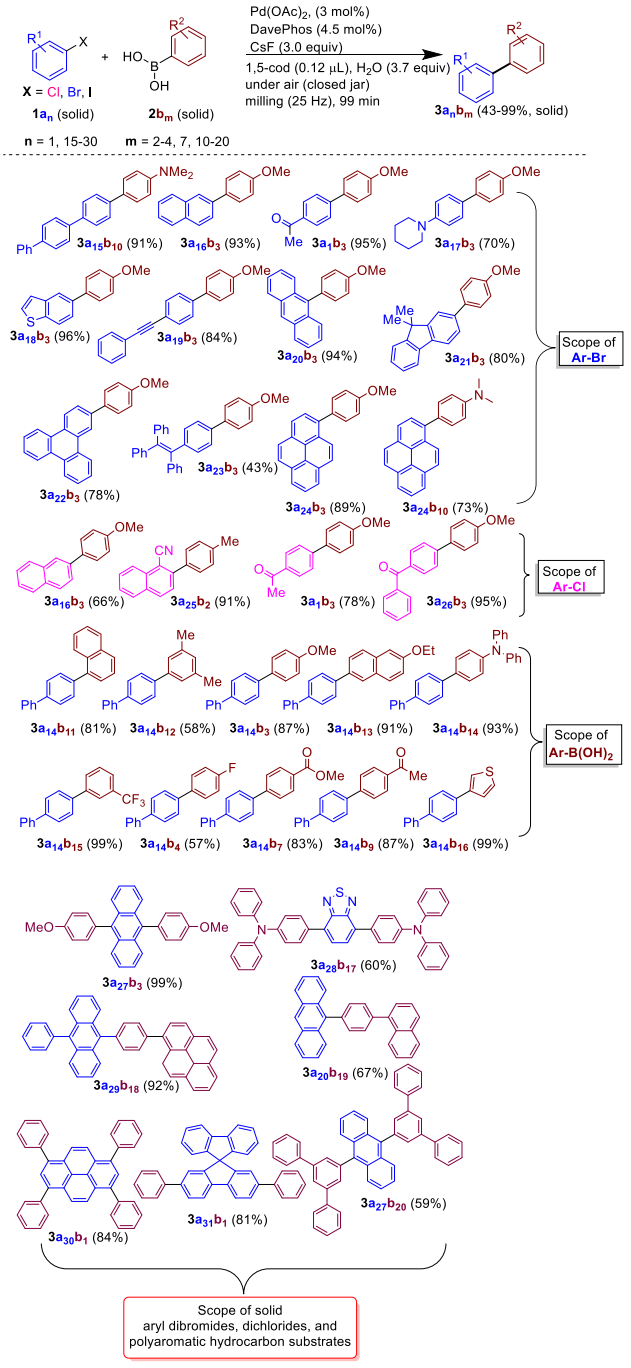

Scheme 7. Solid-Phase Suzuki−miyaura Reaction. Adapted with Permission from Ref 54. Copyright 2019 Wiley-VCH

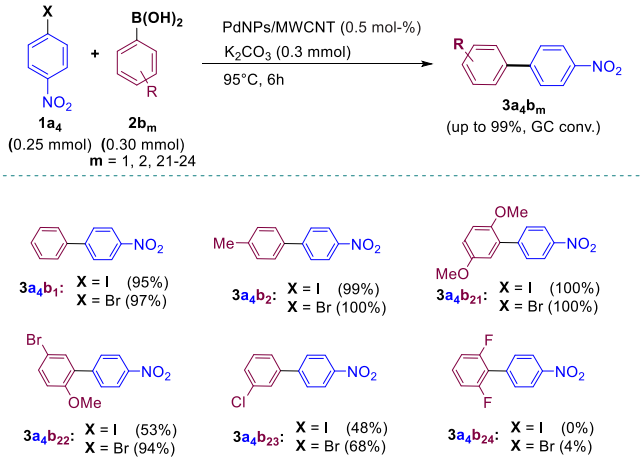

The model reaction has been fine-tuned by reacting solid 1-iodo-4-nitrobenzene (171−173 °C) and 1-bromo-4-nitrobenzene (124−126 °C), which can be heated to relatively high temperatures without melting (Scheme 7). Therefore, the reaction mixture was heated at 95 °C for 6 h, excluding the possibility of reaction in the molten crude. A composite of palladium nanoparticles supported on multiwalled carbon nanotubes (PdNPs/MWCNT, 0.5 mol %) in the presence of K_2CO_3 as a base was used to catalyze the model reaction with quantitative conversion (97% yield). In contrast to Ito's procedure, the conversions were almost quantitative in the presence of potassium (99%) and cesium (96%) carbonates or potassium hydroxide (97%). At the same time, the reaction nearly did not proceed with the addition of potassium fluoride and sodium acetate. The authors once again question whether the cross-coupling really proceeded solvent-free or other side reactions released "liquids" in the reaction medium. More in-depth investigation revealed that the formation of H_2O, as a byproduct of arylboronic acid trimerization, enhanced the mass transfer promoting the formation of the corresponding biphenyl product.

In fact, under the same experimental conditions, the usage of nontrimerizable borate salts (potassium phenyltrifluoroborate and tetraphenylborate) or phenylboronic and tolylboronic acids calcinated at 150 °C for the elimination of any trace of water completely suppressed the Suzuki−Miyaura process. Ananikov assumes that the water can play several critical roles in the route of the reaction mechanism providing as a medium, diffusion, mass transfer, and mobility of the interacting hydrophilic species. Moreover, hydroxide anions generated by the interaction of water with carbonate base could take part in many complex dynamic reaction pathways, especially in the transmetalation step leading to the formation of organo-palladium specie as depicted in Scheme 8.

Regardless of the path, the transmetalation stage generates the boric acid, which in turn converted to tetraborate and water in basic media (Scheme 8, green arrow), closing the catalytic cycle with no water consumption. This solid-phase Suzuki−Miyaura coupling protocol was successfully applied to a wide range of differently decorated arylboronic acids and aryl halides. Notably, the absence of a liquid phase avoids metal leaching during the solid-phase Suzuki−Miyaura reaction, and the PdNPs/MWCNT catalyst can be reused multiple times without loss of efficiency.

3.2. Mechanochemical-Assisted Negishi Reaction.

Browne and co-workers, in a relevant paper from both a scientific and educational point of view, has recently highlighted the advantages of Negishi reaction carried out under mechanochemistry conditions.[55] The Negishi coupling, first published in 1977, is a widely employed nickel- or palladium-catalyzed cross-coupling reaction (Scheme 9), which involves the addition of nucleophilic organozinc compounds to organohalides, forming new C−C bonds in good yields.[56] The reaction has a broad scope and is more versatile than Suzuki or Stille couplings because the organozinc represents a

https://dx.doi.org/10.1021/acscatal.0c00142
ACS Catal. 2020, 10, 8344−8394

Scheme 8. Schematic Representation of Water and Hydroxide Anion Transformations. Adapted with Permission from Ref 54. Copyright 2019 Wiley-VCH

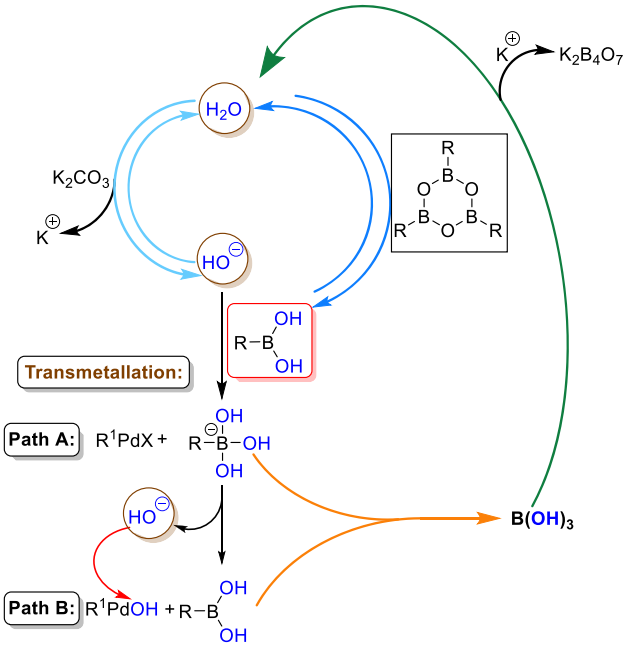

Scheme 9. Negishi Coupling Reaction

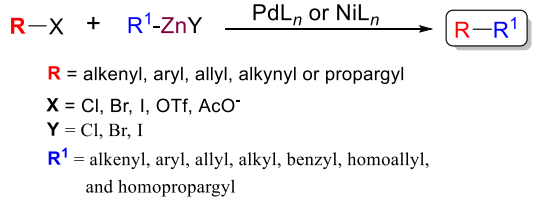

class of organometallic compounds with broad functional group tolerance and require milder reaction conditions.[57] Nevertheless, this procedure has a variety of shortcomings which have limited its widespread. Compared with boronic derivatives, organozinc species are not commercially available and must be in situ generated as necessary following tedious procedures.

Organozinc compounds can be prepared following well-established transmetalation procedures with organomagnesium or organolithium, which unfortunately limit the scope of the method. An alternative source of organozinc compounds for cross-coupling is the metalation of C−X bonds followed by a metal−halogen exchange, but again this approach leads to a substantial loss of the broad functional group tolerance caused by organozinc reagents. An alternative tactic involves the use of activated zinc metal generated by chemical treatments under an inert atmosphere for removing zinc oxide layers on the metal surface. Within this context, Browne group developed an interesting mechanochemical procedure to prepare and subsequently use organozinc reagents, avoiding the need for strictly dry solvents and specific physical metal forms. The model reaction was fine-tuned by grinding ethyl-4-bromobutanoate with dimethylacetamide (DMA, 1.5 equiv) in the presence of granular zinc (1.1 equiv, 20−30 mesh, Table 3, entry 1).

After 4 h, the acidic quench of the jar contents gave ethylbutanoate in 76% yield (**4a$_{32}$H**, scheme in Table 3). The optimized procedure was then extended to 11 commercially available zinc forms, which vary in their particle size and, consequently, also in zinc oxide to zinc metal ratio (Table 3, entries 2−12). As expected, zinc forms (puriss >99%, shot, mossy), with a lower surface-area-to-volume ratio performed better. Negishi reaction was next studied in a one-pot fashion using bromobenzene as the coupling partner in the presence of Pd-PEPPSI-*i*-Pent catalyst (1 mol %), which possess high air stabilities and exhibits good applicability for the Negishi coupling (Scheme 10). The addition of tetrabutylammonium bromide (TBAB, 1.5 equiv) as an additive improved the isolated yields slightly up to 74% (Scheme 10, compound **3a$_{32}$a$_7$**). The optimized mechanochemical Negishi procedure exhibited a broad substrate scope and widely tolerant to many important functional groups when applied for both C(sp^3)−C(sp^2) and C(sp^2)−C(sp^2) couplings.

3.3. Mechanochemical-Assisted Mizoroki−Heck Reactions. The palladium-catalyzed cross-coupling of an aryl or vinyl halide and an alkene in the presence of a base, known as the Mizoroki−Heck reaction, is one of the most useful and versatile strategies for the construction of a new carbon−carbon bond in a target molecule.[58] This procedure has been successfully applied in different academic and industrial applications for the manufacturing of fine chemicals and pharmaceuticals.[59] In 2006, Frejd reported for the first time, a modified Heck reaction under mechanochemical conditions.[60] These first synthetic protocols allowed the cross-coupling of electron-rich unsubstituted and monosubstituted aryl halides (**1a$_{53-61}$**) with protected amino acrylate (**5b$_1$**) in the presence of Pd(OAc)$_2$ (5 mol %) to give Z olefins (**6a$_{53-61}$b$_1$**) in 29−85% yields (Scheme 11). The addition of NaCl (5 mg/mg aryl halide) as grinding auxiliary was critical for having a good final conversion yield.

In general, this optimized mechanical Heck−Jeffery protocol performs considerably better in comparison to analogous procedures in solution affording unnatural amino acids (**6a$_n$b$_1$**) and indoles (**7a$_n$b$_1$**) in good yields (Scheme 11). Many of these procedures have been discussed and comprehensively summarized in several useful review articles and a recent chapter book by Davor Margetic and Vjekoslav Štrukil.[61] The synthetic procedures described in the literature in recent years have been developed, preferably using aryl iodides, which are both the most efficient but also the most expensive substrates. Therefore, the couplings of bromo and chlorine substrates with unactivated alkenes remain challenging today for many industrial applications. However, their utility is limited as they faced the problem of dehalogenations especially under metal-catalyzed reactions and in the presence of a base.[62] In 2018, Su et al. developed a solvent-free, chemoselective Heck cross-coupling protocol for the synthesis of 3-vinylindazoles by tuning of the chemical and mechanical parameters under ball-milling conditions.[63] A thorough study of the experimental parameters of the model reaction between 3-bromo-1-methyl-1*H*-indazole (**1a$_{62}$**) and *n*-butyl acrylate (**5b$_2$**) emphasized that the bromide salts not only suppressed the dehalogenation of 3-bromoindazoles but also assisted in grinding (Scheme 12). NaBr, as grinding auxiliary, exhibited the most efficiency, while other solid auxiliaries such as γ-Al_2O_3 and sand yielded poor results in terms of yield and selectivity of **6a$_{62}$b$_2$**. A catalytic amount of tetrabutylammonium bromide (TBAB), as dehalogenation restrained, was also sufficient to stabilize Pd(0) and to promote this mechanically activated chemoselective Heck protocol. The methodology has a broad scope

https://dx.doi.org/10.1021/acscatal.0c00142
ACS Catal. 2020, 10, 8344−8394

Table 3. Mechanochemical Preparation of Organozinc Reagents. Adapted with Permission from Ref 55. Copyright 2019 Wiley-VCH

entry	Zn (form)	hydrolysis yield (% $\mathbf{4a_{32}H}$)
1	Zinc granular 20-30 mesh	76
2	Zinc granular 20 mesh	73
3	Zinc foil, thickness 0.25 mm 99.9%	72
4	Zinc dust< 10 nm	65
5	Zinc puriss. ACS reagent >99.9%	82
6	Zinc shot, 10 mm (dia), 2 mm (thick), 99.99%	82
7	Zinc flake 325 mesh, 99.9%	63
8	Zinc wire (0.04 in) dia 99.95%	74
9	Zinc powder 6-9 micron 97.5%	61
10	Zinc, metal (powder)	84
11	Zinc 99^{+}% mossy	79
12	Zinc foil, 0.38 mm	69

and the procedure was successfully extended to a series of olefins and nonactivated indazoles affording the corresponding coupling products ($\mathbf{6a_{63}b_2}$-$\mathbf{6a_{66}b_5}$) in high yields and excellent selectivity (Scheme 12). Notably, the application of this protocol for preparing axitinib in short reaction time and high efficiency following a two-step mechanochemical Heck/Migita cross-coupling (Scheme 12).

3.4. Mechanochemical-Assisted Cross-Metathesis Reactions. The alkene metathesis is a catalyzed reaction that proceeds by interchange of substituents of two reacting olefins in an equilibrium reaction to form two new compounds (Scheme 13).[64]

Evolution of ethylene or propylene is favored entropically and drives the cross-metathesis to completeness.[65] Discovered almost 50 years ago,[66] the development of olefin metathesis procedures has introduced a breakthrough in C−C bond formation, leading to remarkable achievements in organic and polymer chemistry.[67] Ruthenium-based olefin metathesis catalysts have opened new routes to design olefins with desirable structures for improved performance in applications ranging from medicinal chemistry to material science[68] catalysts generally exhibit broad functional group tolerance and are relatively stable toward air and water.[69] In 2015, Friščić et al. focused their attention on some relevant cross-metathesis and ring-cross metathesis reactions by using a mechanochemical approach.[70] The model protocol was set up using three different types of olefins: styrene ($\mathbf{5b_6}$, liquid), methyl 4-vinylbenzoate ($\mathbf{5b_7}$, a low-melting solid: 37 °C), 4-vinylbenzoic acid ($\mathbf{5b_8}$, a high-melting solid: 144 °C) (Table 4). Since steel jars gave irreproducible results, olefins were milled at 30 Hz in a 14 mL Teflon milling jar containing one stainless steel ball (10 mm diameter). The procedure was developed by comparing the performance of Grubbs (**A**, **B**, and **C**) and Hoveyda−Grubbs catalysts (**D**), among the best performing for similar reactions in solution. As expected, the reaction with liquid olefin proceeded smoothly and was completed in 30 min (Table 4, entries 2−4), while low melting (LM) alkene $\mathbf{5b_7}$ provided poor conversions (about 30%, after 1.5 h, Table 4, entries 6, and 8). In contrast, the high melting (HM) olefin $\mathbf{5b_8}$ did not exhibit any significant reactivity even after 5 h of milling (Table 4, entries 9−12). Overall, the second generation Hoveyda−Grubbs catalyst (**D**) proved to be the most reliable and efficient of the explored catalysts (Table 4, entry 8). The addition of a substoichiometric amount of a liquid (LAG, η = 0.1−1 μL/mg) significantly improved the yield of $\mathbf{9b_7b_7}$, also enabling the metathesis of $\mathbf{5b_8}$ (Table 4, entries 13 and 14).

Moreover, the use of an inert, water-soluble grinding auxiliary avoided the formation of a thick shell around the

https://dx.doi.org/10.1021/acscatal.0c00142
ACS Catal. 2020, 10, 8344−8394

Scheme 10. Scope of the Mechanochemical Negishi Reaction. Adapted with Permission from Ref 55. Copyright 2019 Wiley-VCH

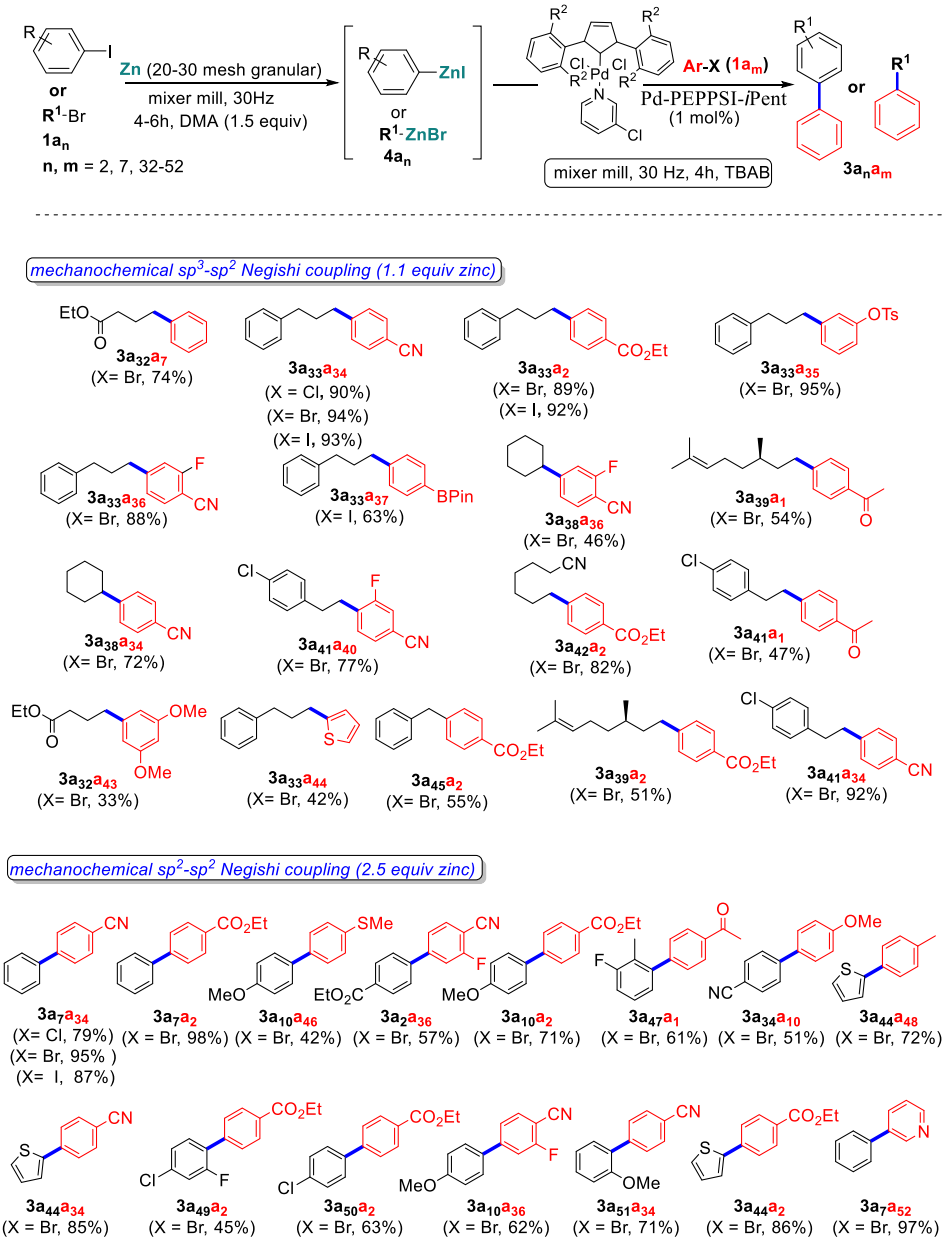

ball and led to a considerable increase in terms of yield and reproducibly of $\mathbf{9b_7b_7}$ (>90%, Table 5, entries 2−6) and $\mathbf{9b_8b_8}$ (>70%, Table 5, entries 7−11), independent of the choice of the auxiliary.

Once established the optimal conditions for cross-metathesis of solid olefins, Friščić et al. extended the protocol to ring-closing-metathesis reactions. In this context, a non-negligible aspect has to be considered; most of the examples described in the literature run in a noncoordinating solvent (CH_2Cl_2) and at a concentration of <0.1 M.[66b] Interestingly, the mechanochemical reaction proceed smoothly with the liquid $\mathbf{5b_9}$ (product $\mathbf{9b_9b_9}$ in Scheme 14), while with solid olefins, it required a further fine-tuning of the process parameters, such as catalytic liquids and solid auxiliaries (Table 6).

Again, combining propylene carbonate (PC, LAG) with different water-soluble salts (NaCl, KCl, NaBr, NaI, and K_2SO_4) as solid auxiliary (150% by weight) ring-closing metathesis resulted in almost quantitative yield of $\mathbf{9b_{12}b_{12}}$ (Table 7). Notably, the amount of grinding auxiliary is comparable to that of reactant, in contrast to conventional solution procedures, which run diluted and generally need a 10- or 100-fold excess of bulk solvent.

3.5. Mechanochemical-Assisted Friedel−Crafts Reactions. Friedel−Crafts reaction is probably one of the oldest reactions and widely used procedure for the construction of carbon−carbon bonds involving an aromatic moiety (Scheme 15). Still today, it is an attractive methodology for the synthesis of aromatic ketones loading acyl substituents directly onto aromatic rings.[71] In recent years, Friedel−Crafts reactions have found increasingly widespread industrial and academic application in the design of targeted complex bioactive molecules and the preparation of fine chemicals.[72]

The rising public awareness of the tremendous impact of chemical contaminants on human health and the environment

https://dx.doi.org/10.1021/acscatal.0c00142
ACS Catal. 2020, 10, 8344−8394

Scheme 11. Mizoroki–Heck Coupling Reactions under Ball-Milling Conditions. Adapted with Permission from Ref 60. Copyright 2006 Thieme

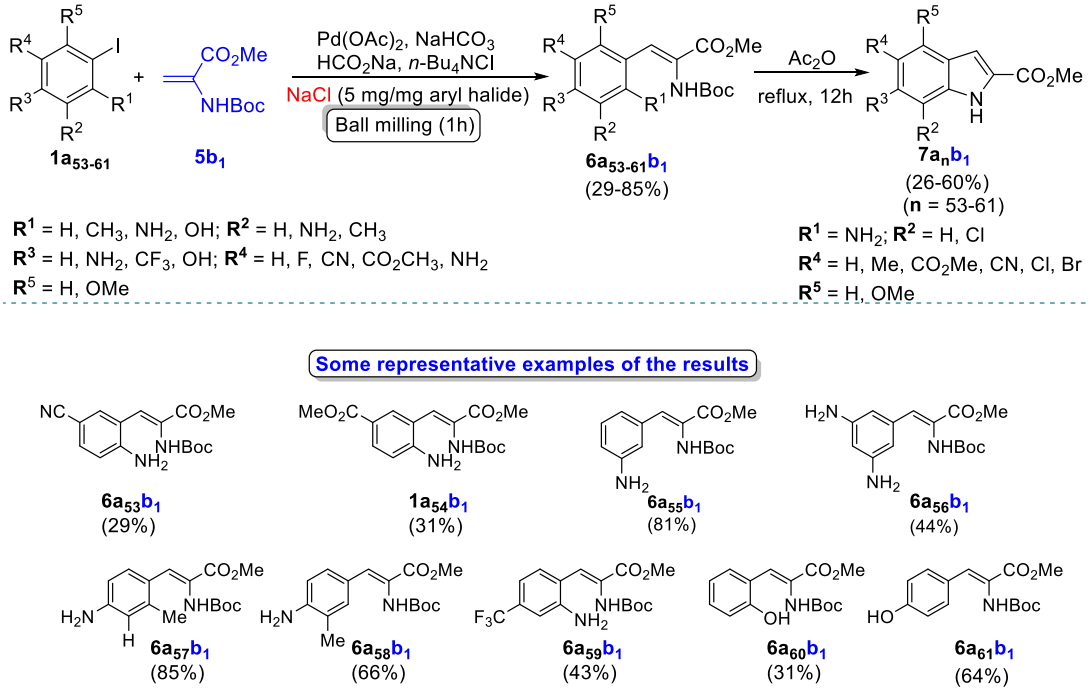

Scheme 12. Optimization of the Reaction Conditions for the Olefination of 3-Bromoindazoles and Examination of the Substrate Scope[a]. Adapted with Permission from Ref 63. Copyright 2018 Beilstein Institute

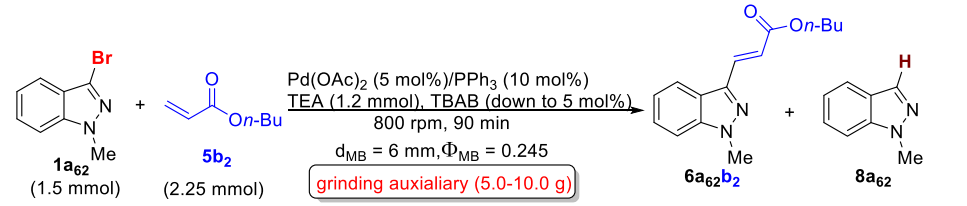

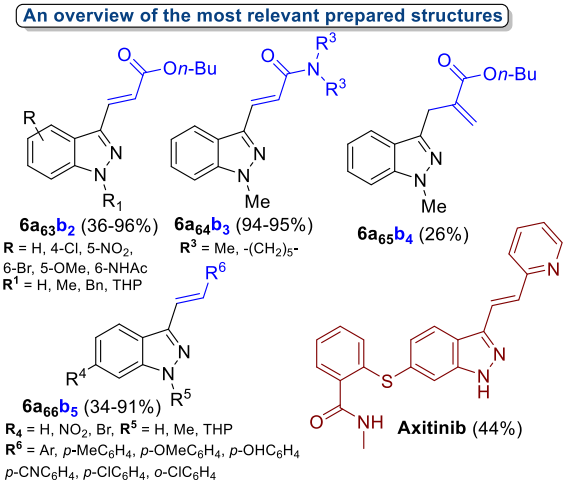

Entry	Grinding Auxiliary	Yield (%) $6a_{62}B_2/8a_{62}$
1	-	10/trace
2	silica gel	53/19
3	**NaBr (10 g)**	**69/trace**
4	KBr	63/trace
5	KBr (10g)	69/trace
6	NaCl	27/5
7	γ-Al_2O_3	20/6
8	sand	30/10

[a] d_{MB} = milling ball diameter, Φ_{MB} = milling ball filling degree.

prompts chemists to design new improvements to reduce waste generation, reactant materials, and save energy consumption. In this regard, Davor Margetić et al., developed at room temperature a solvent-less Friedel–Crafts protocol improving the eco-friendliness of the reaction.[73] The hygroscopic nature of the aluminum trichloride catalyst, when exposed to air humidity, has been a significant factor limiting the application of this methodology to solid-state reactions. The use of an automated ball milling combined with a closed jar can not only help to overcome this problem but also to cut the reaction times, improving the reaction yields, too. The mechanochemical Friedel–Crafts process parameters have been optimized milling together pyrene ($10a_1$) and

https://dx.doi.org/10.1021/acscatal.0c00142
ACS Catal. 2020, 10, 8344–8394

Scheme 13. Olefin Metathesis Processes

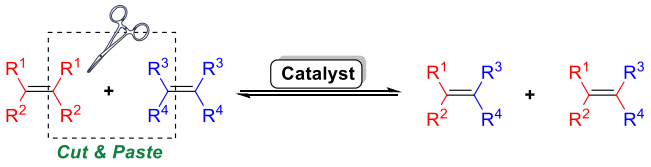

phthalic anhydride ($\mathbf{11b_1}$) in the presence of $AlCl_3$; all reagents and catalyst are solids (Scheme 16).

In solution, this reaction proceeds well, affording the corresponding 1-(*o*-carboxybenzoyl)pyrene ($\mathbf{12a_1b_1}$) in quantitative yield, in general. The mechanochemical reaction involving an equimolar amount of pyrene ($\mathbf{10a_1}$) and phthalic anhydride ($\mathbf{11b_1}$) in the presence of 2.5 equiv of $AlCl_3$ performed best and gave product $\mathbf{12a_1b_1}$ in 79% isolated yield. The addition of various grinding auxiliaries (silica gel, NaCl, Na_2SO_4) to improve mass transfer and prevent pasting of the reaction mixture as well as the use of a small amount of solvents (LAG: THF, CH_2Cl_2) turned out to be detrimental to the reaction yields. Lewis acid catalysts ($FeCl_3$, $ZnCl_2$, $ZnBr_2$, ZnI_2, $CuBr_2$, CuI_2) other than $AlCl_3$ were of no synthetic use whatsoever. With optimized conditions established, the scope of the reaction with respect to a series of acylation reagents in conjunction with pyrene and a variety of aromatic substrates was assessed (Scheme 17). This screening revealed that differences in chemical structures led to different chemical reactivities with final yields ranging from quantitative to low (Scheme 17). In situ Raman and ex situ IR spectroscopy analyses of the solid-state reaction of phthalic anhydride with *p*-xylene pointed out that the process was promoted by the initial formation of a complex between the carbonyl group of the acylation reagent with $AlCl_3$.

In the same context, Borchardt described the utility of the mechanochemical method in the synthesis of porous covalent triazine frameworks (CTFs).[74] Friedel–Crafts alkylation of cyanuric chloride with carbazole under mechanochemical condition gave easy access to different porous polymers in almost quantitatively yields after only 60 min (Scheme 18).

Chiral indole scaffolds, particularly, 3-decorated ones, constitute a central building block in the design of bioactive natural products, active pharmaceutical ingredients (APIs), and synthetic chemicals.[75] The asymmetric Friedel–Crafts alkylation of indoles represents a valuable and widely used strategy to prepare enantioenriched derivatives.[76] To date, the reaction of indole with arylidene malonates in the presence of chiral copper(II) complexes constitutes one of the most promising procedures for preparing 3-decorated indoles being available in the literature, and there are still several unresolved issues to be addressed.[77] The strong dependence of the catalytic activity of the metal complex on the nature of the solvent significantly restricts the widespread use of this technique. Moreover, the need for an inert atmosphere, strictly anhydrous conditions, and prolonged cooling periods render these synthetic procedures tedious and time-consuming. The removal of the solvent could significantly reduce the cost and simplify the

Table 4. Performance of the First- (A) and Second-Generation (B) Grubbs Catalysts, a Fast-Initiating Catalyst (C), and the Second-Generation Hoveyda–grubbs Catalyst (D) in the Mechanochemical Ruthenium-Catalyzed Olefin Metathesis. Adapted with Permission from Ref 70. Copyright 2015 American Chemical Society

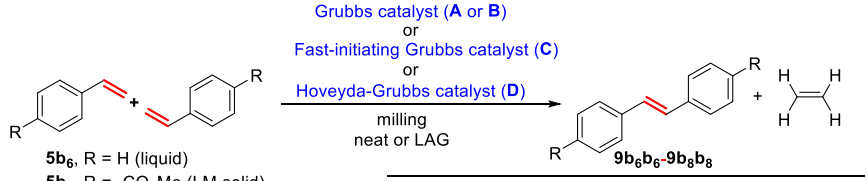

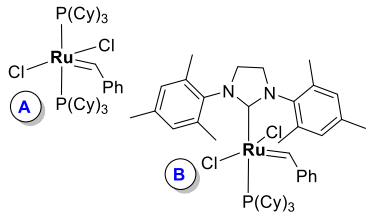

First- (**A**) and second-generation (**B**) Grubbs catalysts

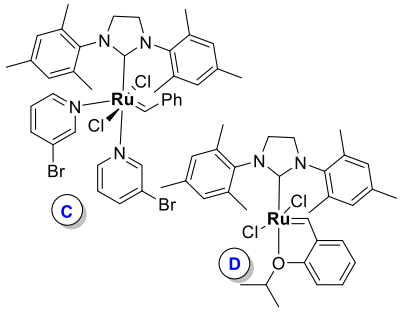

Fast-initiating Grubbs catalyst (**C**), and the second-generation Hoveyda-Grubbs catalyst (**D**)

Entry	Olefin	catalyst (mol%)	liquid (μL)	time (h)	Yield (%)
1	$\mathbf{5b_6}$	A (5)	-	1	-
2	$\mathbf{5b_6}$	B (1)	-	0.5	92
3	$\mathbf{5b_6}$	C (2)	-	0.5	80
4	$\mathbf{5b_6}$	D (0.5)	-	0.5	90
5	$\mathbf{5b_7}$	A (5)	-	1	-
6	$\mathbf{5b_7}$	B (5)	-	1.5	31
7	$\mathbf{5b_7}$	C (2)	-	1.5	0
8	$\mathbf{5b_7}$	D (1)	-	1.5	30
9	$\mathbf{5b_8}$	A (5)	-	5	-
10	$\mathbf{5b_8}$	B (5)	-	5	-
11	$\mathbf{5b_8}$	C (5)	-	5	-
12	$\mathbf{5b_8}$	D (2)	-	5	-
13	$\mathbf{5b_7}$	D (1)	THF (50)	1.5	40
14	$\mathbf{5b_8}$	D (2)	THF (50)	5	49

https://dx.doi.org/10.1021/acscatal.0c00142
ACS Catal. 2020, 10, 8344–8394

Table 5. Mechanochemical Ruthenium-Catalyzed Olefin Metathesis in the Presence of Solid Auxiliary Using Catalyst D. Adapted with Permission from Ref 70. Copyright 2015 American Chemical Society

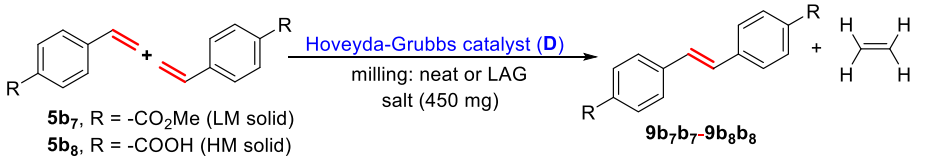

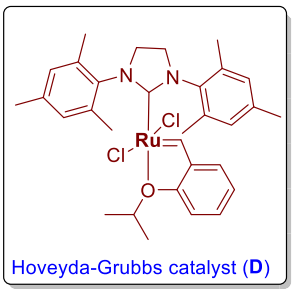

Entry	Olefin	catalyst (mol%)	liquid (μL)	Solid auxiliary	time (h)	Yield (%)
1	$\mathbf{5b_7}$	D (1)	-	-	1.5	**30**
2	$\mathbf{5b_7}$	D (1)	-	NaCl	1.5	93
3	$\mathbf{5b_7}$	D (1)	-	NaBr	1.5	92
4	$\mathbf{5b_7}$	D (1)	-	NaI	1.5	92
5	$\mathbf{5b_7}$	D (1)	-	KCl	1.5	91
6	$\mathbf{5b_7}$	D (1)	-	K_2SO_4	1.5	92
7	$\mathbf{5b_8}$	D (2)	EtOAc (75)	NaCl	5	73
8	$\mathbf{5b_8}$	D (2)	EtOAc (75)	NaBr	5	70
9	$\mathbf{5b_8}$	D (2)	EtOAc (75)	NaI	5	71
10	$\mathbf{5b_8}$	D (2)	EtOAc (75)	KCl	5	74
11	$\mathbf{5b_8}$	D (2)	EtOAc (75)	K_2SO_4	5	71

Scheme 14. Mechanochemical Ruthenium-Catalyzed Ring-Closing Metathesis by Using Liquid Olefin, and Hoveyda–Grubbs Catalyst (D, 0.5 mol %). Adapted with Permission from Ref 70. Copyright 2015 American Chemical Society

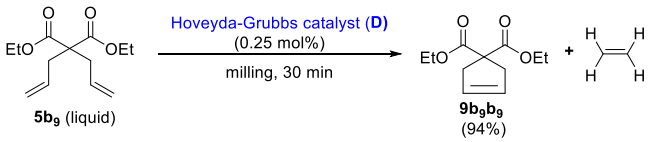

procedure by opening up unexplored paths toward chiral 3-substituted indole derivatives. In 2019, Bolm et al. have developed a valuable mechanochemical copper-catalyzed asymmetric alkylation of indoles with arylidene malonates under the ambient atmosphere.[78] For fine-tuning all the parameters, a mixture of indole ($\mathbf{10a_{12}}$) and benzylidene malonate ($\mathbf{5b_{13}}$) was ground in the presence of a chiral bis(oxazoline)-copper catalyst (CuX_mL_n) by using a mixer mill apparatus (Table 8).

The CuCl/$AgNTf_2$/L_6 combination (5.0 mol %, Table 8, entry 11) has been proven to be the best catalytic system for this mechanochemical asymmetric Michael-type Friedel–Crafts alkylation of indoles, while the addition of pentafluorophenol (PFP, 1.0 equiv, 20 Hz, Table 8, entry 12) led to an almost complete conversion of the starting materials. The optimized conditions were extended to various structurally diverse indoles ($\mathbf{10a_{12}}$-$\mathbf{10a_{17}}$) and arylidene malonates ($\mathbf{5b_{13}}$-$\mathbf{5b_{26}}$) affording products $\mathbf{12a_{12-17}b_{13-26}}$ in excellent yields (up to 98%) and good enantioselectivities regardless of the steric hindrance and electronic properties (Scheme 19).

It is important to emphasize that the reaction times were shorter compared with analogous couplings in solution.

Table 6. Mechanochemical Ruthenium-Catalyzed Ring-Closing Metathesis by Using 0.5 mol % D. Adapted with Permission from Ref 70. Copyright 2015 American Chemical Society

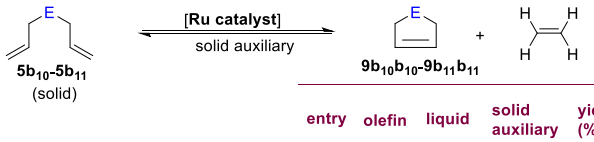

Products synthesised

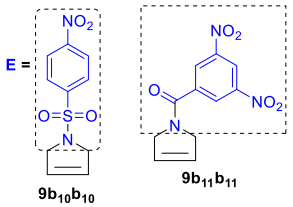

entry	olefin	liquid	solid auxiliary	yield (%)
1	$\mathbf{5b_{10}}$	-	-	-
2	$\mathbf{5b_{10}}$	EtOAc	-	33
3	$\mathbf{5b_{10}}$	EtOAc	NaCl	92
4	$\mathbf{5b_{10}}$	EtOAc	KCl	90
5	$\mathbf{5b_{10}}$	EtOAc	K_2SO_4	91
6	$\mathbf{5b_{11}}$	-	-	-
7	$\mathbf{5b_{11}}$	EtOAc	-	39
8	$\mathbf{5b_{11}}$	EtOAc	NaCl	94
9	$\mathbf{5b_{11}}$	EtOAc	KCl	91
10	$\mathbf{5b_{11}}$	EtOAc	K_2SO_4	89

3.6. Other Mechanochemical-Assisted Processes: Hydroformylation and Multicomponent Reactions. *3.6.1. Hydroformylation Reaction.* The hydroformylation reaction is still today one of the most efficient and promising routes to convert olefins into aldehydes with concomitant homologation of one additional carbon atom (Scheme 20).

In the past, especially during the Second World War, this procedure allowed Germany to develop chemical technologies based on coal and alternatives to oil-based chemistry.[79] By a

https://dx.doi.org/10.1021/acscatal.0c00142
ACS Catal. 2020, 10, 8344–8394

Table 7. Mechanochemical Ruthenium-Catalyzed Ring-Closing Metathesis of $5b_{12}$ by Using 2 mol % D. Adapted with Permission from Ref 70. Copyright 2015 American Chemical Society

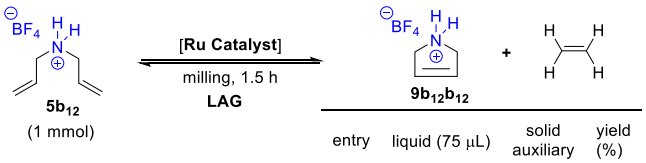

entry	liquid (75 μL)	solid auxiliary	yield (%)
1	-	-	-
2	THF	-	-
3	$BMIMBF_4$	-	15
4	PC	-	13
5	PC	NaCl	96
6	PC	NaBr	92
7	PC	NaI	95
8	PC	KCl	94
9	PC	K_2SO_4	91

Scheme 15. Friedel–Crafts Acylation Reactions

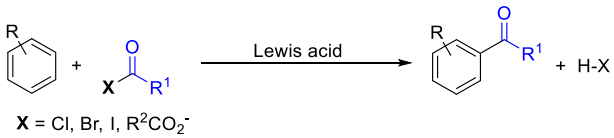

strange twist of fate, the hydroformylation reaction is among the most prominent and useful in the panorama of organic green chemistry in addition to being perfectly in agreement with the 12 principles.[80] Over the years, researchers have developed an increasingly efficient number of transition-metal catalysts and specialized ligands able to improve chemo-, regio-, and enantioselectivities.[81] Several papers in the literature have recently highlighted that supramolecular interactions, such as hydrogen bonding between substrate and ligand, could give rise to a noncovalent substrate preorganization around the active catalytic site.[82] Cyclodextrins and bidentate ligands cooperate with each other via supramolecular interactions promoting the regioselective formation of linear aldehydes.[83] In 2017, Hapiot reported for the first time a Rh-catalyzed hydroformylation of alkenes under ball-milling conditions.[84] In the presence of an in situ-generated $HRh(CO)(PPh_3)_3$ complex, the mechanochemical hydroformylation protocol was set up on 2-vinylnaphtalene ($5b_{27}$, 64–68 °C) as a model substrate and then extended to

Scheme 17. Scope of the Reaction with Respect to a Series of Aromatic Reagents under Mechanochemical Activation Conditions. Adapted with Permission from Ref 73. Copyright 2019 Beilstein Institute

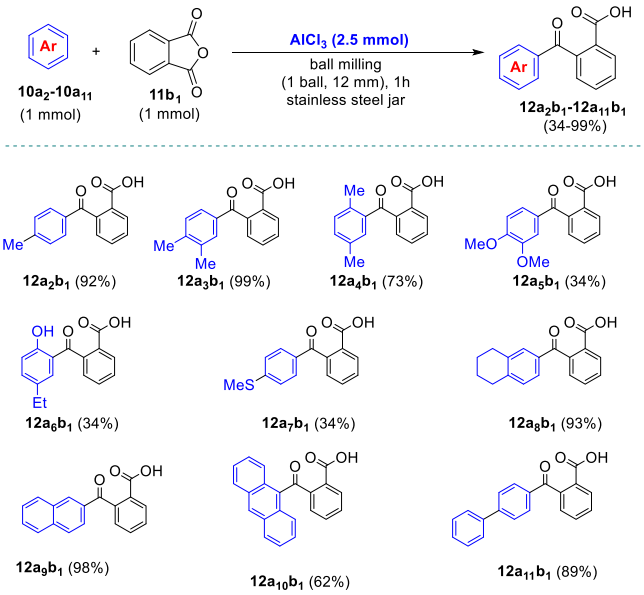

an array of aromatics substituted alkenes ($5b_{28}$-$5b_{31}$, Scheme 21). Olefins were exposed to syngas (CO/H_2: 1/1) under pressure (220 psi) and in a planetary ball mill (850 rpm) for 4 h (Scheme 21).

^1H and ^{31}P NMR spectroscopy confirmed the formation the hydrido-Rh precursor by milling $Rh(CO)_2(acac)$ (acac = acetylacetonate) with 5 equiv of PPh_3 under 220 psi CO/H_2 (1:1) pressure in the presence of saccharide as additives. A careful choice of the saccharide among methyl-α-D-glucopyranoside (**Add-1**, Scheme 21), acyclic dextrins (**Add-2**, Scheme 21), or cyclodextrins [CDs, cyclic oligosaccharides, (**Add-3**)–(**Add-5**), Scheme 21] assured an adequate dispersion of the substrate molecules and the Rh-catalyst into the grinding jar. Moreover, saccharides controlled the activity and selectivity of Rh-catalyzed hydroformylation of vinyl derivatives providing exclusively the corresponding aldehydes whatever the nature of the saccharide. However, acyclic saccharides significantly promote the diffusion of the components within the solid mixture leading to high and chemoselective conversions of alkenes into *α-aldehyde* products during the course of the reaction. The steric hindrance exerted by the cyclic saccharides, such as CDs, on the primary coordination sphere of the metal modify the regioselectivity via through-space control and favor hydroformylation at the less-hindered position of the vinyl function so that the *β-aldehydes* were

Scheme 16. Mechanochemical Friedel–Crafts Reaction of Pyrene and Phthalic Anhydride. Adapted with Permission from Ref 73. Copyright 2019 Beilstein Institute

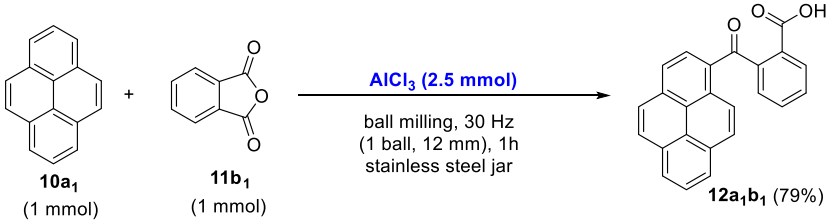

https://dx.doi.org/10.1021/acscatal.0c00142
ACS Catal. 2020, 10, 8344–8394

Scheme 18. Mechanochemical Syntheses of Porous Covalent Triazine Frameworks by Friedel–Crafts Alkylation of Different Aromatic Monomers with Cyanuric Chloride. Adapted with Permission from Ref 74. Copyright 2017 Wiley-VCH

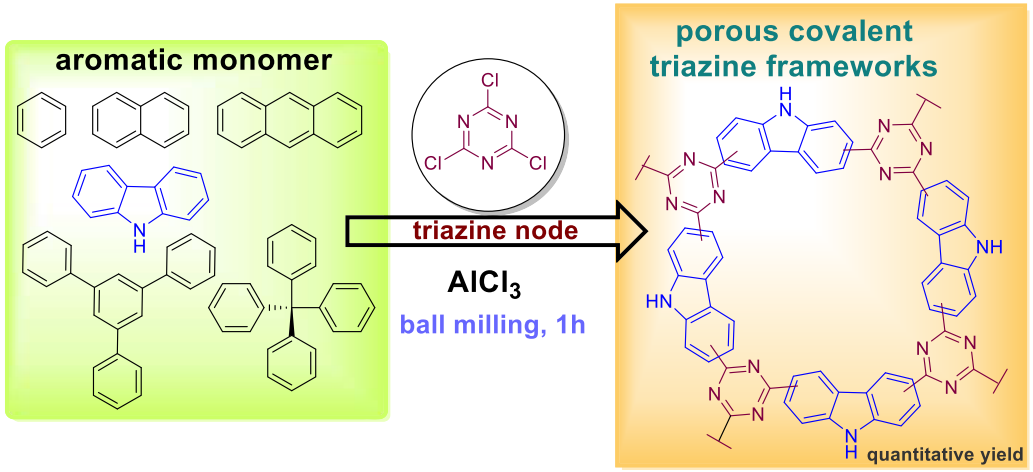

formed in non-negligible proportions. The use of bulkier bidentate ligands, such as BIPHEPHOS (Figure 4) further amplifies this effect paving the road to further developments of catalytic hydroformylation processes in the solid-state.

3.6.2. Strecker Reaction. When and how life began on earth has evolved remains wrapped in a mystery, even today. Along with many other theories proposed for the early generation of biogenic molecules, the formation of prebiotics such as amino acids, etc., due to the physical impact of high-energy extra-terrestrial bodies is not to be excluded a priori. Therefore, the origin of life could also be the result of mechanical actions among the primordial elements: impacts and frictions; theories perfectly correlate to the field of mechanochemistry. In a seminal paper by Hernandez et al., the authors studied the formation of α-amino acids in a ball mill simulating the scenario of early Earth conditions.[85] Strecker reaction allows a simple and direct access to α-amino acids; however, the prebiotic source of HCN still needs to be identified (Scheme 22). Inspired by a recent discovery of Civis, Hernandez used formamide as potential cyanide source in a mechanochemical Strecker-type reaction with benzaldehyde ($\mathbf{13a_1}$) and benzylamine ($\mathbf{14b_1}$) in the presence of SiO_2 using a high-speed mixer mill with a tungsten carbide (WC) jar and one WC ball (d= 15.6 gcm-3) at 30 Hz for 90 min (Table 9).

Despite the high temperatures inside the jar as a result of the highly energetic impacts, only imine $\mathbf{16a_1b_1}$ and unreacted amide were detected in the crude reaction mixture. The use of cyanoferrate as alternative source for generating active CN^- specie ($K_4[Fe(CN)_6]\cdot 3H_2O$ or $K_3[Fe(CN)_6]$) gave α-aminonitrile $\mathbf{15a_1b_1}$ in low amounts, along with imine $\mathbf{16a_1b_1}$ as the major product of the reaction (Table 9, entries 1–2).

Potassium ferricyanide (III) and Prussian blue milled (30 Hz, 90 min) in the presence of silica gel significantly improved the multicomponent Strecker reaction generating preferentially α-aminonitrile $\mathbf{15a_1b_1}$ with little imine $\mathbf{16a_1b_1}$ (95:5) production (Table 9, entries 4 and 6). Powder X-ray diffraction (PXRD) analysis of $K_3[Fe(CN)_6]$ samples milled for 60 min with and without SiO_2 highlighted structural changes in the Fe-complex, but no concrete evidence of KCN in the PXRD patterns suggested a different biogenic CN^- source. Further studies highlighted the formation of gaseous HCN during the grinding process in a high-energy mill. The authors conducted further investigations to detect the formation of gaseous HCN during the grinding process in a high-energy mill. When all reaction conditions were unchanged, the use of a suitably modified sealed jar allowed to bubble and trap the developed gas inside an aqueous solution. After15 min of milling, the formed gas was bubbled in an aqueous media, and a commercially available paper test (Cyantesmo strip) sensitive to the presence of HCN assessed the releasing of hydrogen cyanide inside the jar, as depicted in Figure 5. In confirmation of this hypothesis, the gas bubbled through the vial containing a solution of $\mathbf{13a_1}$ and $\mathbf{14b_1}$ afforded α-aminonitrile $\mathbf{15a_1b_1}$.

The scope of this mechanochemical Strecker reaction was further expanded to various aromatic and aliphatic aldehydes, which were milled together with benzylamine ($\mathbf{14b_1}$) or aniline ($\mathbf{14b_2}$) and $K_3[Fe(CN)_6]$ to afford the expected α-aminonitriles $\mathbf{15a_{1-10}b_{1-2}}$ in good yields (Scheme 23).

A quick hydrolysis (30 min) of the resulting α-aminonitriles in a ball-mill and under prebiotic condition (in the presence of paraformaldehyde, PFA) led to the corresponding amino amides in moderate yields. Aging reactions, under prebiotic conditions, could promote the subsequent transformation of these products into the corresponding amino acids.

3.6.3. Preparation of Propargylamines and Cumulenes. The development of synthetic protocols involving one or more gaseous reagents is one of the most important challenges facing chemists from both the academy and industry.[86] Among these reagents, acetylene plays a key role, because it is an important and widely used building block for the construction of even more complex molecular architectures.[87] Besides, it allows the formation of new C–C and C–X (X = heteroatom) bonds, and the economy of these molecular transformations, in terms of atom economy and step economy, is particularly attractive and of increasing importance nowadays. Acetylene gas is also potentially hazardous and difficult-to-handle, and calcium carbide (CaC_2) has been extensively used as a safe, solid replacement.[88] Unfortunately, calcium carbide is almost insoluble in most organic solvents, and current processes for using CaC_2 often need three-phase reaction mixtures, extreme reaction media, high temperatures, and long reaction times.[89] The use of solventless methodologies could help to overcome these practical drawbacks beforehand, thereby also promoting the valorization of CaC_2 as a solid surrogate for acetylene. The activation of CaC_2 under mechanochemistry conditions not only breaks its crystal structure, accelerating its availability for

https://dx.doi.org/10.1021/acscatal.0c00142
ACS Catal. 2020, 10, 8344–8394

Table 8. Screening of the Catalytic System for the Alkylation of Indole ($10a_{12}$) with Benzylidene Malonate ($5b_{13}$). Adapted with Permission from Ref 78. Copyright 2019 Wiley-VCH

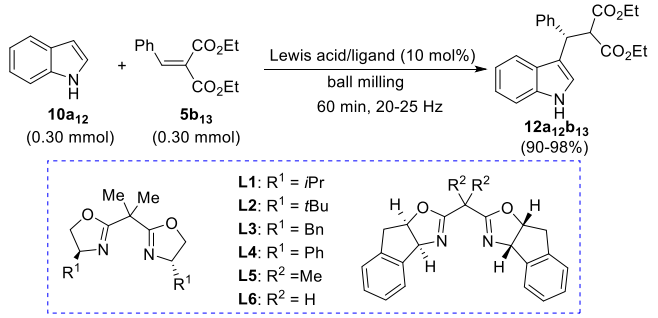

entry	Lewis acid	ligand	milling auxiliary	additive	milling frequency (Hz)	yield (%)	e. r.
1	$Cu(OTf)_2$ (10 mol%)	-	silica gel (60 mg)	-	25	94	-
2	$Cu(OTf)_2$ (10 mol%)	L1	silica gel (60 mg)	-	25	98	50:50
3	$Cu(OTf)_2$ (10 mol%)	L2	silica gel (60 mg)	-	25	95	65:35
4	$Cu(OTf)_2$ (10 mol%)	L3	silica gel (60 mg)	-	25	90	52:48
5	$Cu(OTf)_2$ (10 mol%)	L4	silica gel (60 mg)	-	25	96	50:50
6	$Cu(OTf)_2$ (10 mol%)	L5	silica gel (60 mg)	-	25	97	62:38
7	$Cu(OTf)_2$ (10 mol%)	L6	silica gel (60 mg)	-	25	97	78:22
8	$CuCl_2/AgNTf_2$ (10 mol%)	L6	silica gel (60 mg)	-	25	97	81:19
9	$CuCl/AgNTf_2$ (10 mol%)	L6	silica gel (60 mg)	-	25	97	85:15
10	$CuCl/AgNTf_2$ (10 mol%)	L6 (Cu complex prepared in solution)	silica gel (60 mg)	-	25	97	85:15
11	$CuCl/AgNTf_2$	L6 (5 mol%)	silica gel (60 mg)	-	25	97	85:15
12	$CuCl/AgNTf_2$ (5 mol %)	L6 (5 mol%)	silica gel (60 mg)	PFP	20	95	91:9
13	$CuCl/AgNTf_2$ (5 mol %)	L6 (5 mol%)	silica gel (60 mg)	*i*PrOH	20	95	85:15

the reaction, but also provides new synthetic routes that differ from those of their solution-based thermal counterpart. With that as the premise, Bolm and Hernandez attempted to develop a methodology for quick access to propargylamines by grinding together benzaldehyde ($13a_1$, Table 10), pyrrolidine ($14b_3$, Table 10), and calcium carbide in the presence of a copper catalyst.[90] In contrast to similar experiments performed in a solution, ^{1}H NMR analysis of the crude reaction mixture revealed that the mechanochemical reaction afforded 1,4-diamino-2-butyne ($16a_1b_3$) as the main product (Table 10). The authors screened a wide selection of Cu(I) and Cu(II) salts as a catalyst for this mechanochemical A3 coupling and observed that copper(I) bromide (20 mol %) and CuI (20 mol %) catalyze the reaction to a similar extent, providing $16a_1b_3$ as the major product after 90 min of milling at 25 Hz ($16a_1b_3$/$17a_1b_3$: 85/10, Table 10, entry 3). The presence of water in $Cu(BF_4)_2{\cdot}6H_2O$ during the milling determined a remarkable change in selectivity preferentially leading to the formation of propargylamine $17a_1b_3$ over $16a_1b_3$ ($16a_1b_3$/$17a_1b_3$: 16/74; Table 1, entry 6). Once all the parameters have been set as 90 min of milling at 25 Hz (Table 10, entry 9), the substrate scope of the mechanochemical A3 coupling was extended to a broad set of aldehydes and amines to afford the corresponding bis substituted propargylic products $16a_{1-14}b_{3-4}$ in good yield

https://dx.doi.org/10.1021/acscatal.0c00142
ACS Catal. 2020, 10, 8344−8394

Scheme 19. Mechanochemical Cu-Catalyzed Asymmetric Friedel–Crafts Alkylations of Indoles with Various Arylidene Malonates. Adapted with Permission from Ref 78. Copyright 2019 Wiley-VCH

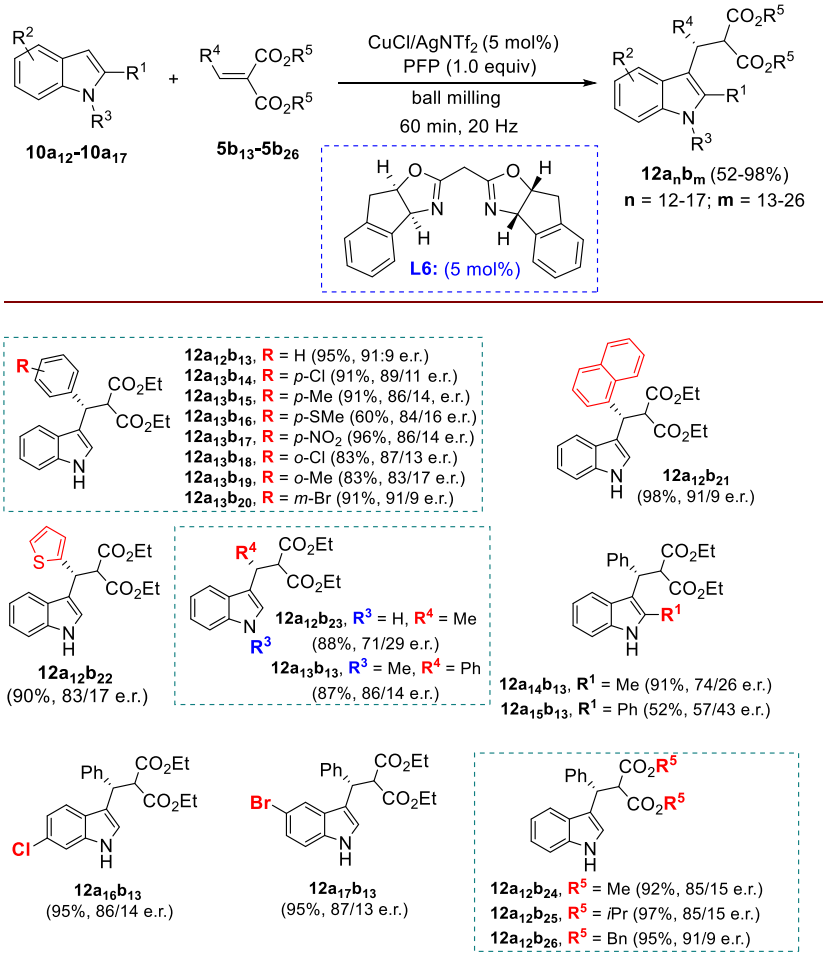

Scheme 20. Hydroformylation, Also Known as Oxo Synthesis or Oxo Process

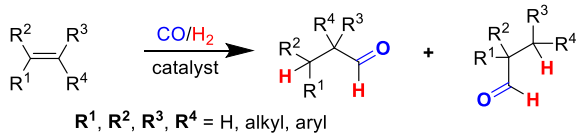

after column chromatography (Scheme 24). In contrast to previous solution procedures, the milling of calcium carbide with 2-cyanobenzaldehyde ($\mathbf{13a_{11}}$) led to isoindolinone $\mathbf{18a_{11}b_3}$ instead of the expected product $\mathbf{16a_{11}b_3}$ suggesting that intramolecular hydrolysis of the nitrile group proceed faster than the addition of the carbide anion to the iminium ion intermediate.

Conversely, the mechanochemical A^3 coupling of primary amines did not proceed beyond the formation of the corresponding imines, whereas acyclic secondary amines (e.g., diethylamine) provided the desired 1,4-diamino-2-butynes in low yields. In this paper, the authors have successfully demonstrated the ability of mechanochemistry to alter established pathways in solution exploring otherwise dormant chemical reactivity.

Nevertheless, there are still a few questions to be answered: what happens when using solid acyclic or high boiling amines? Why has $Cu(BF_4)_2{\cdot}6H_2O$ not been investigated in detail for an in-depth understanding of mechanochemistry processes for preparing propargylamines?

Following this line of research, Bolm et al.[91] have recently established an efficient two-stage procedure for the synthesis of tetraaryl[*n*]cumulenes (*n* = 3, 5) based on the mechanochemical activation of ketones, calcium carbide, and potassium hydroxide via an initial Favorskii alkynylation-type reaction in a ball mill (Schemes 25 and 26).

The subsequent solventless and acid-free reductive elimination of propargylic diols $\mathbf{20a_{(1-10)}a_{(1-10)}}$ in the presence of a stoichiometric amount of $SnCl_2{\cdot}2H_2O$ is crucial for the mechanosynthesis of the cumulenic carbon nanostructures (Scheme 25). The authors also highlighted how the reductive elimination of the alkynediol $\mathbf{20a_1a_1}$ (1 mmol) with substoichiometric amounts of $SnCl_2$ $2H_2O$ (0.5 mmol) led to the formation of the corresponding [3]cumulene $\mathbf{22a_1a_1}$ together with the intermediate 1,1,4,4-tetra-phenyl-2-chloro-buta-2,3-dien-1-ol, which allowed the team to gain significant insights on the reaction mechanism. This mechanochemical protocol was further applied to the synthesis of the illustrative tetraphenyl[5]cumulene ($\mathbf{24a_1a_1}$). Once the propargyl alcohols $\mathbf{21a_1}$ have been prepared, the reaction proceeds through two further steps: a mechanochemical copper-assisted oxidative coupling of propargylic alcohols $\mathbf{21a_1}$ (Scheme 26, step 2) followed by reductive elimination of diyne diol $\mathbf{23a_1a_1}$ with $SnCl_2{\cdot}2H_2O$ (Scheme 26, step 3).

https://dx.doi.org/10.1021/acscatal.0c00142
ACS Catal. 2020, 10, 8344–8394

Scheme 21. Optimization of the Reaction Conditions. Adapted with Permission from Ref 84. Copyright 2017 Wiley-VCH

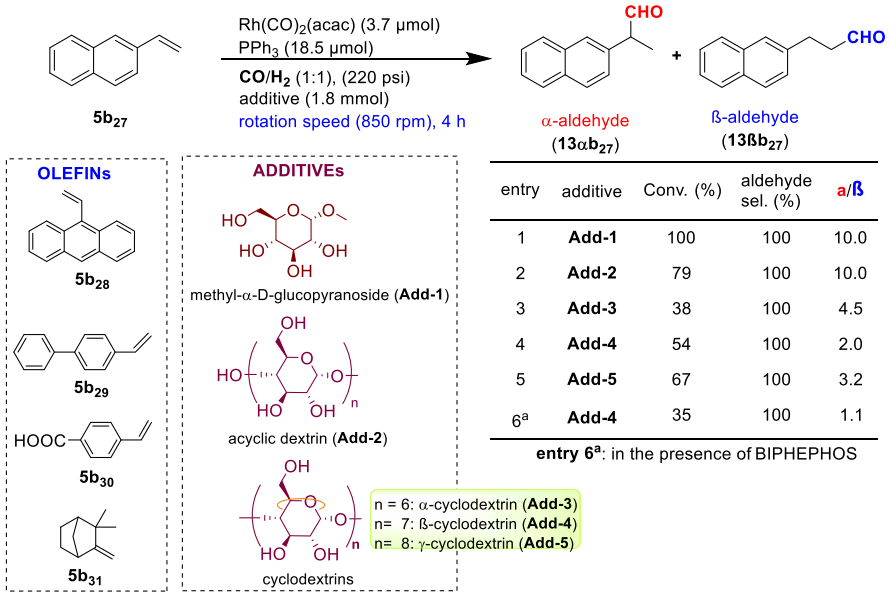

entry	additive	Conv. (%)	aldehyde sel. (%)	a/ß
1	**Add-1**	100	100	10.0
2	**Add-2**	79	100	10.0
3	**Add-3**	38	100	4.5
4	**Add-4**	54	100	2.0
5	**Add-5**	67	100	3.2
6[a]	**Add-4**	35	100	1.1

entry 6[a]: in the presence of BIPHEPHOS

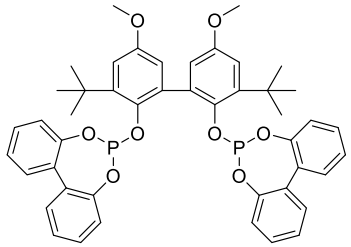

Figure 4. BIPHEPHOS structure.

Such studies could contribute to further development in the mechanosynthesis of carbon-based materials from CaC_2; for example, in supramolecular chemistry for preparing conjugated polycyclic hydrocarbons and cumulenes starting from poorly soluble reagents or acid-labile precursors.

4. MECHANOCHEMISTRY FOR C−H BOND ACTIVATION

4.1. Mechanochemistry for C−N Bond Formation. The development of new synthetic strategies aimed at promoting the formation of new carbon−nitrogen bonds plays a central role in organic synthesis and represents one of the most challenging topics in modern organic synthesis.[92] Although many studies on this topic are available in the literature, the discovering of new routes could pave the way to design new complex synthetic targets that cannot be synthesized following classical pathways.[93] Over the years, direct metal-catalyzed C−H functionalization of unactivated aromatic compounds has emerged as a general, powerful, and attractive strategy for constructing a wider variety of C−C, C−N bonds.[94] Within this overall context, Chang et al., have developed a direct amidation of arene C−H bonds where sulfonyl azides have been used as the amino source releasing N_2 as the only byproduct.[95] Iridium(III) complexes are particularly effective catalysts for the activation of the C−H bond in the aromatic ring bearing weakly coordinating directing groups in the ortho position.[96] While these procedures represent a huge step forward compared to classical S_NAr reactions, most of the current protocols require substantial amounts of solvents, which significantly reduce their environmental sustainability. In 2016, Bolm et al., for the first time, reported an iridium(III)-catalyzed mechanochemical C−H bond functionalization process for the ortho-selective amidation of benzamides by using sulfonyl azides as the nitrogen source in a mixer mill.[97a] With the aim of optimizing the mechanochemical process, *N*-(*tert*-butyl)benzamide (**25a$_1$**) and phenylmethanesulfonyl azide (**26b$_1$**) were ground together (one milling balls, 1.0 cm diameter) with $[\{Cp^*IrCl_2\}_2]$ (2.5 mol %) and $AgBF_4$ (10 mol %) as the catalyst and AgOAc (10 mol %) as an additive for 99 min at 30 Hz to give the amidated product **27a$_1$b$_1$** in high yields (Scheme 27).

Then, this Ir(III)-catalyzed mechanochemical protocol was extended to various sulfonyl azides providing the corresponding derivatives **27a$_{1-12}$b$_{1-6}$** in yields ranging from 49% to 97% (Scheme 27). The reaction proceeds under solvent-free conditions without external heating, the active catalyst is formed in situ, and the amidated products were obtained after shorter reaction times than in solution. In general, this mechanochemical iridium(III)-catalyzed process constitutes an efficient and environmentally benign alternative to the conventional solvent-based procedures.

Scheme 22. Mechanochemical α-Aminonitrile Synthesis with Prebiotic Sources of Cyanide. Adapted with Permission from Ref 85. Copyright 2018 Wiley-VCH

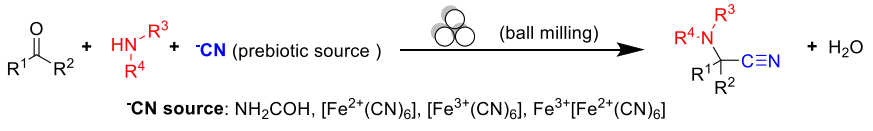

https://dx.doi.org/10.1021/acscatal.0c00142
ACS Catal. 2020, 10, 8344−8394

Table 9. Alternative Source for Generating Active CN^- Specie. Adapted with Permission from Ref 85. Copyright 2018 Wiley-VCH

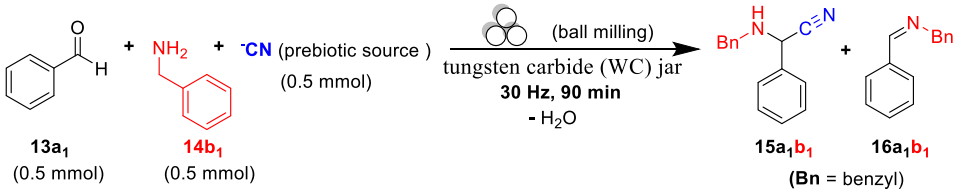

entry	additive	-CN source	ratio (%) of $15a_1b_1/16a_1b_1$
1	-	$K_4[Fe(CN)_6] \cdot 3\,H_2O$	3/97
2	-	$K_3[Fe(CN)_6]$	24/76
3	SiO_2	$K_4[Fe(CN)_6] \cdot 3\,H_2O$	49/51
4	SiO_2	$K_3[Fe(CN)_6]$	95/5
5	-	Prussian blue	16/84
6	SiO_2	Prussian blue	86/14

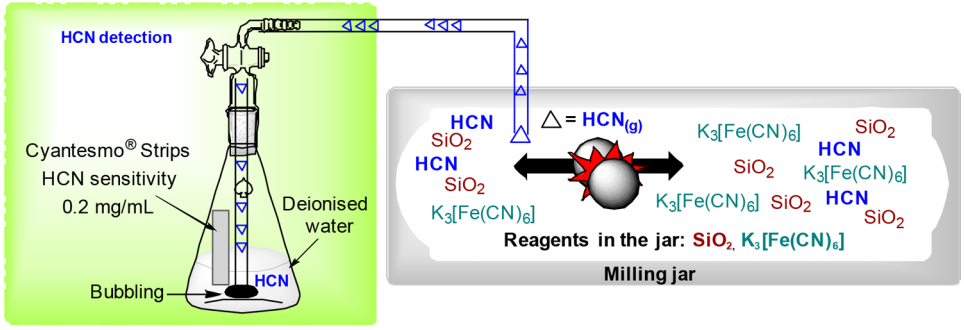

Figure 5. Grinding of $K_3[Fe(CN)_6]$ with SiO_2 by ball milling and formation of HCN. Adapted with permission from ref 85. Copyright 2018 Wiley-VCH.

Scheme 23. Scope of This Mechanochemical Strecker Reaction. Adapted with Permission from Ref 85. Copyright 2018 Wiley-VCH

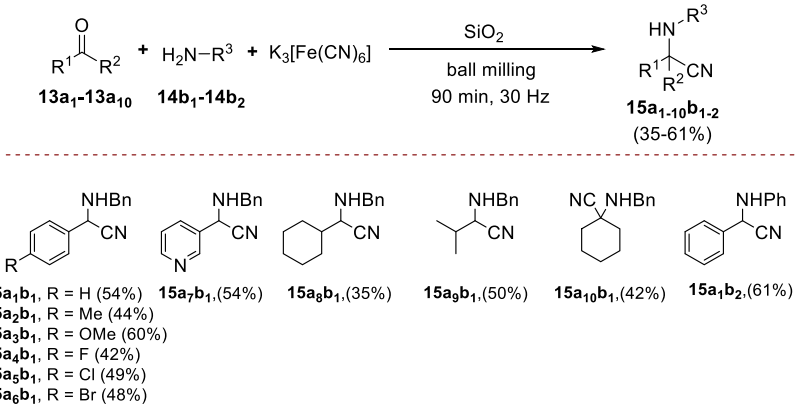

Along these lines, Bolm et al. reported a procedure for the direct mechanochemical rhodium(III)-catalyzed C–H bond amidation of arenes using 1,4,2-dioxazol-5-ones (dioxazolones) as the amidation reagents, where carbon dioxide is being formed as the sole byproduct.[97b] As a starting point, *N*-(*tert*-butyl)benzamide ($\mathbf{25a_1}$) and methyl-1,4,2-dioxazol-5-one ($\mathbf{28b_1}$) were milled for 99 min at 30 Hz with a combination of $[\{Cp^*RhCl_2\}_2]$ (2.5 mol %) and $AgSbF_6$ (10 mol %) as the catalyst and AgOAc (10 mol %) as an additive in a mixer mill to provide the amidated product $\mathbf{29a_1b_1}$ in 76% yield (Scheme 28). This mechanochemical protocol has been optimized by varying several experimental parameters such as the nature and/or the amount of the active catalyst as well as the additive and reaction time. The use of 5 mol % of the Rh(III) catalyst in combination with $AgSbF_6$ (20 mol %) and AgOAc (20 mol %) afforded the amidated product $\mathbf{29a_1b_1}$ in 97% yield. The

https://dx.doi.org/10.1021/acscatal.0c00142
ACS Catal. 2020, 10, 8344–8394

Table 10. Optimization of the Reaction Conditions of the Copper-Catalyzed A3 Coupling. Adapted with Permission from Ref 90. Copyright 2018 Wiley-VCH

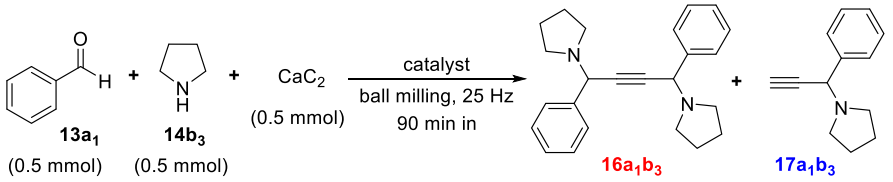

entry	catalyst (mol%)	conv. (%)	yield[a] (%): $16a_1b_3$/ $17a_1b_3$
1	-	-	-
2	CuI (20)	> 99	85/11
3	CuBr (20)	>99	85/10
4	CuCl (20)	83	47/46
5	$CuBr_2$ (20)	99	79/14
6	$Cu(BF_4)_2{\cdot}^6H_2O$ (20)	96	16/74
7[b]	CuI (20)	98	44/31
8[c]	CuI (20)	95	82/13
9	**CuI (10)**	**> 99**	88/12
10	CuI (5)	98	83/13
11[d]	CuI (20)	> 99	74/6

[a]Determined by ^{1}HNMR spectroscopy of the crude reaction mixture using 1,3,5-trimethoxybenzene as the internal standard. [b]Water (1.2 equiv) was added to the milling jar. [c]After 30 min of milling. [d]LAG reaction (MeCN); η = 0.25 μL mg^{-1}.

substrate scope of this mechanochemical protocol was investigated under optimized conditions by using various substrates bearing different substituents in para or meta position of the arene, and the results are illustrated in Scheme 28. To study the influence of the directing moiety group, the scope of the mechanochemical C−H amidation has been broadened significantly.

Generally, the desired ortho amidated products were isolated in good to moderate yields and in shorter reaction times than in solution. It is important to recognize that although the last two mechanochemical C−H bond functionalizations are efficient and complement classic methods for the C−N bond formation, the rhodium- and iridium-based complexes are rather expensive, especially when used on a macro scale. With the aim of replacing precious metal catalysts, Bolm et al. focused their attention on widely abundant and cost-effective first-row cobalt complexes having a high mechanical stress tolerance.[98] The overall design of the synthetic process is divided into two steps where the first process involves the in situ preparation of pentamethylcyclopentadienyl cobalt complex $Cp^*Co(CO)I_2$ [Cp^* = η^5-$C_5(CH_3)_5$], the catalyst and, second, the use of this organocobalt catalyst in mechanochemical C−H bond functionalizations (Scheme 29). Specifically, [$Cp^*Co(CO)I_2$] was applied in indol amidations with 1,4,2-dioxazol-5-ones as the nitrogen source under neat grinding in a mixer ball mill (Scheme 29). [$Cp^*Co(CO)I_2$] was prepared by milling together a mixture of dicobalt octacarbonyl and pentamethylcyclopentadiene (Cp^*H, under argon for 60 min at 25 Hz to provide the intermediate [$Cp^*Co(CO)_3$]. The milling jar was opened under argon, iodine was added, and grinding continued for an additional hour. ^{1}H NMR analysis confirmed the formation of [$Cp^*Co(CO)I_2$], which also highlighted that the cobalt complex was stable under the ball-milling conditions.

With this stable catalyst in hand, the authors next explored its utility in C−H mechanochemical amidation reactions. In the pivotal reaction, 1-(pyrimidin-2-yl)-1*H* indole ($\mathbf{10a_{18}}$) and 3-phenyl-1,4,2-dioxazol-5-one ($\mathbf{28b_4}$) (in a ratio of 1.0:1.5) were ball milled in the presence of 2.5 mol % of [$Cp^*Co(CO)I_2$], 5 mol % of silver hexafluoroantimonate ($AgSbF_6$) and NaOAc (5 mol %) as additive to afford $\mathbf{30a_{18}b_4}$ in 96% yield after only 99 min of milling at 30 Hz (Scheme 30). At ambient conditions, product $\mathbf{30a_{18}b_4}$ was isolated in comparable yields proving that the protocol also works under an aerobic atmosphere. After establishing the optimal reaction conditions for the mechanochemical C−H bond amidation, the substrate scope of indoles and dioxazolones was investigated, and the results are shown in Scheme 30. Interestingly, substantial differences were observed using alkyl-substituted dioxazolones $\mathbf{28b_1}$ and $\mathbf{28b_3}$, which afforded products $\mathbf{30a_{18}b_1}$ and $\mathbf{30a_{18}b_3}$ in low yields (Scheme 30), which is probably due to lower stability of these dioxazolones under the mechanochemical reaction conditions.

4.2. Mechanochemistry for C−C Bond Formation. In recent years, transition-metal-catalyzed hydroarylations of alkynes by innovative C−H bond activation have collected considerable interest because of their potential applications in the design of complex molecular architectures in a single run.[99]

https://dx.doi.org/10.1021/acscatal.0c00142
ACS Catal. 2020, 10, 8344−8394

Scheme 24. Substrate Scope for the Mechanochemical Synthesis of Symmetric 1,4-Diamino-2-butynes $16a_nb_m$. Adapted with Permission from Ref 90. Copyright 2018 Wiley-VCH

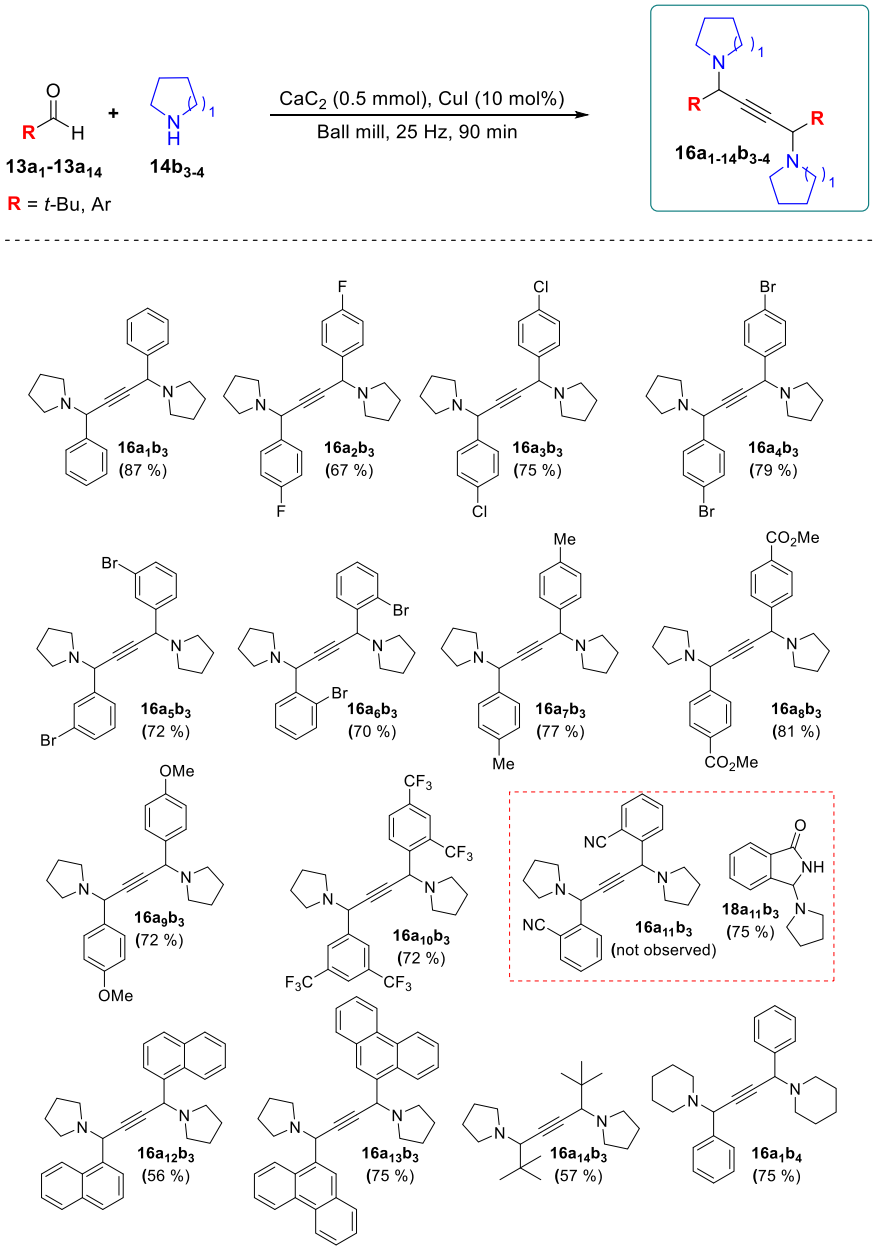

Ruthenium, rhodium, and cobalt complexes promote regio- and stereoselective ortho-alkenylations of aromatic rings bearing directing groups, in a simple and highly atom-economical fashion. Unfortunately, the activation of these catalytic systems, mainly with ruthenium-based catalysts, need a stoichiometric amount or even an excess of an organic acid, long reaction times, and high temperatures. To overcome all these shortcomings, Bolm et al. developed a grinding mechanochemical ruthenium-catalyzed hydroarylations of acetanilides with alkynes to afford trisubstituted alkenes in good to high yields and with high positional- and diastereoselectivity (Scheme 31).[100] The experimental conditions for the mechanochemical reaction were optimized by grinding for 99 min *N*-phenylacetamide (**31a**$_1$, 0.60 mmol) together with diphenylacetylene (**32b**$_1$, 0.72 mmol) in the presence of a mixture of $[RuCl_2(p\text{-cymene})]_2$ (5.0 mol %), pivalic acid (20 mol %) or copper acetate (20 mol %), and $AgSbF_6$ (20 mol %) as catalytic system (Scheme 31). In contrast to a similar reaction in solution, the mechanochemical hydroarylation occurs faster (99 min at 30 Hz vs ^{i}PrOH at 100 °C for 12 h), and oxidative cyclization toward indoles was utterly negligible. The scope of the reaction was successfully extended to a variety of electron-deficient and electron-rich substituted anilides, to study the influence of the substituents (Scheme 31). The optimized mechanochemical procedure preserved its efficiency and selectivity working well also with symmetric and nonsymmetrical alkynes, leading to good results as summarized in Scheme 31.

The mechanochemically prepared hydroarylation products were further converted into indoles through a palladium-catalyzed intramolecular oxidative annulation in a mixer a mill (Scheme 32).

In contrast to similar methods in the homogeneous phase, most of the procedures developed under mechanochemical

https://dx.doi.org/10.1021/acscatal.0c00142
ACS Catal. 2020, 10, 8344−8394

Scheme 25. Alkynylation-Type Reaction in a Ball Mill. Adapted with Permission from Ref 91. Copyright 2019 Wiley-VCH

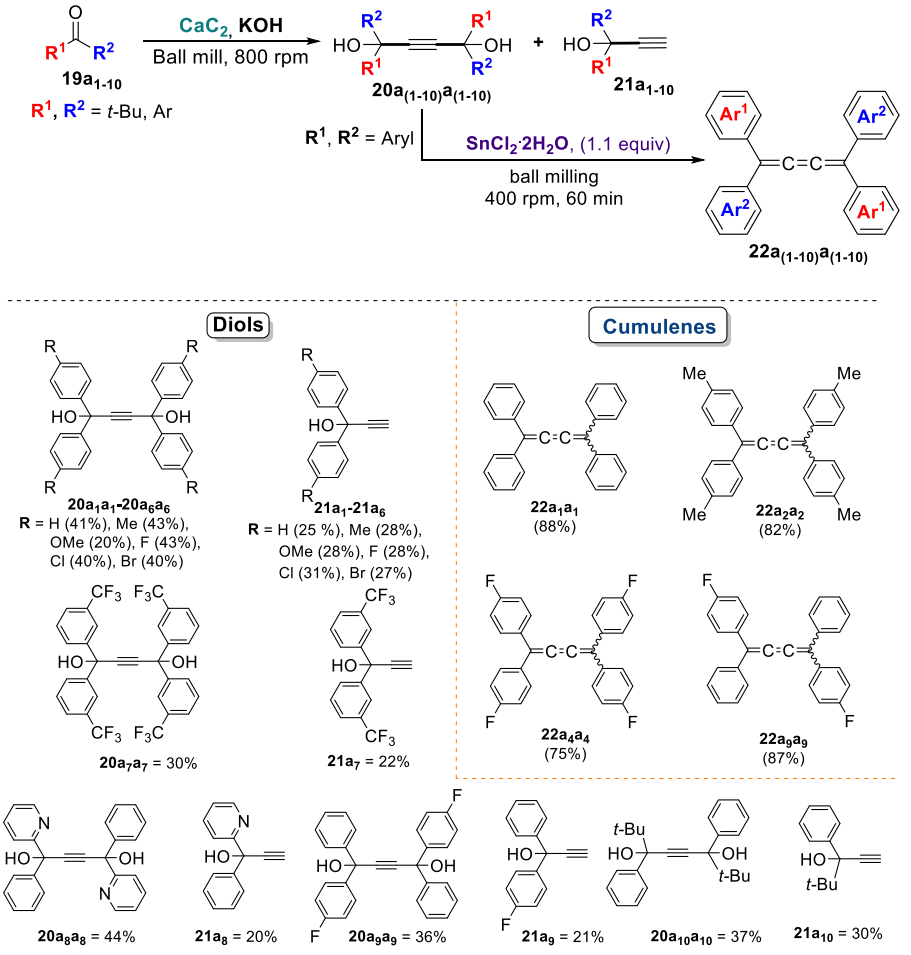

Scheme 26. Mechanosynthesis of [5]cumulene 24a$_1$a$_1$. Adapted with Permission from Ref 91. Copyright 2019 Wiley-VCH

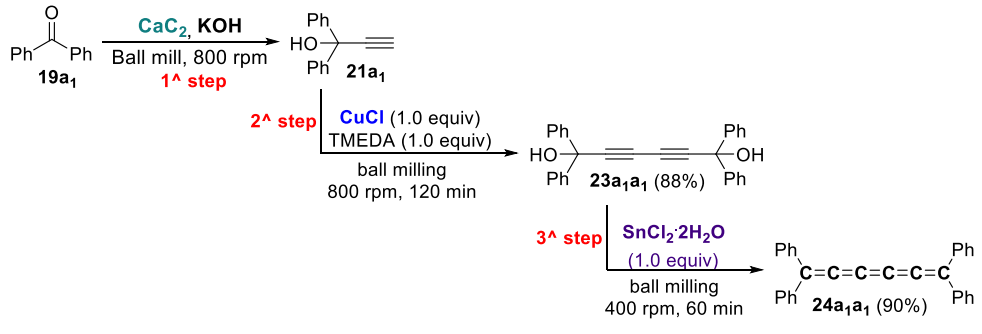

conditions drastically reduce or eliminate the use of organic solvents significantly shorten reaction time, giving better reaction yields. Nevertheless, the overall efficiency of the catalytic system remains comparable both in solution and mechanochemical protocols with, on average, the metal-assisted procedures under mechanochemical conditions requiring a higher load of metal complexes. Bolm et al. working in this direction developed an interesting mechanochemical procedure catalyzed by Rh(III) and Au(I) for the selectively C−H alkynylations of indoles at the C_2- and C_3-position, respectively (Schemes 33 and 34).[101] Both mechanochemical processes showed excellent functional group tolerance, were highly efficient, demanding significantly smaller quantities of catalysts and shorter reaction times than their solvent-based counterparts (Schemes 33 and 34). Also, the optimized protocol does not necessitate additional heating and works in mixer mills under an ambient atmosphere in solvent less conditions resulting in high product yields.

The substrate scope of the gold-catalyzed mechanochemical C−H alkynylation was also assessed by using unsubstituted indole (**10a$_{12}$**) in the coupling with **35b$_1$** (Scheme 34). This gold-catalyzed reaction provided **37a$_{12}$b$_1$** in 75% isolated yield along with a small amount (6%) of an undefined side-product. The optimized procedure has been successfully extended to other substrates as shown in Scheme 34.

The 2-arylindole substructure is a prominent motif present in a nearly ubiquitous range of biologically active compounds, and many of them are used frequently in medicinal and

https://dx.doi.org/10.1021/acscatal.0c00142
ACS Catal. 2020, 10, 8344−8394

Scheme 27. Substrate Scope of the Mechanochemical Ir(III)-Catalyzed C−H Amidation. Adapted with Permission from Ref 97a. Copyright 2016 Wiley-VCH

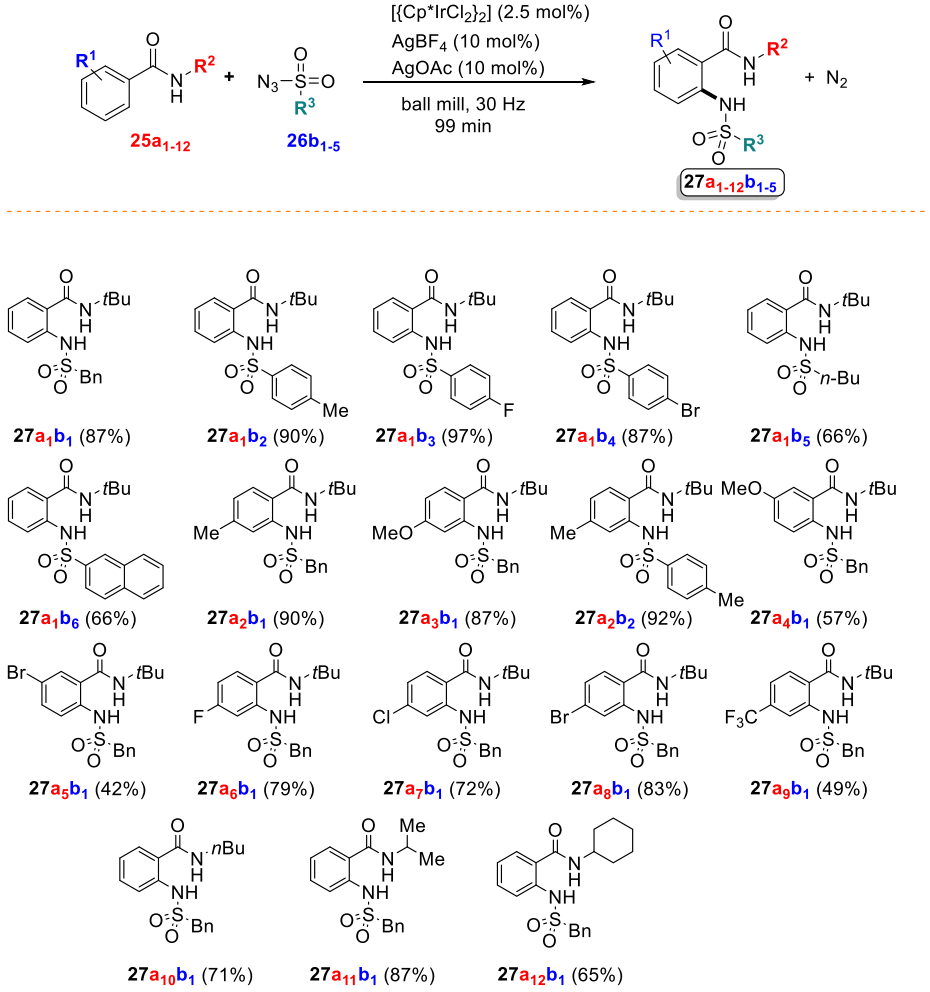

pharmaceutical chemistry.[102] The classical protocols for the decoration of the indole nucleus at C-2 position provide for the metal-catalyzed cross-coupling reaction between preactivated electron-rich indoles with functionalized arene derivatives such as aryl halides. However, most of the procedures adopted for the C-2 arylation have significant limitations in that they require capricious phosphine-based ligands, high temperature, additional steps for the activation of the indolic nucleus, and lack of selectivity (C-2 vs C-3) and atomic economy.[103] In two seminal papers, Sanford[104] and Larrosa[105] separately developed a phosphine ligand-free regioselective C-2 arylation of indoles in the presence of an acid, and under mild conditions. However, these procedures still have several drawbacks, and their scope, limiting their generalization, has caused researchers to develop other innovative strategies. In a work relevant not only from the significant results achieved but also from an academic perspective to the problem, Chatterjee, and Mainak Banerjee[106] developed a mechanochemical protocol for preparing synthetically useful 2-arylindoles by using Pd(II) catalyst in the absence of phosphine ligands.

At the outset, the model reaction has been fine-tuned by reacting *N*-methylindole (**10a**$_{13}$), with iodobenzene (**1a**$_7$) in the presence of $Pd(OAc)_2$ (5 mol %) as the catalyst in a RETSCH mixer mill (MM 400) at 30 Hz (Scheme 35). The oxidizing agent AgOAc (1.2 equiv), in combination with glacial acetic acid (0.5 equiv), also assisted this mechanochemical protocol. The reaction carried out in the presence of silica gel as grinding auxiliary went to completion after 1 h of grinding. Nevertheless, the recovery of the final indole **38a**$_{13}$**a**$_7$ by elution of silica with solvents, even polar ones, did not exceed 72%. The problem becomes even more problematic for the C-2 arylation of unprotected indole (**10a**$_{12}$), where the final isolated yields fell to 53% since a part of the product gets adhered to the solid matrix. The model reaction between **10a**$_{13}$ and **1a**$_7$ either under neat condition or using neutral Al_2O_3, Na_2SO_4, NaCl, and KCl as the milling auxiliary in place of silica gel did not go to completion even after prolonged milling, and a lower yield of **38a**$_{13}$**a**$_7$ was obtained. The use of 0.3 mL of PEG per mmol of indole derivative **10a**$_{13}$ allowed the investigators to overcome the recovery problem, affording the sole 2-phenyl-*N*-methylindole (**38a**$_{13}$**a**$_7$) in 91% yield with exclusive C-2 selectivity within 1 h (Scheme 35). The scope of the reaction was broad and the optimized mechanochemical conditions were suitable with a broad set of functionalities both in the indole and in the aryl iodide units, and the desired 2-arylindoles were achieved up to 99% yields (Scheme 35). Direct C-2 selective arylation of indoles was possible in both unprotected indoles and *N*-alkyl indoles, although with the former substrate, the reaction rate was relatively slower, and yields were a little less. Moreover, indoles with a deactivated five-membered ring provided 2-arylindole derivatives in high

https://dx.doi.org/10.1021/acscatal.0c00142
ACS Catal. 2020, 10, 8344−8394

Scheme 28. Mechanochemical Rh(III)-Catalyzed C−H Bond Amidation of Benzamides. Adapted with Permission from Ref 97b. Copyright 2017 American Chemical Society

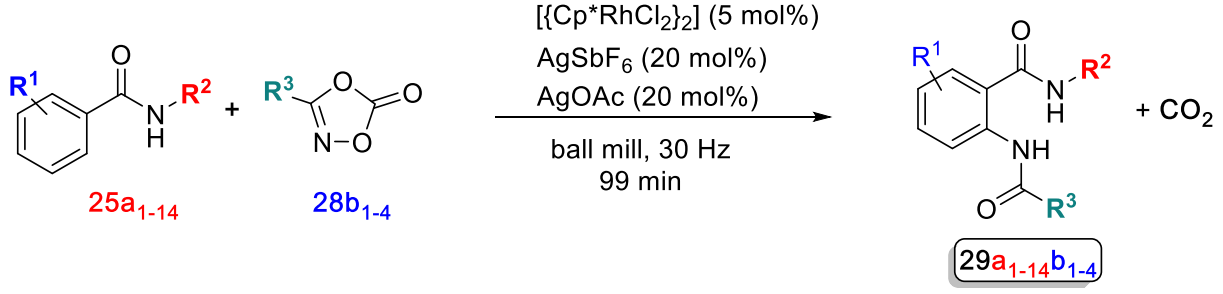

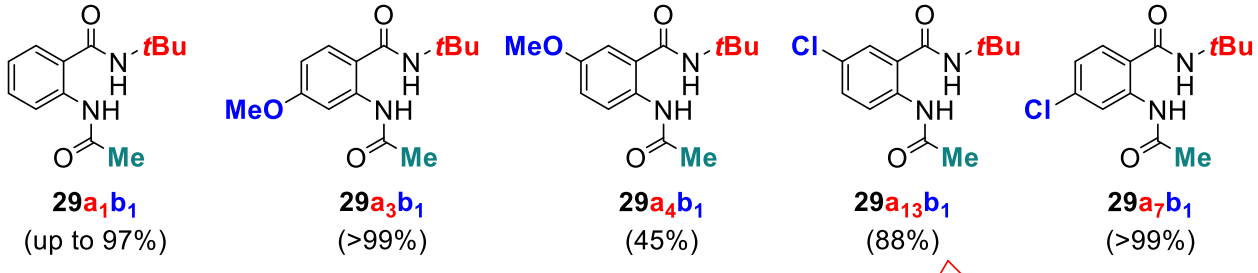

Scheme 29. Mechanosynthesis of [Cp*Co(CO)I$_2$] and Its Use in C−H Bond Activation by Milling. Adapted with Permission from Ref 98. Copyright 2018 Wiley-VCH

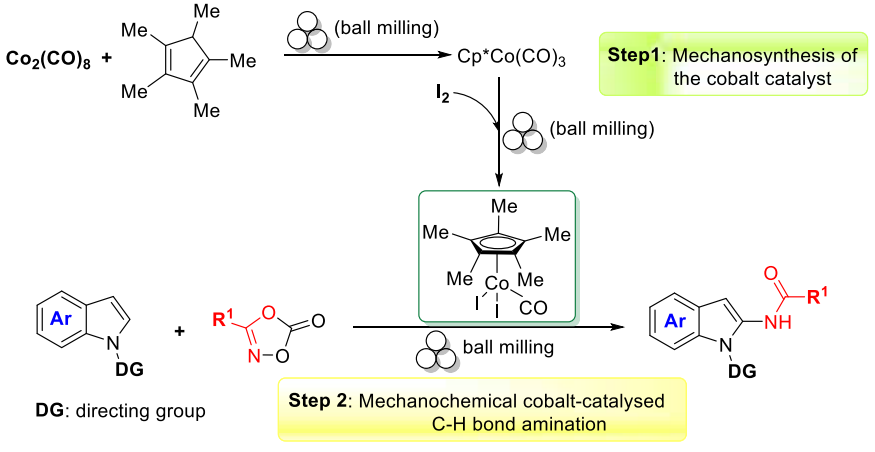

https://dx.doi.org/10.1021/acscatal.0c00142
ACS Catal. 2020, 10, 8344−8394

Scheme 30. Substrate Scope of Indoles and Dioxazolones in the Mechanochemical Amidation Process. Adapted with Permission from Ref 98. Copyright 2018 Wiley-VCH

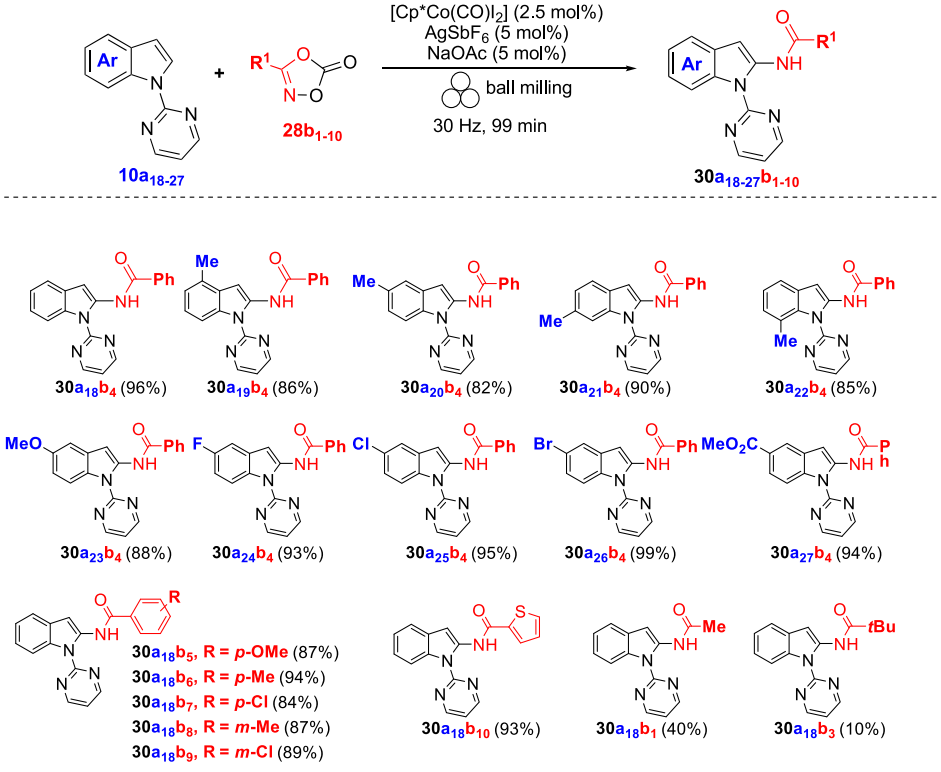

Scheme 31. Mechanochemical Ruthenium-Catalyzed Hydroarylations of Alkynes with Acetanilides. Adapted with Permission from Ref 100. Copyright 2017 American Chemical Society

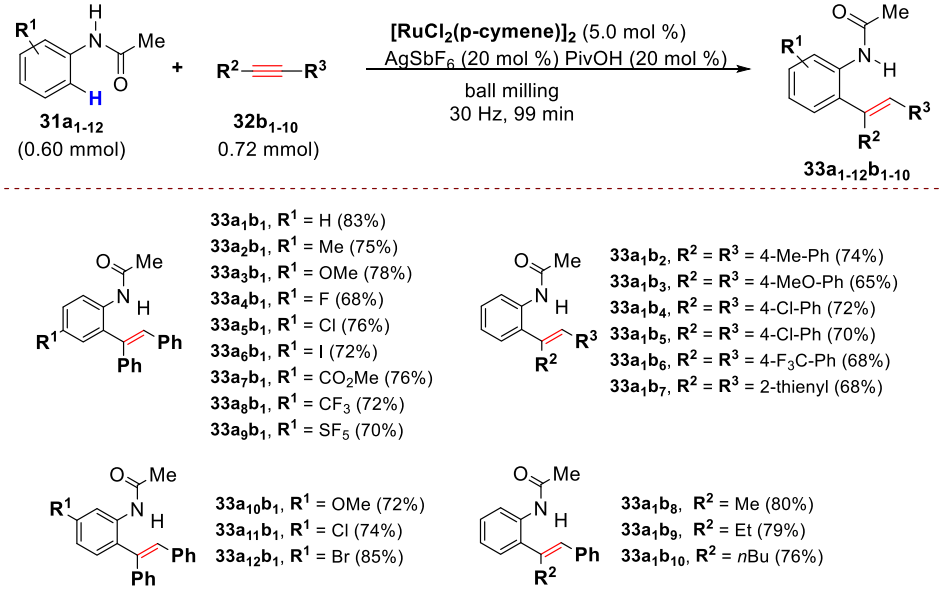

yields. The present mechanochemical method can also be successfully extended to gram-scale.

In this context, Su et al.[107] developed a mechanochemically induced synthesis of 3-acylindoles by a facile copper-catalyzed decarboxylative acylation of *N*-free indoles with α-ketonates via a liquid-assisted grinding (LAG) approach (Scheme 36). The addition of a catalytic amount of $Cu(OAc)_2 \cdot H_2O$ in the presence of O_2 as the terminal oxidant promotes the mechanosynthesis of various 3-acylindoles in high yields. Additionally, this mechanochemical protocol, which tolerates a wide range of functional groups, was also applicable to a gram-scale synthesis.

Boronic acids are among the most versatile, efficient, and widely used building blocks involved in the synthesis of relevant pharmaceutical scaffolds and new materials.[108] Although the synthetic routes for this class of compounds are well established, these protocols present serious concerns in terms of their environmental impact. Most of the procedures

https://dx.doi.org/10.1021/acscatal.0c00142
ACS Catal. 2020, 10, 8344−8394

Scheme 32. Mechanochemical Palladium-Assisted Synthesis of Indoles. Adapted with Permission from Ref 100. Copyright 2017 American Chemical Society

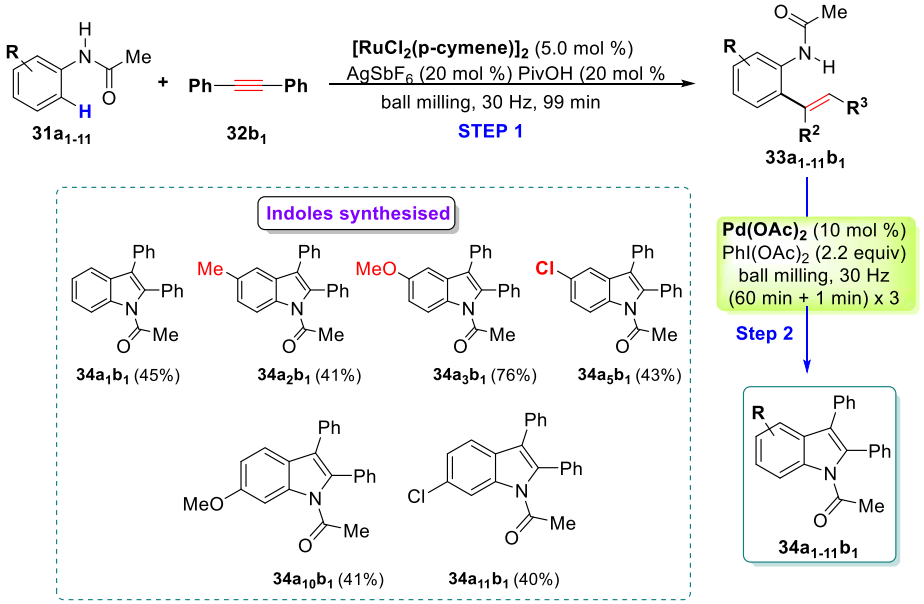

Scheme 33. Substrate Scope of the Mechanochemical Rh(III)-Catalyzed C−H Alkynylation. Adapted with Permission from Ref 101. Copyright 2018 Wiley-VCH

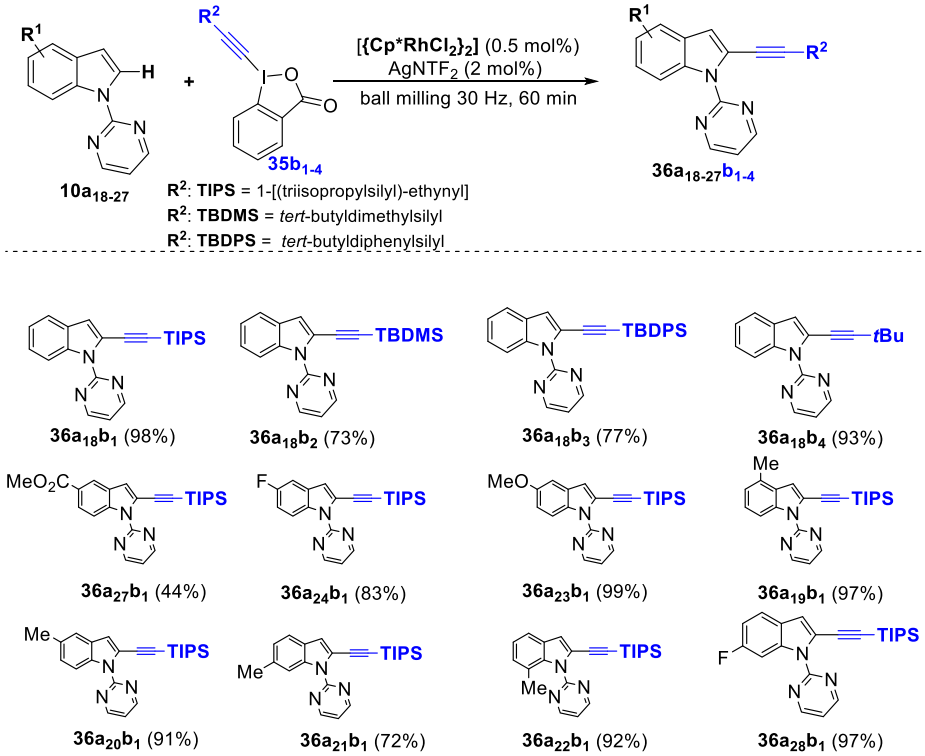

described in the literature require significant amounts of dry and degassed organic solvents, and they are carried out in anhydrous conditions under a nitrogen atmosphere, which are still important limiting factors. Compared with traditional solvent-based protocols, mechanochemistry allow avoiding harmful organic solvents, significantly shorten reaction time, and does not require external heating, opening new routes to different product compositions. In an important paper, Ito et al.[109] have applied mechanochemistry to iridium(I)-catalyzed C−H borylation reactions by using a diboron reagent (Scheme 37). This mechanochemical protocol was set up grinding indole **10a**$_{12}$ (1 mmol) with bis(pina-colato)diboron [(**pin**)-**B**-**B**-(**pin**), 0.6 mmol] in the presence of [Ir(OMe)cod]$_2$ (0.75 mol %) and 4,4′-di-*tert*-butyl-2,2′-bipyridine (dtbpy; 1.5 mol %) in a Retsch MM 400 mill in a stainless milling jar by using one stainless steel ball (Scheme 37). The results depend on the ratio of ball size/jar volume, and the borylation reaction performed better (NMR yield: 84%, isolated yileld: 59%) using

https://dx.doi.org/10.1021/acscatal.0c00142
ACS Catal. 2020, 10, 8344−8394

Scheme 34. Substrate Scope of the Mechanochemical Au(I)-Catalyzed C−H Alkynylation. Adapted with Permission from Ref 101. Copyright 2018 Wiley-VCH

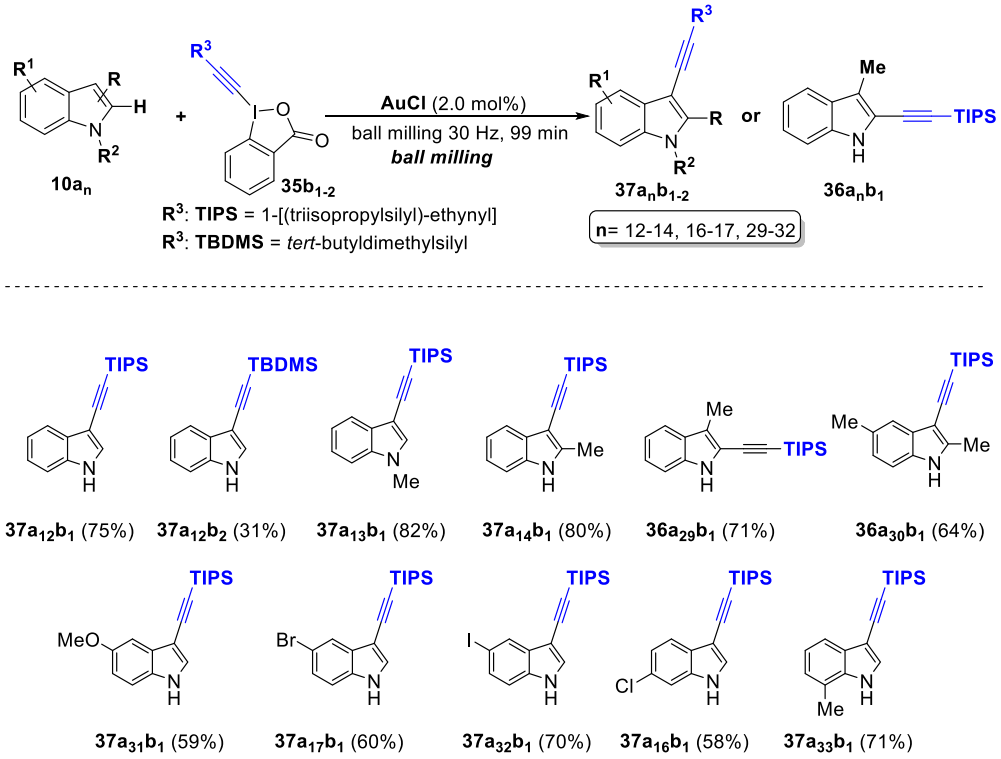

7.5 mm balls in a 5 mL jar and does not require the use of inert gas. Compared with traditional solvent-based protocols, where one or two of the boryl groups in the diboron reagent [$(pin)_2B_2$] might be inserted into the substrates, depending on the conditions applied, under the applied mechanochemical conditions, both boryl groups in (pin)-B-B-(pin) were available for inclusion in **10a$_{12}$**. This optimized mechanochemical procedure was extended to a variety of heteroaromatic compounds, giving the corresponding C2-borylated indoles in moderate to good yield with excellent regioselectivity (Scheme 37).

7-Methyl-substituted indole, pyrroles bearing ester (**42a$_1$**) and ketone (**42a$_2$**) moieties, did not provide the corresponding borylated product **40a$_{33}$**, **45a$_1$**, and **45a$_2$** due to drastic changes in rheology that did not allow the efficient mixing of the reactants and catalyst (Scheme 38). The use of LAG additive as DCM and THF (25 μL/mg of reactants) changed the resulting starting solid-state mixture to a viscous oil, allowing to overcome these issues. A comparison of the kinetic data of the model reaction conducted in solution or under mechanochemical conditions shows extremely interesting results. In THF solution, the reaction rate was initially high, decreased after 20 min, and was almost complete in about 90 min. Under mechanochemical conditions, the C−H borylation reaction did not proceed in the first 60 min but reached quick completion within 70 min following a sigmoidal kinetic. The reaction start was contemporary to the change of the physical state (rheological change) of the reaction mixture from a solid to a viscous oil of the reactive mixture. An induction period (60 min) is required to promote the formation of the catalytically active trisboryl iridium complex from the iridium precursor under mechanochemical conditions, and this might be another plausible explanation.

5. OTHER MECHANOCHEMICAL-ASSISTED PROCESSES FOR C(sp_2)−N BOND-FORMATION

Aromatic carbon−nitrogen bonds are among the most ubiquitous in functional materials and C−N bonds can be found in a plethora of molecules, which are key building blocks for preparing valuable pharmaceutical agents, agrochemicals, natural product, and polymers, among others. The Buchwald−Hartwig amination is one of the most robust and versatile oxidative coupling reactions for the formation of a carbon−nitrogen bond.[110] In recent years, numerous catalytic systems have been developed, expanding the scope and the range of amenable substrates. Despite the significant progress achieved so far, most catalytic systems are sensitive to air, which limits the reproducibility of the outcomes. The discovery and subsequent development of the PEPPSI series of catalysts by Organ et al. have represented a turning point to overcome the mentioned limitations.[111] Recently, automated ball-milling techniques made it possible to conduct reactions with low organic solvent content improving selectivity or differing reaction outcomes over solution results. Moreover, ball-milling procedures have allowed oxygen- and moisture-sensitive reactions to be successfully achieved. In 2018, Browne and co-workers merged with the Pd-catalyzed Buckwald−Hartwig reaction with a ball-milling strategy, observing very interesting results.[112] The referral reaction was fine-tuned by evaluating under ball-milling conditions the model coupling of morpholine (**14b$_5$**) with chlorobenzene (**1a$_7$**) in the presence of Pd-PEPPSI-^{i}Pent (1% loading) as a catalyst and using KOtBu as a base (Scheme 39). The reagents were weighed in the air, added to the jar, and then milled for 3 h without special precautions. The resulting cross-coupled product was obtained in 56% yield. These results were further enhanced up to 91%, improving the flowability and mixing of the reaction mixture by

https://dx.doi.org/10.1021/acscatal.0c00142
ACS Catal. 2020, 10, 8344−8394

Scheme 35. Substrate Scope of the Mechanochemical Pd(II)-Catalyzed C−H Arylation. Adapted with Permission from Ref 106. Copyright 2019 American Chemical Society

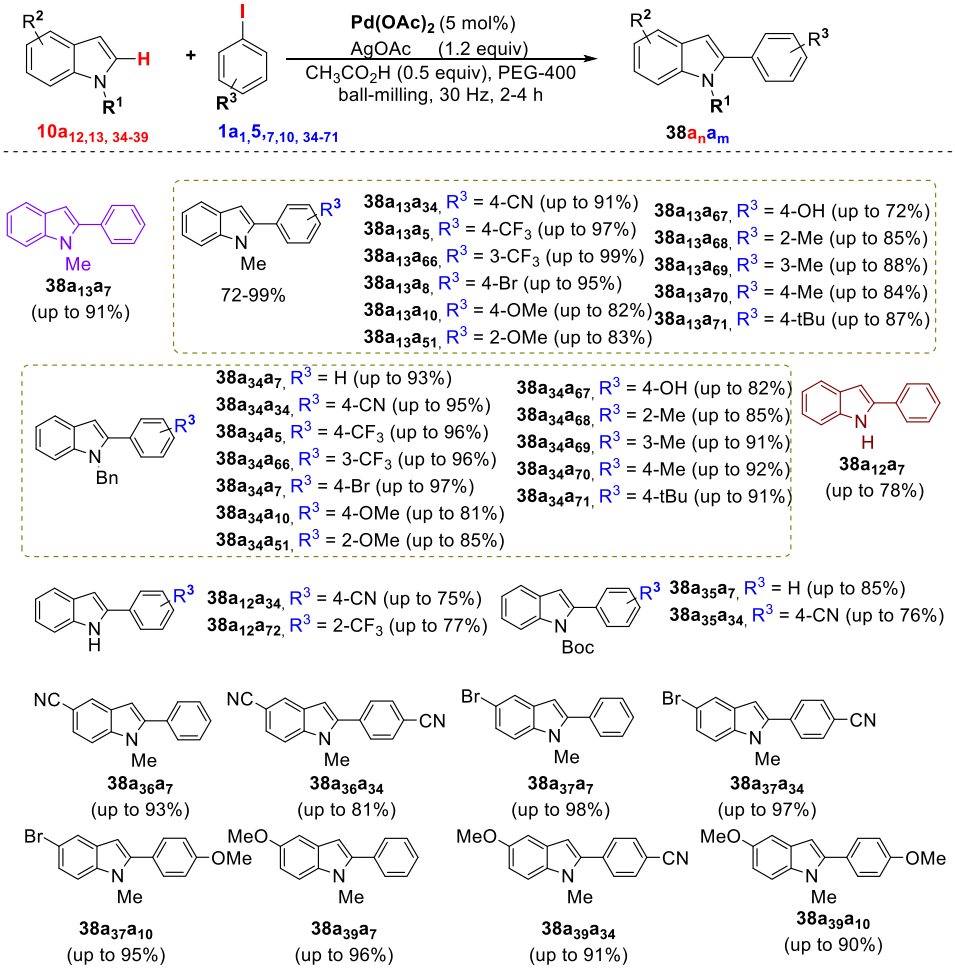

using 3 mass equivalents of sand. No appreciable improvement was observed by using other bases or catalysts, while halving the catalyst loading the reaction yield remained almost unchanged. However, a decrease in catalyst loading (up to 0.2 mol %) led to a significant increase in reaction times (up to 8 h). Once the author pointed-out the reaction, the procedure was extended to 15 aryl halides affording the products in moderate to excellent yield (32−91% isolated yields, Scheme 39). Afterward, a row of 14 secondary amines in place of starting and highly nucleophilic morpholine highlighted the robustness of the method (Scheme 40).

The amine scope of mechanochemical Buchwald−Hartwig amination showed that the reaction yields were dependent on the substrate evaluated. Conversely, this procedure failed with primary amines, and any attempted cross-coupling of aniline or octylamine with chlorobenzene **1a**$_7$ afforded the desired cross-coupled product in less than 5% GC yield.

Notably, Browne and co-workers examined the performance of the Buchwald−Hartwig reaction model carried out both under ball-milling and traditional aerobic solution conditions by comparing the experimental data. Among the tested solvents (including THF, 1,4-dioxane, and toluene), THF provided the best results affording the cross-coupled product in only 37% yield (Scheme 41). The authors justified these results hypothesizing that under milling conditions, the rate of C−N bond formation is faster, or the rate of catalyst degradation is slower relative to the solution phase.

In many cross-coupling processes described in the literature, at least one of the substrates is a liquid and could also act as a solvent for promoting reactions under neat conditions. The benefits of these solution-based reactions are now well-established, while solid-state palladium-catalyzed cross-coupling reactions remain an opened and motivating challenge for the research community. In this scenario, Ito et al. developed an efficient and scalable solvent-free procedure for solid-state palladium-catalyzed C−N cross-coupling reactions under mechanochemistry conditions.[113] Initially, the authors made a comparative study between the reactivity of liquid 1-bromonaphthalene (**1a**$_{79}$) and solid 1-bromopyrene (**1a**$_{24}$) in the palladium-catalyzed cross-coupling amination reactions with diphenylamine **14b**$_{18}$ using a solvent-free mechanochemical approach (Scheme 42). The C−N coupling reaction of liquid substrate **1a**$_{79}$ in the presence of the Pd(OAc)$_2$/XPhos (**P1**) catalyst system or the much more performing Pd(OAc)$_2$/*t*-Bu$_3$P (**P2**) gave the desired tertiary amine **49a**$_{79}$**b**$_{18}$ in a yield of 41% and 95%, respectively (Scheme 42). Pd(OAc)$_2$/^{t}Bu$_3$P (**P2**) exhibited high catalytic activities for the coupling of several other liquid aryl halides with diphenylamine **14b**$_{18}$, providing high yields. The results changed dramatically switching to a solid aryl halides such as 1-bromopyrene (**1a**$_{24}$) in the pivotal reaction by using either the Pd(OAc)$_2$/

https://dx.doi.org/10.1021/acscatal.0c00142
ACS Catal. 2020, 10, 8344−8394

Scheme 36. Decarboxylative Acylation of N-Free Indoles. Adapted with Permission from Ref 107. Copyright 2019 The Royal Society of Chemistry

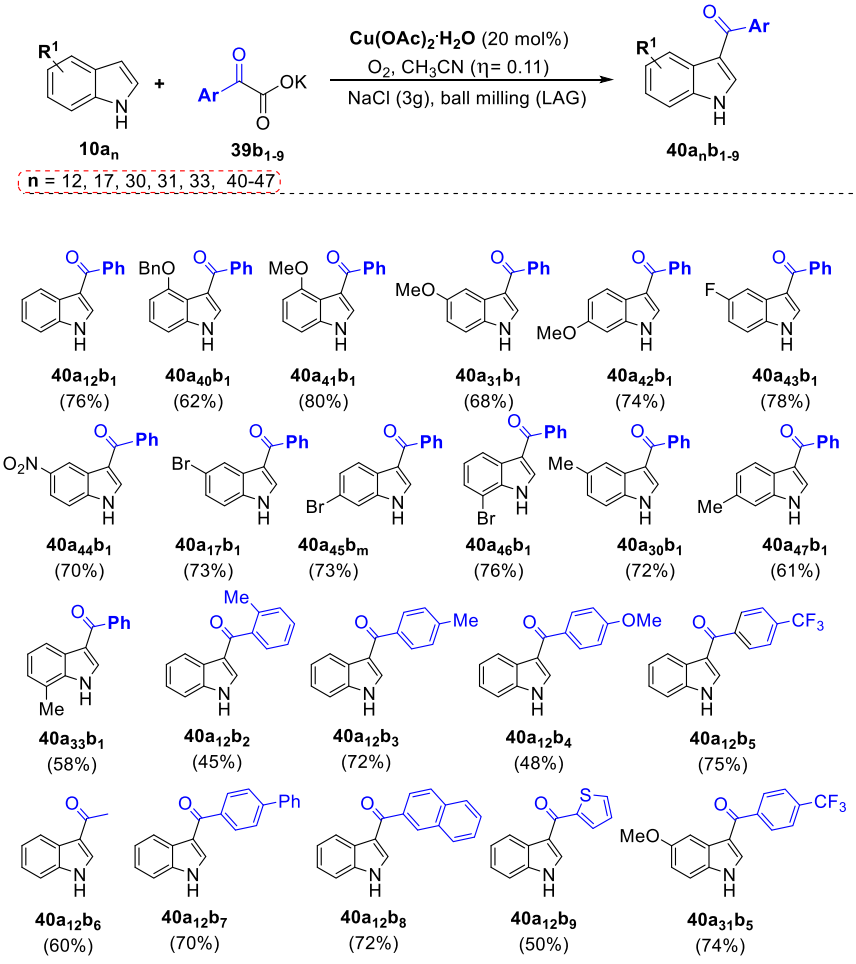

Scheme 37. Substrate Scope of the Mechanochemical C−H Borylation of Indoles. Adapted with Permission from Ref 109. Copyright 2019 Wiley-VCH

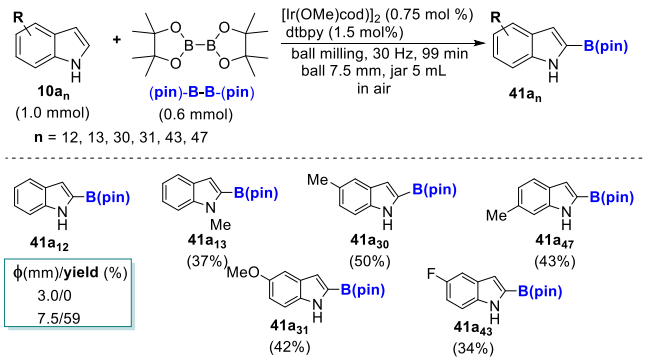

XPhos (**P1**) or the $Pd(OAc)_2/{}^tBu_3P$ (**P2**) catalyst system ($\mathbf{49a_{24}b_{18}}$, 3% and 28% yield, respectively, Scheme 42).

Ito et al. pointed out that in mechanosynthesis, there was a significant difference in terms of reactivity between liquid and solid aryl halides. Higher-performance catalyst systems for Hartwig C−N coupling in solution such as Ad_3P (**P3**), Cy_3P (**P4**) provided poor results of $\mathbf{49b_{24}b_{18}}$, 18%, and 0%, respectively. Increasing the amounts of the catalyst did not bring significant improvements. The addition of substoichiometric liquid additives (toluene, benzene, THF) into the jar slightly improved the reaction yield of $\mathbf{49b_{24}b_{18}}$ (20−55%). Cycloalkanes, unlike hexane, prevent catalyst deactivation because of the facile aggregation of the palladium catalyst in the solid-state and promoted more effectively the cross-coupling reaction (54% yield). The use of olefin additives (1,5-cyclooctadiene, cyclohexene, 1-hexene, (*E*)-hex-3-ene, etc.) as a dispersant for the palladium specie suppressed any aggregation of catalyst in the solid-state ($\mathbf{49b_{24}b_{18}}$, 96−99% yield). Transmission electron microscopy (TEM) images of the crude mixture with cycloocta-1,5-diene (1,5-cod) unequivocally showed the formation of palladium nanoparticles (3−5 nm) in the reaction mixture after 99 min of milling. Also, the coordination of palladium with the olefins accelerated the leaching rates for active monomeric Pd(0) specie from the palladium nanoparticles. The dissociated Pd(0) species were subsequently cached by $^tBu_3P$, releasing the olefin ligands to generate $[(t\text{-}Bu_3P)Pd(0)]$, which subsequently induced the activation of the C−X bond of aryl halides. Next, the scope of the reaction was extended to a broad set of aryl halides allowing the preparation of a wide range of functionalized triarylamines having large polycyclic hydrocarbon cores (Scheme 43).

The progress of the cross-coupling amination reaction between $\mathbf{1a_{24}}$ and $\mathbf{14b_{18}}$ in the presence of 1,5-cod was monitored in situ by the powder X-ray diffraction (PXRD) analysis. The temperature inside the milling jar after the grinding at 30 Hz for 60 min was about 30 °C, and only the

https://dx.doi.org/10.1021/acscatal.0c00142
ACS Catal. 2020, 10, 8344−8394

Scheme 38. Iridium(I)-Catalyzed C−H Borylation in Air by Using LAG Mechanochemistry. Adapted with Permission from Ref 109. Copyright 2019 Wiley-VCH

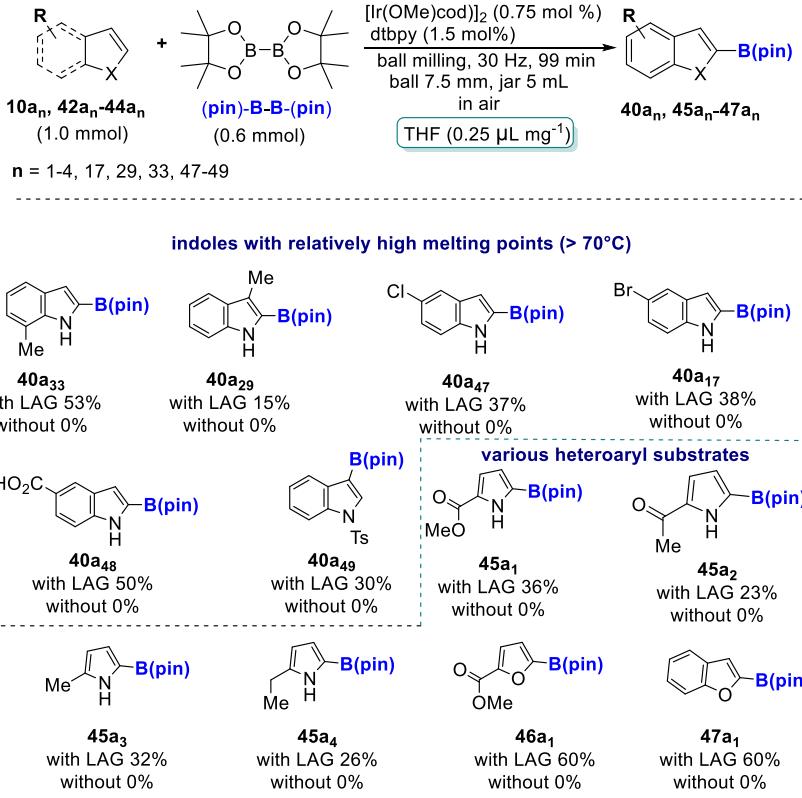

Scheme 39. Aryl Halide Scope of Mechanochemical Buchwald−Hartwig Reaction. Adapted from Adapted with Permission from Ref 112. Copyright 2019 The Royal Society of Chemistry

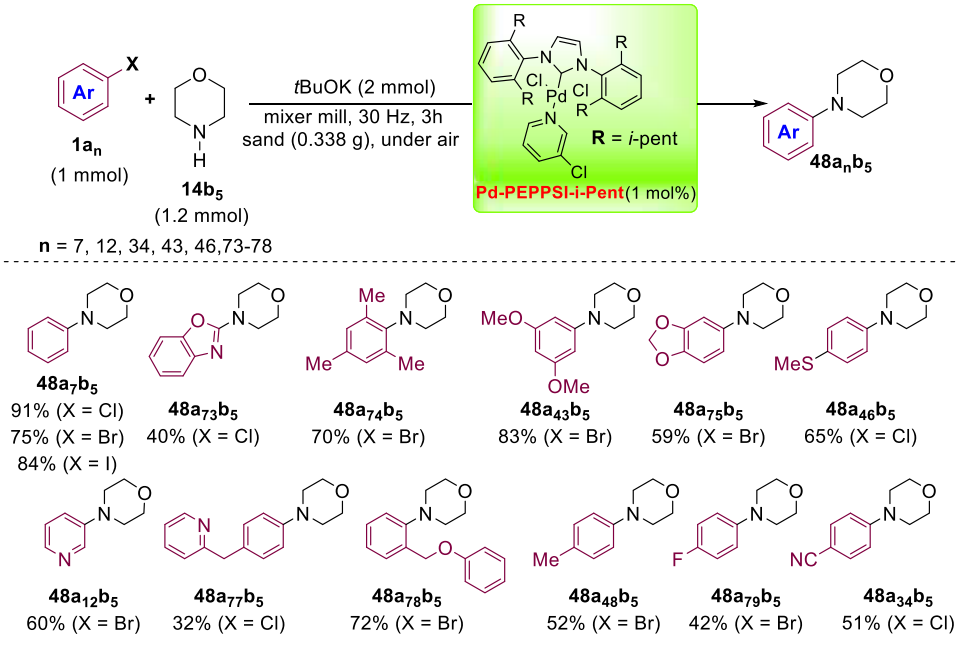

diffraction peaks of the coupling product **49a$_{24}$b$_{18}$** and NaBr were observed, clearly demonstrating that this reaction proceeded via a solid-to-solid conversion without melting. Notably, the debate between Ito and Mack on the determination of the critical parameters that promote the mechanosynthesis of some Buckwald−Hartwing reactions have been taken into account. In-depth studies of the issue pointed out that the model amination reaction, in the presence of 1,5-cod, follows simple first-order kinetics without noting any relevant changes in rheology. These results were confirmed by TEM analysis, which showed and further corroborated the formation of higher aggregates of dense palladium particles after grinding for 30 min.

https://dx.doi.org/10.1021/acscatal.0c00142
ACS Catal. 2020, 10, 8344−8394

Scheme 40. Amine Scope of Mechanochemical Buchwald–Hartwig Reaction. Adapted with Permission from Ref 112. Copyright 2019 The Royal Society of Chemistry

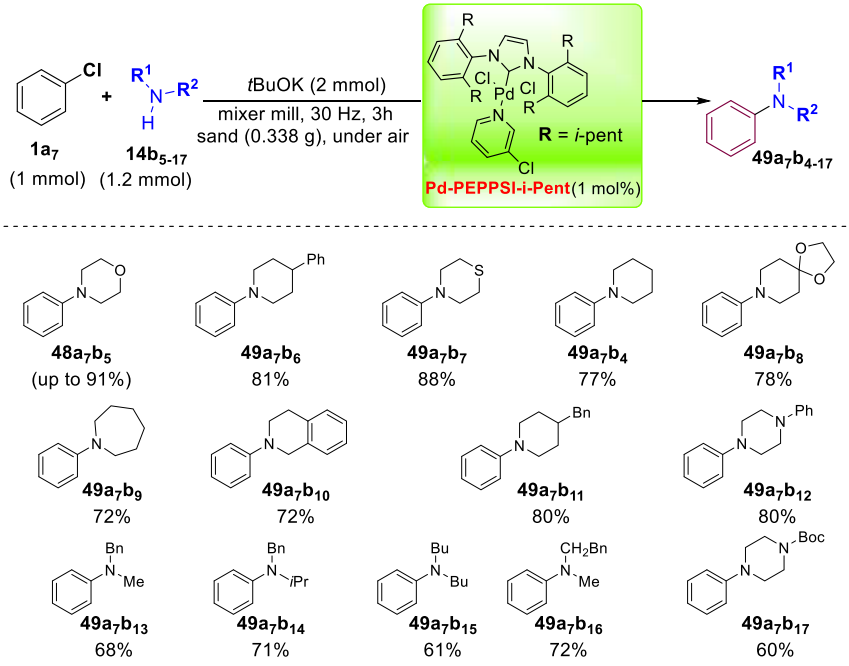

Scheme 41. Buchwald–Hartwig Reaction, Milling Vs Solution. Adapted with Permission from Ref 112. Copyright 2019 The Royal Society of Chemistry

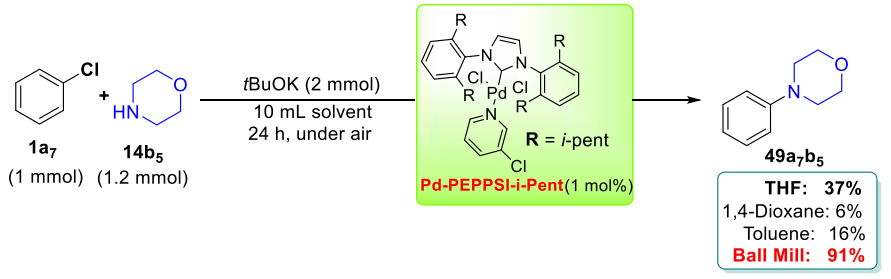

Scheme 42. Comparison of the Reactivity of Liquid and Solid Aryl Bromides. Adapted with Permission from Ref 113. Copyright 2019 Springer Nature

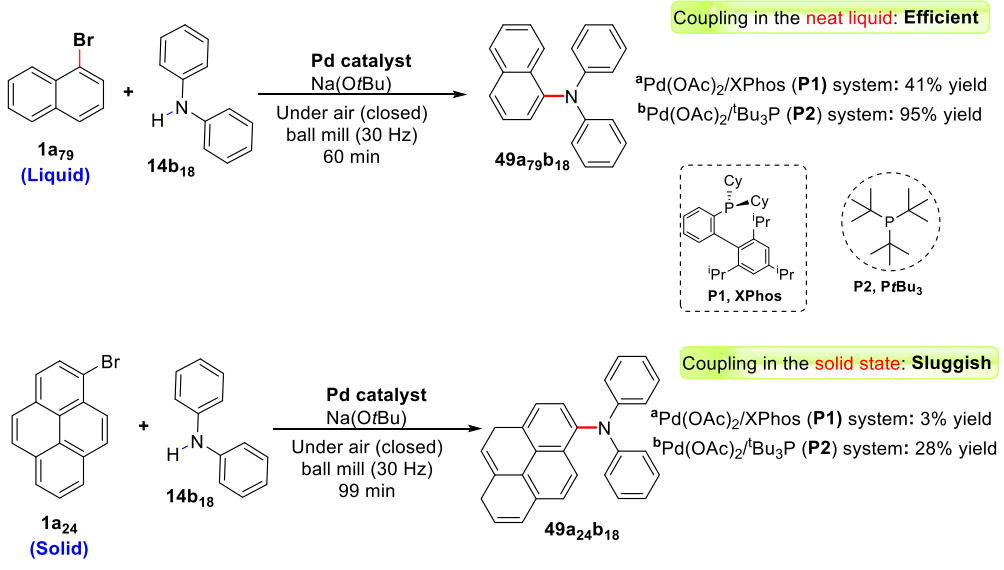

https://dx.doi.org/10.1021/acscatal.0c00142
ACS Catal. 2020, 10, 8344–8394

Scheme 43. Olefin-Accelerated Solid-State C−N Cross-Coupling Reactions. Adapted with Permission from Ref 113. Copyright 2019 Springer Nature

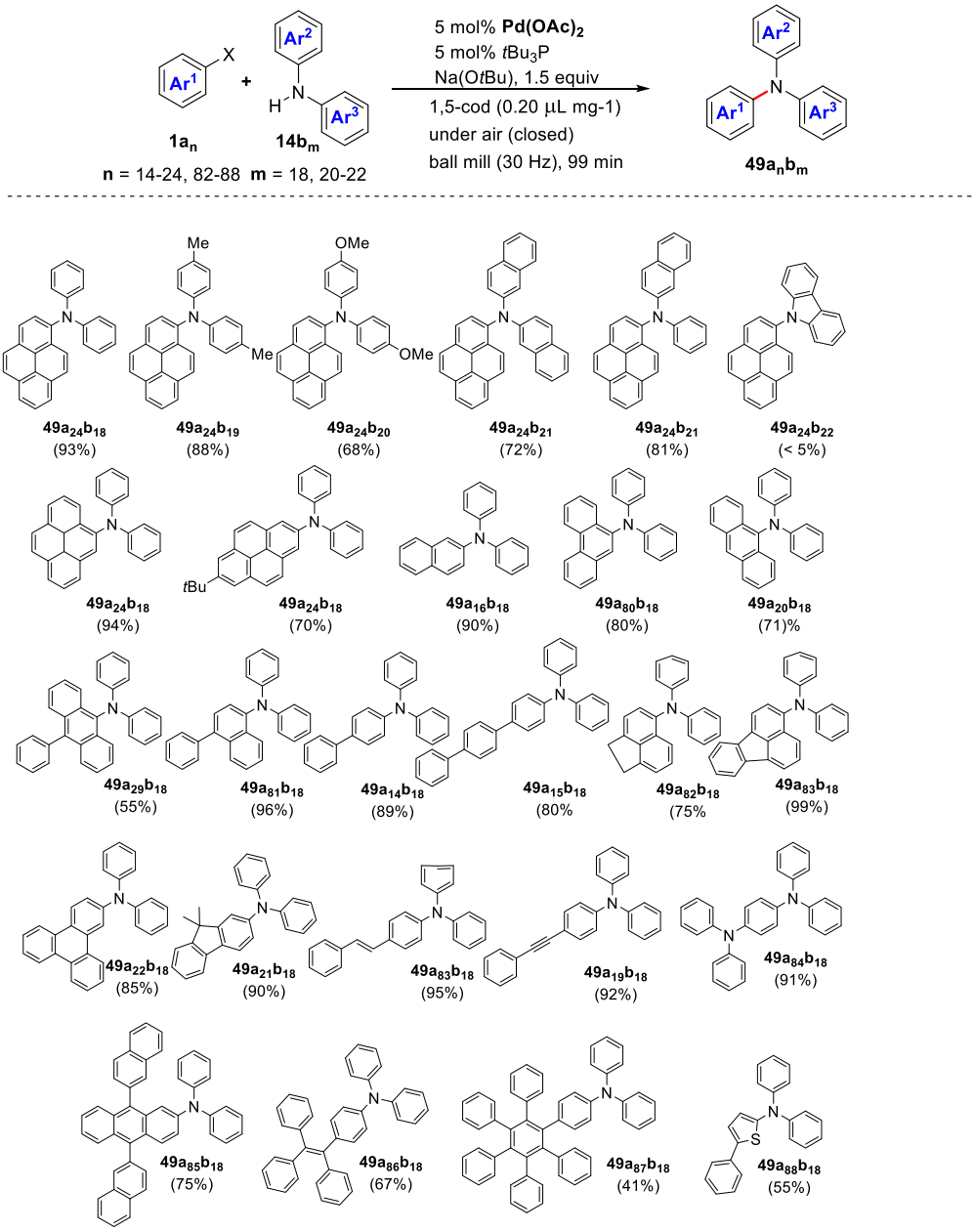

6. MECHANOCHEMISTRY FOR METAL-ASSISTED HETEROCYCLIC SYNTHESIS

Heterocycles play a key role in different sectors of chemistry, an essential core in medicinal chemistry,[114] and an essential building block in the preparation of materials chemistry, etc. Metal-assisted catalysis represents a powerful tool for designing and developing heterocyclic structures, even very complex ones. Nevertheless, the recovery of the metal complex, especially for homogeneous catalysis, is still today an open challenge. Heterogeneous catalysis in a solvent-free matrix is unquestionably an ambitious goal from an environmental impact point of view. James Mack et al., combining heterogeneous catalysis and mechanochemistry, succeeded in fully achieving this objective.[115] They developed a solvent- and ligand-free nickel-catalyzed [2+2+2+2] cycloaddition of alkynes that led to the formation of substituted cyclooctatetraene (COT) derivatives (Scheme 44). The procedure is simple, effective, versatile, inexpensive, and uses a recyclable Ni(0) source. The reaction was fine-tuned using ethyl propionate, and the best results were obtained milling the alkyne in a steel jar filled with nickel pellets that work as grinding balls. The conversion of $\mathbf{32a_8}$ to cyclooctatetraenes (COT) $\mathbf{51a_8}$-$\mathbf{51d_8}$ was 54% within 1 h and reached a maximum (94%) after 16 h (Scheme 44, entries 7 and 8).

Other combinations of both jar coating and grinding balls material resulted in less effective in terms of conversions and isolated yields (Scheme 44, entries 1−6 and 10−12). Unlike what has been reported in previous studies on solution chemistry, the major products are cyclooctatetraene isomers rather than substituted benzenes. This mechanochemical approach takes advantage of the ferromagnetic properties of nickel (0) pellets, which were easily separated from the

https://dx.doi.org/10.1021/acscatal.0c00142
ACS Catal. 2020, 10, 8344−8394

Scheme 44. Nickel Catalysis in a High-Speed Ball Mill. Adapted with Permission from Ref 115. Copyright 2016 American Chemical Society

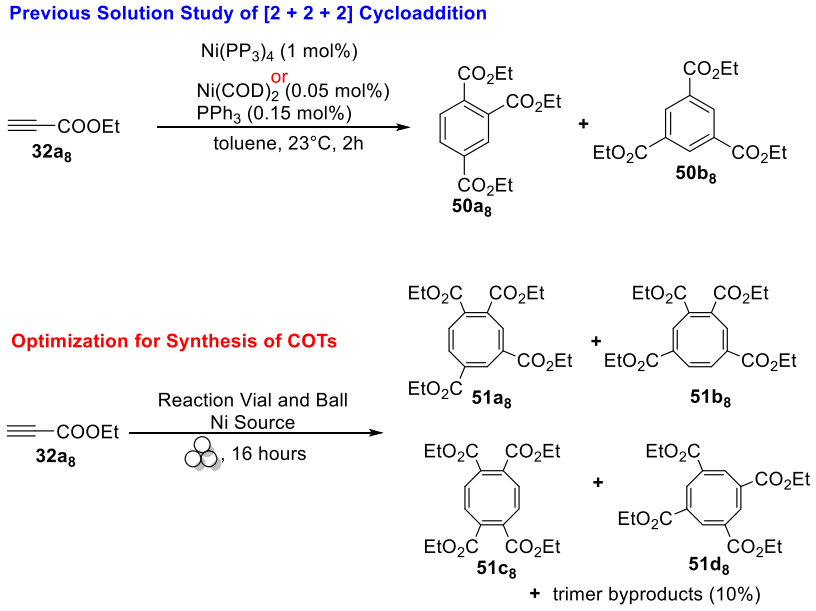

entry[a]	vial	ball	Ni source	time (h)	% conversion[b]
1	nickel	nickel	vial/ball	16	10
2	stainless steel	stainless steel	Ni foil	16	0
3	stainless steel	tungsten carbide	Ni foil	16	37
4	nickel	stainless steel	vial	16	28
5	nickel	tungsten carbide	vial	16	85
6	nickel	none	Ni pellets	1	39
7	stainless steel	none	Ni pellets	1	54
8	stainless steel	none	Ni pellets	16	94
9[c]	stainless steel	stainless steel	Ni powder	16	57
10	stainless steel	stainless steel	-	16	0
11	stainless steel	tungsten carbide	-	16	0
12	Teflon	Teflon	-	16	0

[a]Reactions were performed on a 2.48 mmol scale (250 μL). [b]Determined by ^{1}H NMR. [c]Multiple stainless steel balls were used to emulate nickel pellet conditions.

product mixture by using a strong neodymium magnet and recycled for later use. The scope of the reaction was successfully extended to a broader collection of terminal alkynes, and the results are summarized in Scheme 45.

Continuing this line of research, Coleman and Mack found that silver and copper foil inserted into a stainless steel (S.S) jar could function as an efficient heterogeneous catalyst for the cyclopropenation of terminal and internal alkynes under mechanochemical reaction conditions.[116] Despite the broad usefulness of cyclopropenyl-containing compounds, the harsh reaction conditions, nonrecoverable transition metal catalysts, poor atom economy, large volumes of solvent required, and slow syringe pump additions used in classical synthetic procedures have severely restricted access to this class of compounds. Mechanochemical heterogeneous transition metal-catalyzed [2+1] cycloadditions of unsaturated hydrocarbons (alkynes and alkenes) and diazoacetates into catalysts represent a general, robust, and straightforward methodology for the synthesis of these cycloadducts (Scheme 46).

The metal foil is switchable and can be recyclable at least 20 times without any appreciable drop in yield or diastereoselectivity without the need for fresh distilled solvent, inert gas to preserve the catalytic activity, or heat. In the same batch reactor, copper- and silver-foil were able to heterogeneously catalyze the cyclopropenation of internal and terminal alkynes, respectively, in excellent overall yields. The reactions occurred at room temperature and were completed after 16 h of grinding. This mechanochemical [2+1] cycloaddition has also

https://dx.doi.org/10.1021/acscatal.0c00142
ACS Catal. 2020, 10, 8344−8394

Scheme 45. Substrate Scope for Cycloaddition Reaction. Adapted with Permission from Ref 115. Copyright 2016 American Chemical Society

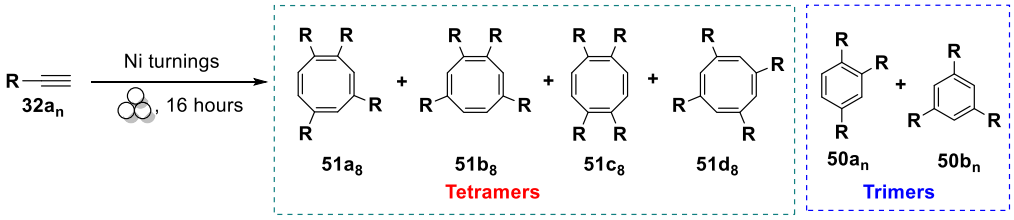

entry	alkyne	yield (%)	tetramer/timer ratio
1	CO_2Et	66	93/7
2	CO_2Me	68	98/2
3	$CO_2{}^tBu$	89	81/19
4	Ph	74	94/6
5	Ar-*p*(Me)	50	71/29
6	Ar-*p*(*t*Bu)	18	80/20
7	Ar-*p*(OMe)	42	15/85
8	Ar-*p*(F)	42	68/32
9	Ar-*p*(CO_2Me)	45	89/11

Scheme 46. Metal Foil-Catalyzed Cycloaddition of Unsaturated Hydrocarbons with Methyl Phenyldiazoacetate. Adapted with Permission from Ref 116. Copyright 2018 The Royal Society of Chemistry

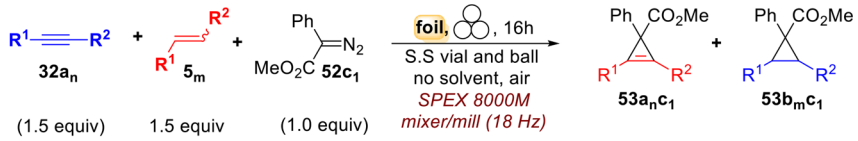

			Ag Foil		Cu Foil	
entry	R^1	R^2	yield (%)	(53a$_n$c$_1$ /53b$_m$c$_1$)	yield (%)	(53a$_n$c$_1$ /53b$_m$c$_1$)
1	Ph	H	91	2/98	92	65/35
2	*n*-Butyl	*n*-Butyl (*trans*)	80	75/25	40	15/85
3	*n*-Butyl	*n*-Butyl (*cis*)	83	70/30	48	10/90
4	Ph	CH_3 (*trans*)	90	55/45	86	15/85
5	Ph	CH_3 (cis)	90	55/45	88	15/85
6	Ph	Ph (*trans*)	80	95/5	30	5/95
7	Ph	Ph (*cis*)	82	90/10	42	5/95

effectively been used for cyclopropenation of unsaturated substrates containing unprotected amino and silyl groups that did not work in similar procedures in a homogeneous phase. The authors have also developed a versatile *one-pot* domino Sonogashira coupling/cyclopropenation solvent-free mechanochemical procedure as an organometallic-catalyzed three-component coupling of an aryl halide, terminal acetylene, and diazoacetate for the formation of complex cyclopropenes (Scheme 47).

The quinoline core is an important heterocyclic core present in many natural and synthetic compounds of pharmaceutical and biological relevance. For this reason, there is a growing interest in developing new synthetic protocols for preparing quinoline derivatives bearing diverse substitution patterns.[117] Although most of the procedures reported up to now in the literature are effective and efficient enough, they still have several limitations such as harsh reaction conditions, extended reaction times, tedious workup, and often they require the use of expensive catalysts or environmentally harmful solvents. In this context, Zhang et al. proposed and developed a straightforward methodology for the solvent-free synthesis of 2,4-diphenylquinolines via a one-pot reaction of anilines, benzaldehydes, and phenylacetylenes in the presence of $FeCl_3$ under solvent-free mechanochemical conditions.[118] This

https://dx.doi.org/10.1021/acscatal.0c00142
ACS Catal. 2020, 10, 8344−8394

Scheme 47. One-Pot Domino Sonogashira Coupling/Cyclopropenation Mechanochemical Reaction. Adapted with Permission from Ref 116. Copyright 2018 The Royal Society of Chemistry

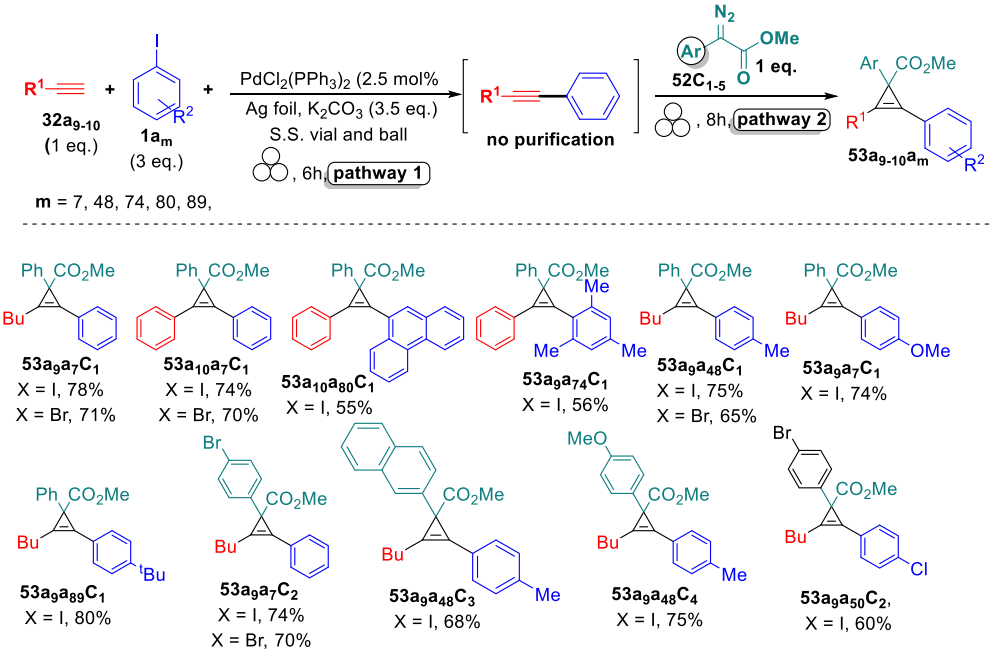

Scheme 48. Synthesis of 2,4-Diphenyl-quinolines $54a_nb_m$ via Imino Diels–Alder and Aromatization of In Situ-Generated Imine. Adapted with Permission from Ref 118. Copyright 2018 Wiley-VCH

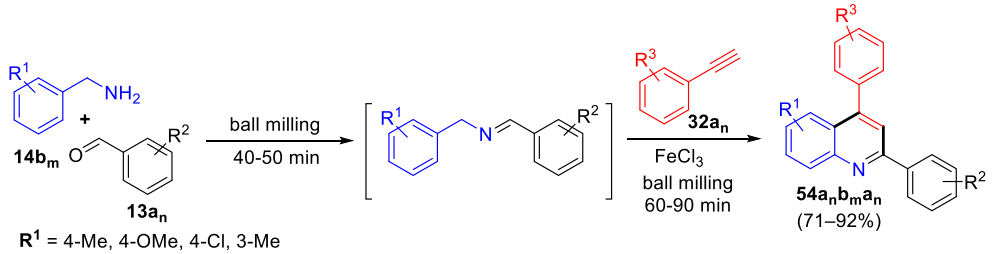

Scheme 49. Copper-Catalyzed Azide–Alkyne Cycloaddition under Mechanochemical Activation. Adapted with Permission from Ref 119. Copyright 2015 MDPI

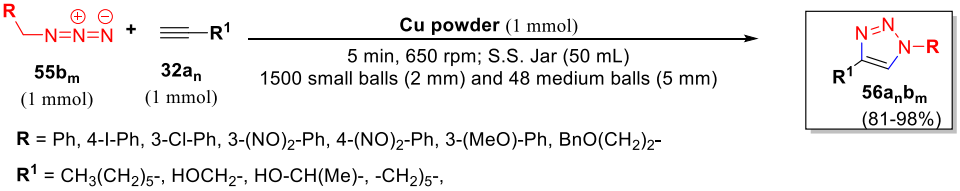

mechanochemical procedure allowed the synthesis of a series of 2,4-diphenylquinolines in good to excellent yield (74–95%) after a very easy workup avoiding any extraction or column chromatography workup (Scheme 48).

The Cu(I)-catalyzed alkyne–azide click reaction (CuAAC) is considered to be the "click chemistry" reaction par excellence, and in 2001, Sharpless coined this term. Cravotto et al. observed that the mechanochemical activation of metallic copper powder promotes solvent-free alkyne–azide click reactions (CuAAC).[119] They investigated and tuned a broad set of reaction parameters (i.e., milling time, revolutions/min, size, and milling ball number) that affect the outcomes of this mechanochemical click procedure significantly. Under optimized conditions, this eco-friendly procedure has been proven to be effective on a broad collection of different substrates, affording the corresponding 1,4-disubstituted 1,2,3-triazole derivatives in high yields and purities, after a simple filtration (Scheme 49).

In the same line, Raić-Malić and Užarević have successfully applied mechanochemistry in the CuAAC click reaction to prepare 6-phenyl-2-(trifluoromethyl) quinolines carrying *p*-halogen-substituted and nonsubstituted phenyl-1,2,3-triazole unit on the O-4 position of the quinoline core.[120] In comparison to the corresponding solution reactions, these Cu(II)-, Cu(I)-, and Cu(0)-assisted milling protocols proved to be significantly more efficient, with up to 15-fold gain in

https://dx.doi.org/10.1021/acscatal.0c00142
ACS Catal. 2020, 10, 8344–8394

Scheme 50. Synthetic Procedures for Preparation of *p*-Halogen-Substituted and Nonsubstituted Phenyl-1,2,3-triazole. Adapted with Permission from Ref 120. Copyright 2017 Beilstein Institute

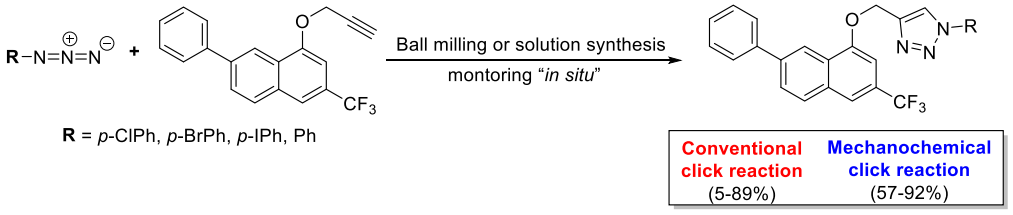

Conventional click reaction. **Method 1a**: $Cu(OAc)_2·H_2O$, CH_3OH, 60 °C, stirring for 3.5 h; **method 1b**: $Cu(OAc)_2·H_2O$, CH_3OH, 60 °C, stirring overnight; **method 1C**: CuI, DIPEA, acetic acid, CH_2Cl_2, rt, 3.5 h stirring. **Mechanochemical click reaction**. **Method 2a**: $Cu(OAc)_2·H_2O$, two stainless-steel milling balls (7 mm), PTFE vessel, 3.5 h, rt, 30 Hz; **method 2b**: CuI, DIPEA, acetic acid, two stainless-steel milling balls (7 mm), PTFE vessel, 3.5 h, rt, 30 Hz; **method 2c**: DIPEA, acetic acid, PTFE vessel, two brass balls (7 mm), rt, 3.5 h.

yield (Scheme 50). In situ monitoring by Raman spectroscopy of milling process in the presence of Cu(II) and Cu(I) catalysts highlighted the direct involvement of the copper species in the reaction and generation of highly luminescent compounds. On the contrary, in situ monitoring of the mechanochemical reaction by using Cu(0) catalysts in the form of brass milling media showed that the catalysis is most likely conducted on the surface of milling balls. The oxidation and spin states of the respective copper catalysts were determined by electron spin resonance spectroscopy.

7. MECHANOCHEMISTRY FOR REDOX REACTIONS

7.1. Mechanochemistry for Oxidation Reactions.

Redox reactions constitute the pillars of organic chemistry knowledge, and, together with substitution and elimination reactions, they also form the basis of the education of chemists. In this context, aldehydes/ketones, which are the oxidized forms of primary and secondary alcohols, likely are the most important and versatile building blocks in organic synthesis. Carbonyl compounds and alcohols represent the two sides of the same coin, with aldehydes and ketones that are reactive but unstable and toxic reagents. On the contrary, alcohols are rather stable and widely diffused in nature (biomass) but showed poor reactivity. Until a few decades ago, the selective oxidation of primary alcohols to aldehydes and secondary alcohols to ketones required the use of extremely toxic reagents, hazardous, and expensive having an extremely harmful environmental impact. The introduction of the stable 2,2,6,6-tetramethylpiperidine-1-oxyl radical (TEMPO) as the catalytic oxidizing agent by Anelli and Montanari has radically changed, from an environmental point of view, the synthetic route to aldehydes and ketones.[121] The classic Anelli–Montanari oxidation involves eco-friendly aqueous NaOCl (bleach) as a primary oxidant in a two-phase medium (CH_2Cl_2/H_2O) buffered at pH 8.5–9.5.[122] Over the years, bleach has been successfully replaced by many other co-oxidants, including the oxygen present in the air. Although these CuI/TEMPO-based procedures under ambient aerobic conditions are operationally simple and extremely useful, they require the use of considerable amounts of harmful solvents.[123] To address these issues, Porcheddu et al. have established an eco-friendly and cost-efficient TEMPO-based oxidative procedure for the selective air oxidation of primary and secondary benzyl alcohols to the corresponding aldehydes and ketones under ball-milling conditions.[124] In the control experiment, the active copper catalyst species was prepared by grinding together (1 min) 2,2,6,6-tetramethylpiperidine 1-oxyl (TEMPO, 3 mol %), 2,2′-bipyridyl (3 mol %), $[Cu(CN)_4]OTf$ (3 mol %) and 1-methylimidazole (NMI, 7 mol %) in a zirconia-milling beaker containing four balls (two balls × 5 mm Ø, two balls × 12 mm Ø) of the same material (Scheme 51). Then, 4-nitrobenzyl alcohol (**57a**$_1$, 2 mmol) was

Scheme 51. Mechanical-Assisted Alcohol-to-Aldehyde Oxidation. Adapted with Permission from Ref 124. Copyright 2017 Beilstein Institute

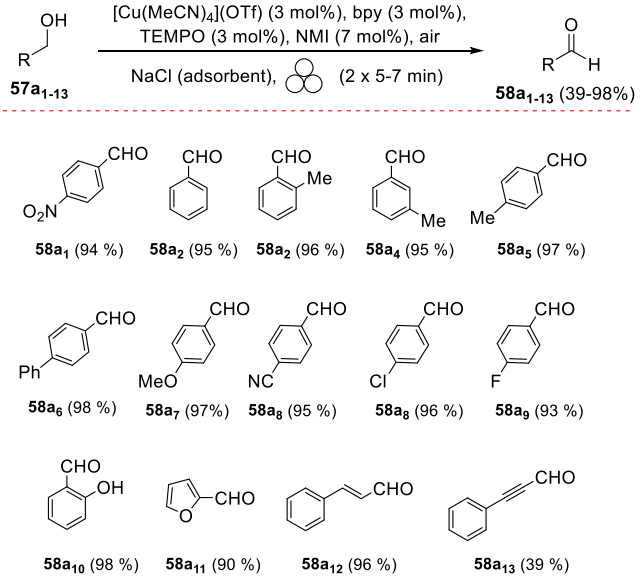

added, and the reaction mixture was subjected to two additional grinding cycles of 5 min, each followed by a break of 2 min leaving in the meantime the uncovered jar in open (10 min overall).

Under mechanical activation conditions, the alcohol-to aldehyde oxidation was faster (15 min overall) than that in solution (1 h), and the absence of any solvent makes the purification protocol easier. A library of common alcohols was efficiently and selectively oxidized to the corresponding carbonyl compounds in high yields and purities (Schemes 51 and 52). Aimed at eliminating or at least significantly reducing the use of metal catalyst and solvents, Porcheddu et al. have successfully used crystalline sodium hypochlorite (NaOCl·

https://dx.doi.org/10.1021/acscatal.0c00142
ACS Catal. 2020, 10, 8344–8394

Scheme 52. Mechanical-Assisted Alcohol-to-Ketone Oxidation. Adapted with Permission from Ref 124. Copyright 2017 Beilstein Institute

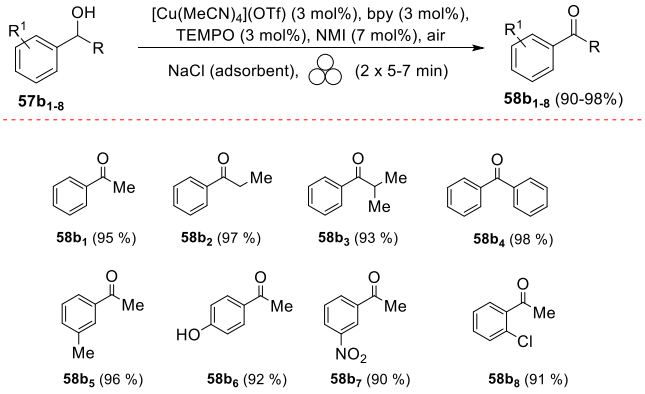

$5H_2O$) in the presence of TEMPO or AZADO (2-azaadamantane *N*-oxyl) to induce mechanochemical oxidative processes on several structurally different primary and secondary alcohols, without using any metal catalyst.[125] The proposed redox procedure is safe, inexpensive, and performed effectively in an Ertalyte jar,[126] whose material has never been used before in mechanochemical processes. Benzylic and aliphatic alcohols with different carbon chain lengths were converted to the corresponding aldehydes or ketones in good yields and no carboxylic acid derivatives were detected.

K_2FeO_4, that is, the hexavalent iron in the highest oxidation state (+6), is known for its environmentally friendly features as an oxidant agent. Ferrate (VI) has higher redox potentials than those of more commonly used oxidants such as $KMnO_4$, $K_2Cr_2O_7$, HNO_3, Cl_2, H_2O_2, O_3. Still, unlike the latter, its nontoxic reduction product Fe (III) is one of the most abundant metal ions on earth. Although the chemistry of ferrates (VI) has been known for over a century, its low solubility and instability in common solvents have severely hindered its applications. Ferrate (VI) salt remains stable for a long time in the as-prepared solid-state. At the same time, in the presence of a solvent, the outer surface will be gradually passivated by the resultant Fe (III), drastically reducing its oxidizing activity. Li et al. used mechanical milling to address the above issues, thus circumventing the problem of insolubility.[127] Moreover, the continuously crushing of the crystals generates new reactive fracture surface to expose into redox reactions. Mechanical milling of primary benzylic alcohols and aldehyde in the presence of a slight excess of ferrate (VI) in its "dry" solid-state enabled within several hours (2−18 h) their near quantitative oxidation to the corresponding acids in high yields (Scheme 53). This is in contrast to what is known in the literature regarding analogue reactions in solution, where ferrate(VI) did not oxidize aldehydes into acids. More significantly, the oxidation reaction of methyl-substituted benzaldehydes gave rise to dicarboxylic products (Scheme 54).

7.2. Mechanochemistry for Reduction Reactions. In organic synthesis, metal-assisted hydrogenations are one of the most effective and efficient classics reducing reactions from an atom economy and environmental point of view. Nevertheless, molecular hydrogen is derived from fossil fuels, and still today, transport, handling, and storage of this gaseous reagent suffer from safety concerns. The in situ generation of hydrogen gas in the minimum amount required for the reaction makes it

Scheme 53. A Solvent-Free Mechanochemical Way for Versatile Green Oxidation. Adapted with Permission from Ref 127. Copyright 2018 Wiley-VCH

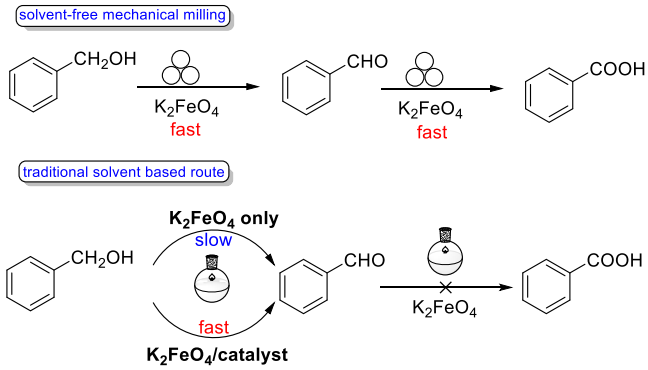

Scheme 54. General Procedure for the Mechanochemical Oxidation of Various Aromatic Aldehydes with Ferrate(VI). Adapted with Permission from Ref 127. Copyright 2018 Wiley-VCH

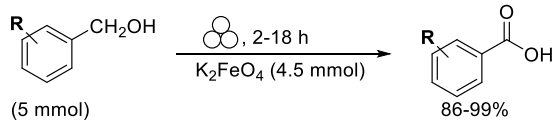

R = H, 4-Me, 2-Me, 3-Me, 2-F, 4-F, 4-OMe

possible to circumvent, at least partially, these problems. Following this approach, Sawama and Sajiki discovered that alkanes (e.g., *n*-pentane, *n*-hexane, etc.) and diethyl ether (Et_2O) generate the appropriate quantities of hydrogen gas by mechanochemical activation using a planetary ball mill stainless-steel (SUS304) equipped with stainless steel (SUS304) balls.[128] The in situ-generated H_2 in a SUS304 ball milling jar has been used for the successful hydrogenation of a variety of reducible functionalities (i.e., olefins, alkynes, and ketones). In particular, the use of pentane as a replacement hydrogen source promoted the reduction of the olefin moieties, while Et_2O was applicable as a pseudoreductant for the arene hydrogenation. Stainless steel (SUS304) utilized for the experiments were mainly composed of Fe (69%), Cr (18%−20%), and Ni (8−10%), but only the metals chromium and nickel play a key role in this process. Specifically, Cr promotes the hydrogen generation from the alkanes and Et_2O, while Ni metal acts as a reducing catalyst (Scheme 55).

Few metal complexes, as well as the Wilkinson's catalyst $[RhCl(PPh_3)_3]$ (WC), can claim such an important role in catalytic studies leading to several advances in that field. Historically, it has been the first catalyst used in the selective hydrogenation of alkenes and alkynes in a homogeneous liquid phase at room temperature and pressure. In 1965, Wilkinson et al. have synthesized for the first time $[RhCl(PPh_3)_3]$ as a red-purple crystalline solid by treating rhodium(III) chloride hydrate with an excess of triphenylphosphine in refluxing ethanol.[129] Single-crystal X-ray diffraction showed that the Wilkinson's catalyst adopts a slightly distorted square planar structure.[130] In the following, it was observed that the reduction of the amount of solvent during the synthesis of the catalyst led to the formation of a polymorphic orange form of the Wilkinson's catalyst **59** (Scheme 56). The thus-prepared catalyst adopts a square planar geometry with a more noticeable distortion toward tetrahedral coordination, in

https://dx.doi.org/10.1021/acscatal.0c00142
ACS Catal. 2020, 10, 8344−8394

Scheme 55. Stainless Steel-Mediated Hydrogen Generation from Alkanes and Diethyl Ether. Adapted with Permission from Ref 128. Copyright 2018 American Chemical Society

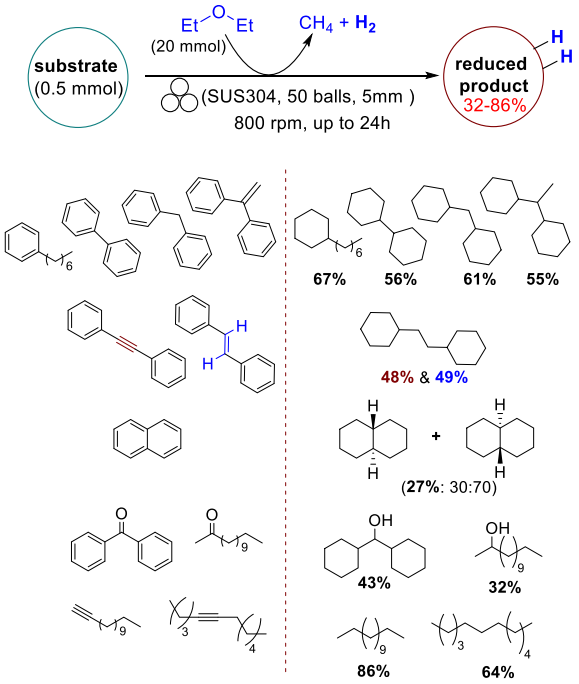

comparison to the red polymorph. In this contest, Hernandez et al. explored the mechanosynthesis of Wilkinson's catalyst $[RhCl(PPh_3)_3]$ employing both a net grinding and a LAG approach.[131] Grinding of a mixture of rhodium(III) chloride hydrate (1 equiv), PPh_3 (5.0 equiv), at 25 Hz for 90 min led to the formation of a pale orange solid. Under liquid-assisted grinding conditions [η = 0.25; η denotes the ratio of liquid additive to solid sample (μL mg^{-1})], ethanol or other superior alcohols afforded similar outcomes.

The removal of residual PPh_3 and Ph_3PO with a minimal amount of Et_2O gave an orange solid having ^{31}P solid-state NMR spectrum and X-ray analysis in agreement with previously published data for the orange polymorph of the Wilkinson's catalyst **59**. The mechanochemically prepared Rh-complex efficiently catalyzed a solventless dehydrocoupling of dimethylamine-borane ($Me_2N{\cdot}BH_3$) in a ball mill (Scheme 56), which occurred faster than its related solution-based counterpart. Under mechanochemical conditions, diborazane $[Me_2N{-}BH_2]_2$ in the presence of the Rh-complex **59** also promoted one-pot hydrogenation of olefins, using close to stoichiometric amounts of dihydrogen. The polymorph of the Wilkinson's catalyst used strongly affected the overall reaction efficiency of this mechanochemical Rh-catalyzed hydrogenation.

A FEW GENERAL REMARKS

The extensive review of the available literature on metal-catalyzed mechanochemical transformations carried out so far allows two main features to emerge. On the one hand, there is great promise that mechanochemical methods show for innovation within the framework of sustainable production of fine chemicals. On the other hand, there is a remarkable wealth of empirical information quickly built up during the recent and current burgeoning developments in the field.

Precisely the enormous interest attracted by the mechanocatalysis of metals and metal complexes is at the origin of the most evident limits that the studies carried out current present, that is, the general lack of a systematic approach to the investigation of mechanochemical transformations. Data scattered in several publications are obtained under different experimental conditions for very different classes of compounds, which significantly hinders proper comparison. Thermodynamic and kinetic factors can hardly be disentangled under these circumstances, and the same holds for truly mechanochemical effects.

Therefore, at the end of this Review paper, the challenge for readers can well be to become familiar with some of the most critical features of the metal-catalyzed processes developed by a mechanochemistry approach, sometimes overturning well-established beliefs for similar solution-based reactions.

Mechanochemical synthesis using ball milling has some indisputable advantages since the reactions occurred in the absence of potentially harmful, degassed, and dry solvents (neat or LAG milling), avoiding additional external heating and using very simple devices that do not require special skills. In contrast to a similar reaction with solvents, metal-assisted mechanochemical processes do not require an inert atmosphere, bypassing the sensitivity of reactions to aerobic conditions. Moisture does not compromise the final results, and of course, the process is not affected by reagent-solubility

Scheme 56. Mechanochemical Dehydrocoupling of Dimethylamine Borane and Hydrogenation Reactions Using Wilkinson's Catalyst. Adapted with Permission from Ref 131. Copyright 2018 The Royal Society of Chemistry

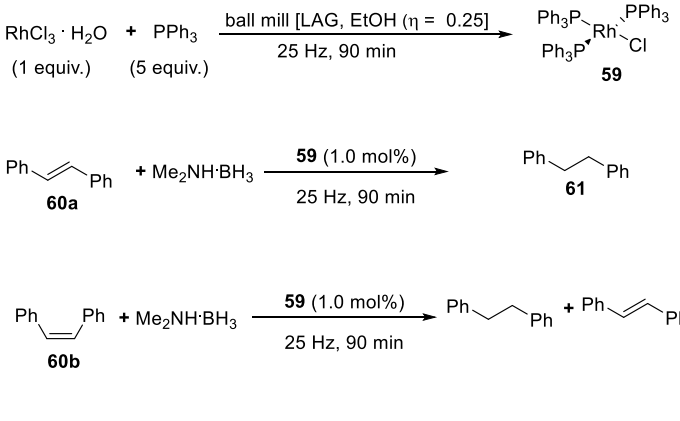

[RhCl(PPh$_3$)$_3$]	Yield
LAG WC	13%
RED WC	99%

[RhCl(PPh$_3$)$_3$]	61	60a
LAG WC	62%	30%
RED WC	77%	23%

https://dx.doi.org/10.1021/acscatal.0c00142
ACS Catal. 2020, 10, 8344−8394

issues.[132] Also, mechanochemically assisted reactions provide the desired products with yields comparable or even higher than those previously reported in the literature for similar systems in solution.

Intending to help the reader with the most convenient perspective in the critical analysis of the available literature and the planning of future research activities, we focus here on a few examples that allow some comparison between chemical reactivity under conventional and mechanical activation conditions. Although not wholly satisfactory, these examples will, hopefully, show the importance of deepening the insight into the reasons underlying experimental observations.

Working in this direction, Kubota et al. have proven that solvent-free mechanochemical synthetic techniques allow drawing a wide range of highly moisture- and oxygen-sensitive Buchwald-type phosphine-ligated palladium(II)-based oxidative addition complexes in air under mild conditions (Scheme 57).[133] In contrast to previously reported procedures for

Scheme 57. Synthesis of Palladium-Based Oxidative Addition Complexes Involving Moisture- and/or Oxygen-Sensitive Pd(0) Intermediates. Adapted with Permission from Ref 133. Copyright 2019 The Royal Society of Chemistry

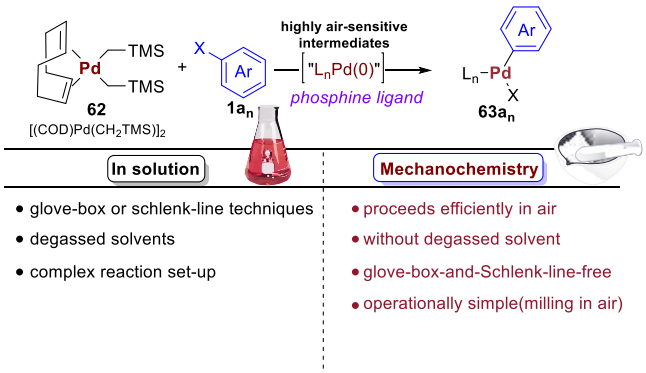

similar systems in solution, this protocol is operationally simple, scalable, and quick, avoiding the use of glovebox-and-Schlenk-line (Scheme 57).

To probe the usefulness of this mechanochemical methodology for synthesizing palladium-based oxidative addition complexes, Kubota initially has fine-tuned the reaction between the palladium precursor **62** and 1-bromopyrene $\mathbf{1a_{24}}$ in the presence of 2-dicyclohexylphosphino-2′,6′-diisopropoxybiphenyl (RuPhos), which is a routinely used Buchwald-type ligand. ^{1}H NMR analysis showed a conversion to the corresponding oxidative addition complex $\mathbf{63a_{24}}$ in moderate yield (40%) upon grinding for 30 min in air (Table11, entry 1). The authors found that better results were obtained by milling with a catalytic amount of liquid (LAG, Table 11, entries 3−12). At the same time, the addition of 0.20 μL of THF per mg of reactant drastically reduced the reaction time to 10 min and significantly improved the yield of $\mathbf{63a_{24}}$ (71% yield, Table 11, entries 3 and 16).

The optimized conditions were successfully applied to electron-rich (35−57%) and -poor aryl bromide (60−76%), heteroaryl bromides such as indole (49%), thiophene (78%), dibenzofuran (51%) derivatives, and polybrominated aromatics (61−88%) for further evaluation of the substrate scope. The authors also provide a comparative study of the performance of solution-based and mechanochemical reactions (Scheme 58). This framework can be used to demonstrate the efficiency and enormous potentiality of mechanochemistry procedures. In this regard, the oxidative solution-based addition of $\mathbf{1a_{22}}$ under a nitrogen atmosphere, using cyclohexane or THF as solvents, gave $\mathbf{63a_{22}}$ in 61% and 87% yield, respectively. However, when the same reactions were realized, exposing the reagents to air the reaction yields have dropped dramatically (8% and 46%, respectively). On the contrary, the mechanochemical oxidative addition of the model reaction, even in air, gave efficiently the desired product $\mathbf{63a_{22}}$ in high yields (92%). These and other studies[134] published in the literature allow assuming that gaseous oxygen does not efficiently diffuse through crystalline or amorphous solid-state reaction mixtures as a result of the low impact of atmospheric oxygen on this moisture- and/or oxygen-sensitive substrates.

For over a hundred years, Grignard reactions have been part of the toolkit of both academic and industrial chemists in the design of new molecular geometries. The classical and direct procedure for preparing Grignard reagents involves the reaction between elemental magnesium and an organic halide, usually in a dry ethereal solvent. All commercial-grade solvents[135] were dried under nitrogen and over an alkali metal (e.g., sodium or potassium) using benzophenone as a dryness indicator and distilled prior to use.[136] The drying process of an organic solvent is an important topic in the first years of study at university. However, as simple as the procedure may seem, there are many examples of unfortunate accidents, including fatal ones, in chemical laboratories around the world. In this framework, Mack et al. have explored some mechanochemical methods for preparing Grignard reagents without special precautions to remove moisture in the air.[137] The reaction between a 3 M ether solution of methyl Grignard (MeMgBr) and 4-bromobenzophenone $\mathbf{58b_9}$ in a stainless-steel jar previously charged with a 1/8 in. stainless steel ball gave 1-bromo-4-(1-phenylethenyl) benzene $\mathbf{57b_9}$ (42% conversion) and 1-(4-bromophenyl)-phenylethanol $\mathbf{5b_{32}}$ (58% conversion) after milling for 1 h (Scheme 59). In a separate Grignard experiment, the same reaction was repeated using the methyl Grignard obtained by evaporation of Et_2O, which results in a slurry. Interestingly, the 17 h milling of the Grignard reagent with 4-bromobenzophenone ($\mathbf{58b_9}$) yielded the 1-bromo-4-(1-phenylethenyl) benzene ($\mathbf{5b_{32}}$) as the major product instead of being quenched by moisture in the air (Scheme 59).[138] Mack claims that the only water present in a 5 mL jar used during the milling reaction is contained in small concentration both in the reactants and/or in the air before the vial is sealed.

The authors estimate that the jar used for their reactions contained a quantity of water altogether in the order of a few ppm, that is, the same level water present in a dry solvent commonly prepared in a laboratory. They assumed that during mechanochemical impacts inside the reaction jar, the gaseous elements (vaporous water and oxygen) simply slipping past the ball and never react with any of the other components in the reaction beaker as depicted in Figure 6 and Figure 7.

On the base of a recent study aimed at improving the general preparation of Grignard reagents in a ball milling, Harrofield et al. observed that a 4-fold excess of magnesium is needed to obtain a manipulable solid, instead of an intractable paste.[139] There is at present still enormous research interest in this topic and our understanding move at a considerable speed. The strength of the C−F bond makes the direct preparation of Grignard reagents extremely challenging by reacting elemental

https://dx.doi.org/10.1021/acscatal.0c00142
ACS Catal. 2020, 10, 8344−8394

Table 11. Optimization of the Reaction Conditions[a]

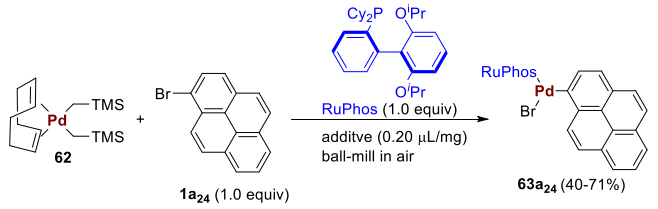

Entry	LAG	Milling frequency (Hz)	Time (min)	NMR yield[b] (%)
1	none	30	30	40
2	none	30	60	43
3	THF	30	30	71
4	Toluene	30	30	61
5	CH_3CN	30	30	71
6	Dioxane	30	30	64
7	DMF	30	30	64
8	Et_2O	30	30	66
9	DMSO	30	30	55
10	Pentane	30	30	58
11	Cyclohexane	30	30	47
12	MeOH	30	30	48
13	THF	25	30	78[e]
14[c]	THF	25	30	55
15[d]	THF	25	30	67
16	THF	25	10	71

[a]Conditions: **1** (0.05 mmol), **2a** (0.05 mmol), RuPhos (0.05 mmol), and the LAG additive (0.2 μL mg^{-1}) in a stainless-steel ball-milling jar (1.5 mL) with a stainless-steel ball (3 mm). [b]Determined by ^{1}H NMR analysis of the crude reaction mixture using an internal standard. [c]Two stainless-steel balls (3 mm) were used. [d]Three stainless-steel balls (3 mm) were used. [e]Isolated yield. Adapted with permission from ref 133. Copyright 2019 The Royal Society of Chemistry.

Scheme 58. A Comparative Study of the Performance of Solution-Based and Mechanochemical Reactions. Adapted with Permission from Ref 133. Copyright 2019 The Royal Society of Chemistry

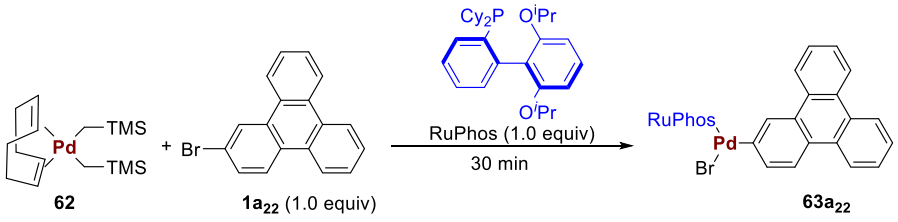

In solution (under N_2)	In solution (in air)	Mechanochemistry (in air)
Cyclohexane: 61%	Cyclohexane: 8%	LAG with THF (0.20 μL/mg): **92%**
THF: 87%	THF: 46%	

https://dx.doi.org/10.1021/acscatal.0c00142
ACS Catal. 2020, 10, 8344−8394

Scheme 59. Comparison of a Grignard Reaction (under Air Condition) between Solution and Ball Milling. Adapted with Permission from Ref 137. Copyright 2012 Elsevier

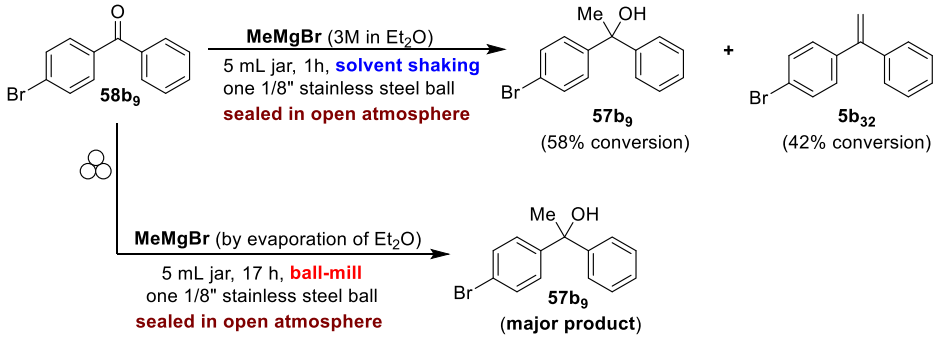

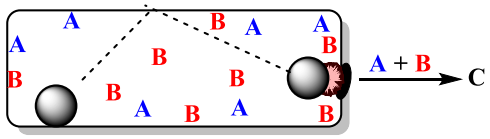

Figure 6. A collision between ball bearing and reagents A and B leads to formation of product C. Adapted with permission from ref 137. Copyright 2012 Elsevier.

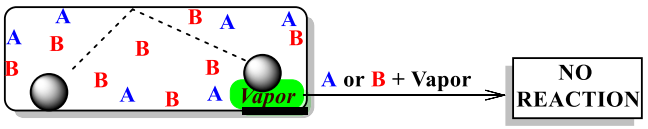

Figure 7. A collision between the ball bearing, reactant A and vaporous O_2 or H_2O leads to no reaction. Adapted with permission from ref 137. Copyright 2012 Elsevier.

magnesium with an organic fluoride, typically in an ethereal solvent. In solution, the direct reaction of many organofluorides with elemental magnesium yield no product, and any other strategy is welcomed. In this regard, Hanusa et al. have successfully developed a mechanochemical procedure to activate the C−F bond and prepare fluoro-Grignard reagents milling together elemental magnesium (8 equiv) with fluoronapthalenes (Scheme 60).[140] Despite these preliminary encouraging results, much work remains to be done in this area.

Scheme 60. Direct Mechanochemical Preparation of a Fluoro Grignard Reagent. Adapted with Permission from Ref 140. Copyright 2020 MDPI

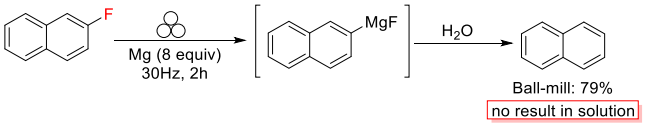

In recent years, visible light-photoredox catalysis as a means to accelerate bond-forming reactions has become a topic of considerable interest in contemporary organic chemistry.[141] In these processes, the photoexcited catalyst can behave like a very efficient single-electron oxidant providing an electron to an acceptor, effectively triggering the reaction (Scheme 61). The following single-electron oxidation of a donor leads to the formation of the final product, together with the concomitant regeneration of the ground-state catalyst (Scheme 61).

Scheme 61. A Commonly Accepted Photoredox Oxidative Quenching Cycle. Adapted with Permission from Ref 142. Copyright 2019 American Association for the Advancement of Science

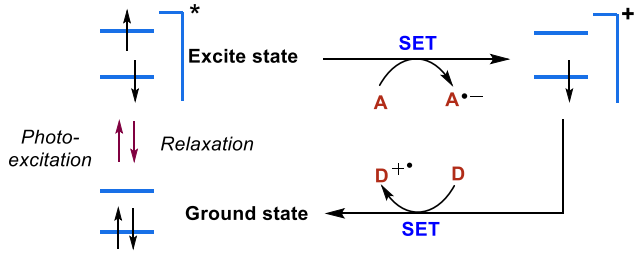

In an extraordinary paper, Hito et al. have recently highlighted how the mechanical action of balls on a piezoelectric material could generate temporarily highly polarized particles (Scheme 62).[142] The mechanically activated

Scheme 62. Proposed Mechanoredox Paradigm Using a Ball Mill and a Piezoelectric Material. Adapted with Permission from Ref 142. Copyright 2019 American Association for the Advancement of Science

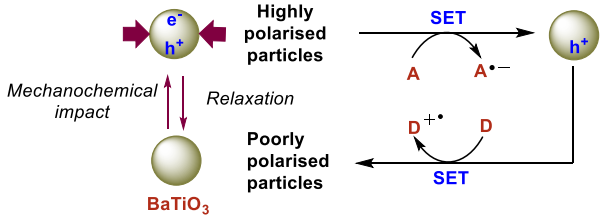

piezoelectric material transfers electrons to target organic molecule promoting the selective formation of new bonds by mimicking photoredox catalysts (Scheme 62). The model reaction has been fine-tuned using the commercially available, inexpensive, and easy-to-handle $BaTiO_3$ nanoparticles as the piezoelectric component.

To support this mechanistic hypothesis, the author investigated the mechanoredox C−H arylation of aryl diazonium salts **55b$_8$** and furan **64** in the presence of $BaTiO_3$ (1.5 mL stainless steel milling jar with 5 mm diameter stainless steel ball, Table 12). The mechanochemical agitation (20 Hz for 1 h under air) of all components provided the corresponding arylated product **65b$_8$** in 40% yield (Table12, entry 1). In contrast, when the same reaction was irradiated with ultrasound in anhydrous dimethyl sulfoxide and under

https://dx.doi.org/10.1021/acscatal.0c00142
ACS Catal. 2020, 10, 8344−8394

Table 12. Optimization for Mechanoredox Arylation. Adapted with Permission from Ref 142. Copyright 2019 American Association for the Advancement of Science

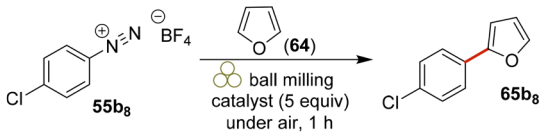

	Entry	catalyst	milling frequency	65b$_8$ (NMR yield %)
	1	$BaTiO_3$	20	40
	2	none	20	<1
IN SOLUTION	3	$BaTiO_3$	-	<1 (In DMSO, with ultrasound, under N_2)
	4	$SrTiO_3$	20	3
	5	TiO_2	20	<1
	6	$BaCO_3$	20	<1
	7	Al_2O_3	20	<1
Ball Mill	8	$BaTiO_3$	30	81
	9	$LiNbO_3$	30	24
	10	ZnO	30	15

nitrogen, the product **65b$_8$** was detected only in trace amount (<1%, Table 12, entry 3). The mechanochemical activation of the model reaction with ceramic materials (TiO_2, $BaCO_3$, Al_2O_3) did not proceed at all, while other piezolelectric items, such as $LiNbO_3$ and ZnO, provided **65b$_8$** in lower yields (24% and 15%, respectively, Table 12). Instead, an increase in the grinding frequency (from 20 to 30 Hz) doubled the yield (81%) of the reaction (Table 12, entry 8).

The scope of the optimized procedure was successfully extended to a wider range of substrates to validate the methodology. Successively, the authors probed the mecanoredox borylation of **55b$_8$** using the same setup to broaden the series, and the desired arylboronate (**66b$_8$**) was recovered in 21% yield (Scheme 63). The addition of a stoichiometric amount of CH_3CN (0.12 μL) as a LAG liquid additive, as well as the prolonging of the milling time to 3 h, led to higher yield (61%).

The outcomes were thoroughly compared with the analogous photoredox reactions reported in the literature,[143] and the mechanochemical procedure provides better results both in terms of overall reaction time and product yield (Scheme 63). In this framework, coronene **67** was arylated in 43% yield under the optimized mechanoredox conditions (**67b$_{12}$**, Scheme 64), while the arylation of coronene **67** in DMSO (König's photoredox procedure)[144] using eosin Y failed to deliver the desired product (**67b$_{18}$**, Scheme 64). The low solubility of coronene **67** in the polar solvents commonly used for photoredox reactions, could rationalize the lack of reactivity. Scanning electron microscopy (SEM) and thermo-

Scheme 63. Scope of Mechanoredox Borylation. Adapted with Permission from Ref 142. Copyright 2019 American Association for the Advancement of Science

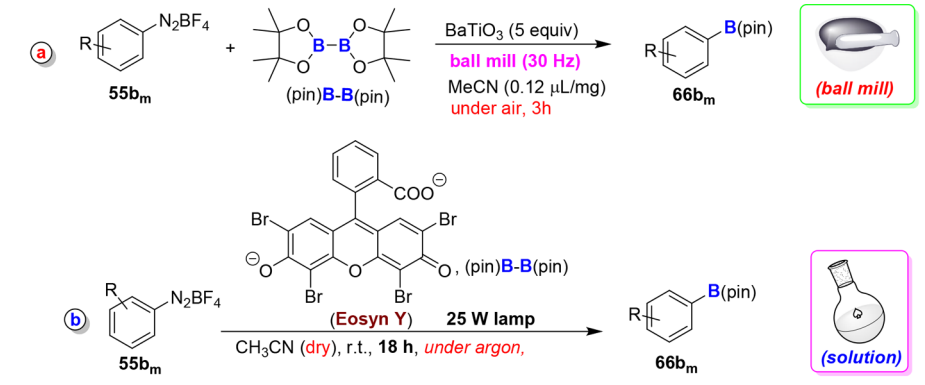

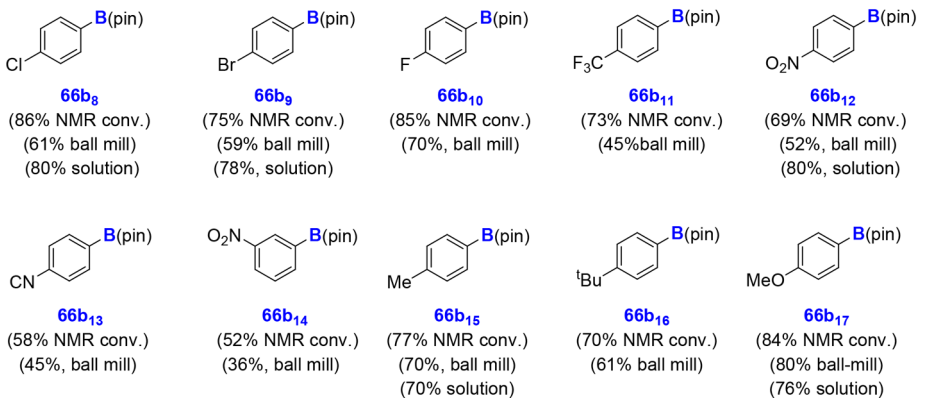

https://dx.doi.org/10.1021/acscatal.0c00142
ACS Catal. 2020, 10, 8344−8394

Scheme 64. C−H Arylation of PAHs Using a Mechanoredox Approach (Top) and under Photoredox Conditions (Bottom, Ref 144). Adapted with Permission from Ref 142. Copyright 2019 American Association for the Advancement of Science

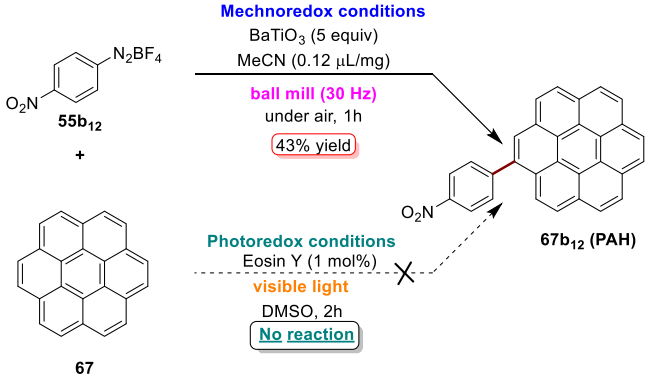

graphic analyses proven that the reaction inside the jar takes place exclusively via a mechanochemical activation.

Finally, the authors successfully validated the robustness of this procedure by "hammering" the raw reaction 200 times.[145] The *sui generis* mechanoredox borylation of **55b$_{16}$** afforded the product **66b$_{16}$** in 43% yield (Scheme 65), as assessed by nuclear magnetic resonance (NMR) integration.

Indisputably, Ito's paper emphasizes the potentialities of mechanochemistry that is a new frontier of research still to be explored. Mechanochemistry is not a panacea for overcoming all challenges. Nevertheless, similarly to other conventional organic procedures, it is a powerful tool in the hands of chemists to reduce the environmental impact of chemical processes.

9. CONCLUSIONS

In the past few years, metal-assisted mechanochemical reactions have become a topic of extreme interest, prompting IUPAC to include mechanochemistry among the top 5 innovations that will change the world.[146] The reactions carried out inside a ball mill provided a new strategy to prepare powerful catalysts and opened the door for synthesizing a more extensive range of complex molecular targets. At this point, a simple transfer of know-how from the homogeneous phase to the jar of a ball mill is no longer the key. Over the next few years, the interest of the scientific community has to focus on to understand better what happens to reagents and catalysts during the milling.[147] Many kinetic and thermodynamic aspects of mechanochemically activated reactions are still poorly understood, as well as everything that happens in the jar during a single mechanochemical impact. Currently, limited information is available in the literature on the chemical structure and surface of catalysts loaded into the volume of the reaction throughout the reactive process. We hope that for any future study on metal-assisted mechanochemical reactions, this Review might significantly inspire and influence the modern metal-assisted catalysis.

AUTHOR INFORMATION

Corresponding Author

Andrea Porcheddu − *Dipartimento di Scienze Chimiche e Geologiche, Università degli Studi di Cagliari, 09042 Cagliari, Italy; Consorzio C.I.N.M.P.I.S., 70125 Bari, Italy;* orcid.org/0000-0001-7367-1102; Email: porcheddu@unica.it

Authors

Evelina Colacino − *ICGM, Univ Montpellier, CNRS, ENSCM, 34296 Montpellier, France;* orcid.org/0000-0002-1179-4913

Lidia De Luca − *Dipartimento di Chimica e Farmacia, Università degli Studi di Sassari, 07100 Sassari, Italy;* orcid.org/0000-0001-7211-9076

Francesco Delogu − *Dipartimento di Ingegneria Meccanica, Chimica, e dei Materiali, Università degli Studi di Cagliari, 09123 Cagliari, Italy*

Complete contact information is available at: https://pubs.acs.org/10.1021/acscatal.0c00142

Author Contributions

The manuscript was written through contributions of all authors. A.P. wrote the first draft of the manuscript. All authors have given approval to the final version of the manuscript.

Funding

Authors are grateful to MIUR (Italy, PRIN project: MultI-Functional poLymer cOmposites based on groWn matERials, n° 2017B7MMJ5_001). A.P. is grateful to MIUR for "Finanziamento delle Attività Base di Ricerca (FABR 2017)".

Notes

The authors declare no competing financial interest.

ACKNOWLEDGMENTS

Authors acknowledge the CeSAR (Centro Servizi d'Ateneo per la Ricerca) of the University of Cagliari, Italy for the NMR experiments at 600 MHz.

REFERENCES

(1) Tarrant, N. Between Aquinas and Eymerich: The Roman Inquisition's Use of Dominican Thought in the Censorship of Alchemy. *Ambix* **2018**, *65*, 210−231.

(2) Ross, J. *Contemporary Catalysis, Fundamentals and Current Applications*, 1st ed.; Elsevier, 2018; pp 1−364.

(3) (a) Anastas, P. T.; Warner, J. *Green Chemistry: Theory and Practice*; Oxford University Press Inc, 2000 (b) Principles of Green Chemisty. https://www.acs.org/content/acs/en/greenchemistry/

Scheme 65. Mechanoredox borylation of 55b$_{16}$ with BaTiO$_3$ in air using a hammer. Adapted with permission from ref 142. Copyright 2019 American Association For The Advanced of Science

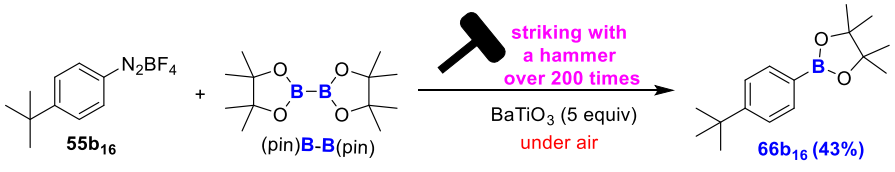

https://dx.doi.org/10.1021/acscatal.0c00142
ACS Catal. 2020, 10, 8344−8394

principles/12-principles-of-green-chemistry.html (accessed March 21, 2020).
(4) Hutchings, G.; Davidson, M.; Catlow, R.; Hardacre, C.; Turner, N.; Collier, P. *Modern Development in Catalysis*; World Scientific Publishing Europe Ltd, 2016. DOI: 10.1142/q0035.
(5) Byrne, F. P.; Jin, S.; Paggiola, G.; Petchey, T. H. M.; Clark, J. H.; Farmer, T. J.; Hunt, A. J.; McElroy, C. R.; Sherwood, J. Tools and techniques for solvent selection: green solvent selection guides. *Sustainable Chem. Processes* **2016**, *4*, 7.
(6) de Marco, B. A.; Rechelo, B. S.; Tótoli, E. G.; Kogawa, A. C.; Salgado, H. R. N. Evolution of green chemistry and its multidimensional impacts: A review. *Saudi Pharm. J.* **2019**, *27*, 1−8.
(7) Alder, C. M.; Hayler, J. D.; Henderson, R. K.; Redman, A. M.; Shukla, L.; Shuster, L. E.; Sneddon, H. F. Updating and further expanding GSK's solvent sustainability guide. *Green Chem.* **2016**, *18*, 3879−3890.
(8) Solvents and sustainability. https://www.chemistryworld.com/features/solvents-and-sustainability/3008751.article#/ (accessed March 21, 2020).
(9) Sheldon, R. The: E factor 25 years on: The rise of green chemistry and sustainability. *Green Chem.* **2017**, *19*, 18−43.
(10) (a) Achar, T. K.; Bose, A.; Mal, P. Mechanochemical synthesis of small organic molecules. *Beilstein J. Org. Chem.* **2017**, *13*, 1907−1931. (b) Do, J. L.; Friščić, T. Mechanochemistry: A Force of Synthesis. *ACS Cent. Sci.* **2017**, *3*, 13−19. (c) Howard, J. L.; Cao, Q.; Browne, D. L. Mechanochemistry as an emerging tool for molecular synthesis: What can it offer? *Chem. Sci.* **2018**, *9*, 3080−3094. (d) Tan, D.; García, F. Main group mechanochemistry: from curiosity to established protocols. *Chem. Soc. Rev.* **2019**, *48*, 2274−2292. (e) Andersen, J.; Brunemann, J.; Mack, J. Exploring stable, sub-ambient temperatures in mechanochemistry: Via a diverse set of enantioselective reactions. *React. Chem. Eng.* **2019**, *4*, 1229−1236.
(11) (a) Butyagin, P. Y. Kinetics and Nature of Mechanochemical Reactions. *Russ. Chem. Rev.* **1971**, *40*, 901−915. (b) Heinicke, G. *Tribochemistry*; Akademie-Verlag: Berlin, 1986. (c) Gutman, E. M. *Mechanochemistry of Materials*; Cambridge International Science Publishing: Cambridge, 1998. (d) Balaz, P.; Achimovicova, M.; Balaz, M.; Billik, P.; Cherkezova-Zheleva, Z.; Criado, M. J.; Delogu, F.; Dutkova, E.; Gaffet, E.; Gotor, F. J.; Kumar, R.; Mitov, I.; Rojac, T.; Senna, M.; Streletskii, A.; Wieczorek-Ciurowa, K. Hallmarks of mechanochemistry: from nanoparticles to technology. *Chem. Soc. Rev.* **2013**, *42*, 7571−7637.
(12) (a) Tan, D.; Friščić, T. Mechanochemistry for Organic Chemists: An Update. *Eur. J. Org. Chem.* **2018**, *2018*, 18−33. (b) Chemists Get Back To The Grind With Mechanochemistryhttps://cen.acs.org/articles/91/i2/Chemists-Back-Grind-Mechanochemistry.html..
(13) (a) Suryanarayana, C. C. Mechanical alloying and milling. *Prog. Mater. Sci.* **2001**, *46*, 1−184. (b) Balaz, P. *Mechanochemistry in Nanoscience and Minerals Engineering*; Springer-Verlag: Berlin, Heidelberg, 2008.
(14) (a) For more technical details about the Fritsch devices, see the following website: a) https://www.fritsch-international.com/ (accessed March 22, 2020).
(15) For more technical details about the Retsch devices, see the following website: https://www.retsch.com/ (accessed March 22, 2020).
(16) (a) https://unionprocess.com/ (accessed March 21, 2020) (b) http://group.zoz.de/ (accessed March 21, 2020).
(17) For more technical details about the InSolido devices, see the following website: https://www.insolidotech.com/ (accessed March 21, 2020).
(18) For more technical details about the Form-Tech devices, see the following website a) https://formtechscientific.com/ (accessed March 21, 2020).
(19) For more technical details about the Nissin Giken devices, see the following website: http://www.nissin-giken.co.jp/ (accessed March 21, 2020).
(20) For more technical details about the Spex devices, see the following website https://www.spexsampleprep.com/ (accessed March 21, 2020).
(21) Michalchuk, A. A. L.; Tumanov, I. A.; Boldyreva, E. V. Ball size or ball mass − what matters in organic mechanochemical synthesis? *CrystEngComm* **2019**, *21*, 2174−2179.
(22) For more technical details about the Pebble devices, see the following website: https://fedequip.com/inventory/ball-mill-pebble-jar-mills (accessed March 22, 2020).
(23) (a) Nash, D. J.; Restrepo, D. T.; Parra, N. S.; Giesler, K. E.; Penabade, R. A.; Aminpour, M.; Le, D.; Li, Z.; Farha, O. K.; Harper, J. K.; Rahman, T. S.; Blair, R. G. Heterogeneous Metal-Free Hydrogenation over Defect-Laden Hexagonal Boron Nitride. *ACS Omega* **2016**, *1*, 1343−1354. (b) Witt, P. J.; Sinnott, M. D.; Cleary, P. W.; Schwarz, M. P. A hierarchical simulation methodology for rotary kilns including granular flow and heat transfer. *Miner. Eng.* **2018**, *119*, 244−262.
(24) Baláž, P.; Baláž, M.; Achimovičová, M.; Bujňáková, Z.; Dutková, E. Chalcogenide mechanochemistry in materials science: insight into synthesis and applications. *J. Mater. Sci.* **2017**, *52*, 11851−11890.
(25) (a) Crawford, D. E.; Miskimmin, C. K. G.; Albadarin, A. B.; Walker, G.; James, S. L. Organic synthesis by Twin Screw Extrusion (TSE): continuous, scalable and solvent-free. *Green Chem.* **2017**, *19*, 1507−1518. (b) Morrison, H.; Fung, P.; Tran, T.; Horstman, E.; Carra, E.; Touba, S. Use of Twin Screw Extruders as a Process Chemistry Tool: Application of Mechanochemistry to Support Early Development Programs. *Org. Process Res. Dev.* **2018**, *22*, 1432−1440. (c) Cao, Q.; Crawford, D. E.; Shi, C.; James, S. L. Greener Dye Synthesis: Continuous, Solvent-Free Synthesis of Commodity Perylene Diimides by Twin-Screw Extrusion. *Angew. Chem., Int. Ed.* **2020**, *59*, 4478−4483.
(26) Friščić, T.; Mottillo, C.; Titi, H. M. Mechanochemistry for Synthesis. *Angew. Chem.* **2020**, *132*, 1030−1041.
(27) Crum, R. S.; Homel, M. A.; Pagan, D. C.; Herbold, E. B.; Miller, D.; Lind, J.; Jensen, B. J.; Iverson, A. J.; Akin, M. C. In situ X-ray imaging of heterogeneity in dynamic compaction of granular media. *J. Appl. Phys.* **2019**, *125*, No. 025902.
(28) Awalt, J. K.; Scammells, P. J.; Singer, R. D. Liquid Assisted Grinding for the N-Demethylation of Alkaloids. *ACS Sustainable Chem. Eng.* **2018**, *6*, 10052−10057.
(29) Belenguer, A. M.; Lampronti, G. I.; Sanders, J. K. M. Reliable Mechanochemistry: Protocols for Reproducible Outcomes of Neat and Liquid Assisted Ball-mill Grinding Experiments. *J. Visualized Exp.* **2018**, *131*, 56824.
(30) Sentence quoted from: Tanaka, K.; Toda, F. Solvent-Free Organic Synthesis. *Chem. Rev.* **2000**, *100*, 1025−1074.
(31) (a) James, S. L.; Friščić, T. Mechanochemistry: a web themed issue. *Chem. Commun.* **2013**, *49*, 5349−5350. (b) Leonardi, M.; Villacampa, M.; Menéndez, J. C. Multicomponent mechanochemical synthesis. *Chem. Sci.* **2018**, *9*, 2042−2064. (c) Cindro, N.; Tireli, M.; Karadeniz, B.; Mrla, T.; Užarević, K. Investigations of Thermally Controlled Mechanochemical Milling Reactions. *ACS Sustainable Chem. Eng.* **2019**, *7*, 16301−16309.
(32) Shu, C.; Zhang, J.; Ge, J.; Sim, J. H.; Burke, B. G.; Williams, K. A.; Rylander, N. M.; Campbell, T.; Puretzky, A.; Rouleau, C.; Geohegan, D. B.; More, K.; Esker, A. R.; Gibson, H. W.; Dorn, H. C. A Facile High-Speed Vibration Milling Method to Water-Disperse Singlewalled Carbon Nanohorns. *Chem. Mater.* **2010**, *22* (2), 347−351.
(33) Li, H.; Walker, G. C. Twist and Shout: Single-Molecule Mechanochemistry. *ACS Nano* **2017**, *11* (1), 28−30.
(34) Caruso, M. M.; Davis, D. A.; Shen, Q.; Odom, S. A.; Sottos, N. R.; White, S. R.; Moore, J. S. Mechanically-Induced Chemical Changes in Polymeric Materials. *Chem. Rev.* **2009**, *109*, 5755−5798.
(35) Avvakumov, E. G.; Senna, M.; Kosova, N. V. *Soft Mechanochemical Synthesis: A Basis for New Chemical Technologies*; Kluwer Academic Publishers: New York, 2002.

(36) (a) Jones, W.; Eddleston, M. D. Introductory Lecture: Mechanochemistry, a versatile synthesis strategy for new materials. *Faraday Discuss.* **2014**, *170*, 9−34. (b) James, S. L.; Adams, C. J.; Bolm, C.; Braga, D.; Collier, P.; Friscic, T.; Grepioni, F.; Harris, K. D. M.; Hyett, G.; Jones, W.; Krebs, A.; Mack, J.; Maini, L.; Orpen, A. G.; Parkin, I. P.; Shearouse, W. C.; Steed, J. W.; Waddell, D. C. Mechanochemistry: opportunities for new and cleaner synthesis. *Chem. Soc. Rev.* **2012**, *41*, 413−447. (c) Fischer, F.; Lubjuhn, D.; Greiser, S.; Rademann, K.; Emmerling, F. Supply and Demand in the Ball Mill: Competitive Cocrystal Reactions. *Cryst. Growth Des.* **2016**, *16*, 5843−5851.

(37) Arnaut, L.; Burrows, H. *Chemical Kinetics: From Molecular Structure to Chemical Reactivity*, 1st ed.; Elsevier Science: New York, 2006.

(38) Schmalzried, H. *Chemical Kinetics of Solids*; VCH Verlagsgesellschaft mbH: Berlin, 1995.

(39) Torre, F.; Barra, P.; Pia, G.; Delogu, F.; Porcheddu, A. Microscopic Kinetic Information from Ag Oxalate Mechanochemistry in Ball Drop Experiments. *Mater. Lett.* **2020**, *267*, 127525.

(40) (a) Rigney, D. A.; Hammerberg, J. E. In *The 1999 Julia R. Weertman Symposium on Advanced Materials for the 21st Century*; Chung, Y. W., Dunand, D. C., Liaw, P. K., Olson, G. B., Eds.; TMS (OH): Cincinnati, 1999; pp 465−474. (b) Kim, H.-J.; Kim, W. K.; Falk, M. J.; Rigney, D. A. MD Simulations of Microstructure Evolution during High-Velocity Sliding between Crystalline Materials. *Tribol. Lett.* **2007**, *28*, 299−306. (c) Kim, H.-J.; Karthikeyan, S.; Rigney, D. A. A simulation study of the mixing, atomic flow and velocity profiles of crystalline materials during sliding. *Wear* **2009**, *267*, 1130−1136. (d) Karthikeyan, S.; Agrawal, A.; Rigney, D. A. Molecular Dynamics Simulations of Sliding in an Fe-Cu Tribopair System. *Wear* **2009**, *267*, 1166−1176. (e) Emge, A.; Karthikeyan, S.; Rigney, D. A. The effects of sliding velocity and sliding time on nanocrystalline tribolayer development and properties in copper. *Wear* **2009**, *267*, 562−567. (f) Rigney, D.; Karthikeyan, S. The *evolution* of *tribomaterial during sliding*: a *brief introduction*. *Tribol. Lett.* **2010**, *39*, 3−7.

(41) (a) Lund, A. C.; Schuh, C. A. Atomistic simulation of strain-induced amorphization. *Appl. Phys. Lett.* **2003**, *82*, 2017−2019. (b) Lund, A. C.; Schuh, C. A. Topological and chemical arrangement of binary alloys during severe deformation. *J. Appl. Phys.* **2004**, *95*, 4815−4822. (c) Delogu, F.; Cocco, G. Molecular dynamics investigation on the role of sliding interfaces and friction in the formation of amorphous phases. *Phys. Rev. B: Condens. Matter Mater. Phys.* **2005**, *71*, 144108. (d) Delogu, F.; Cocco, G. Numerical simulations of structural modifications at a Ni−Zr sliding interface. *Phys. Rev. B: Condens. Matter Mater. Phys.* **2005**, *72*, No. 014124. (e) Odunuga, S.; Krasnochtchekov, Y.; Li, P.; Bellon, P.; Averback, R. S. Forced Chemical Mixing in Alloys Driven by Plastic Deformation. *Phys. Rev. Lett.* **2005**, *95*, No. 045901. (f) Delogu, F. Forced chemical mixing in model immiscible systems under plastic deformation. *J. Appl. Phys.* **2008**, *104*, No. 073533. (g) Vo, N. Q.; Odunuga, S.; Bellon, P.; Averback, R. S. Forced chemical mixing in immiscible alloys during severe plastic deformation at elevated temperatures. *Acta Mater.* **2009**, *57*, 3012−3019. (h) Ashkenazy, Y.; Vo, N. Q.; Schwen, D.; Averback, R. S.; Bellon, P. Shear induced chemical mixing in heterogeneous systems. *Acta Mater.* **2012**, *60*, 984−993. (i) Delogu, F.; Cocco, G. Numerical simulations of atomic-scale disordering processes at impact between two rough crystalline surfaces. *Phys. Rev. B: Condens. Matter Mater. Phys.* **2006**, *74*, No. 035406. (j) Delogu, F. Molecular dynamics of atomic rearrangements at perturbed surfaces. *Phys. Rev. B: Condens. Matter Mater. Phys.* **2009**, *80*, No. 014115. (k) Delogu, F. Molecular dynamics of collisions between rough surfaces. *Phys. Rev. B: Condens. Matter Mater. Phys.* **2010**, *82*, 205415. (l) Delogu, F. Ignition of an exothermal reaction by collision between Al and Ni crystals. *J. Appl. Phys.* **2011**, *110*, 103505. (m) Delogu, F. A possible alloying mechanism in idealized collisions between Cu and Sn crystals. *Chem. Phys. Lett.* **2012**, *521*, 125−129. (n) Arshad, S. N.; Lach, T. G.; Ivanisenko, J.; Setman, D.; Bellon, P.; Dillon, S. J.; Averback, R. S. Self-organization of Cu-Ag during controlled severe plastic deformation at high temperatures. *J. Mater. Res.* **2015**, *30*, 1943−1956. (o) Ashkenazy, Y.; Pant, N.; Zhou, J.; Bellon, P.; Averback, R. S. Phase evolution of highly immiscible alloys under shear deformation: Kinetic pathways, steady states, and the lever-rule. *Acta Mater.* **2017**, *139*, 205−214. (p) Verma, N.; Pant, N.; Beach, J. A.; Ivanisenko, J.; Ashkenazy, Y.; Dillon, S. J.; Bellon, P.; Averback, R. S. Effects of ternary alloy additions on the microstructure of highly immiscible Cu alloys subjected to severe plastic deformation: An evaluation of the effective temperature model. *Acta Mater.* **2019**, *170*, 218−230.

(42) Rigney, D. A.; Hirth, J. P. Plastic deformation and sliding friction of metals. *Wear* **1979**, *53*, 345−370.

(43) Persson, B. *Sliding Friction, Physical Principles and Applications*; Springer-Verlag Berlin Heidelberg: Berlin, 2000.

(44) Honeycombe, R. W. K. *The plastic deformation of metals*, 2nd ed.; Edward Arnold: Ann Arbor, 1984.

(45) Brennhaugen, D. D. E.; Georgarakis, K.; Yokoyama, Y.; Nakayama, K. S.; Arnberg, L.; Aune, R. E. Probing heat generation during tensile plastic deformation of a bulk metallic glass at cryogenic temperature. *Sci. Rep.* **2018**, *8*, 16317.

(46) (a) Delogu, F.; Takacs, L. Mechanochemistry of Ti−C powder mixtures. *Acta Mater.* **2014**, *80*, 435−444. (b) Delogu, F.; Takacs, L. Information on the mechanism of mechanochemical reaction from detailed studies of the reaction kinetics. *J. Mater. Sci.* **2018**, *53*, 13331−13342.

(47) (a) Kubota, K.; Takahashi, R.; Ito, H. Mechanochemistry allows carrying out sensitive organometallic reactions in air: Glovebox-and-Schlenk-line-free synthesis of oxidative addition complexes from aryl halides and palladium(0). *Chem. Sci.* **2019**, *10*, 5837−5842. (b) Shaw, T. E.; Shultz, L. R.; Garayeva, L. R.; Blair, R. G.; Noll, B. C.; Jurca, T. Mechanochemical routes for the synthesis of acetyl- A nd bis-(imino)pyridine ligands and organometallics. *Dalton Trans.* **2018**, *47*, 16876−16884.

(48) (a) Gujral, S. S.; Khatri, S.; Riyal, P.; Gahlot, V. Suzuki Cross Coupling Reaction- A Review. *Indo Glob. J. Pharm. Sci.* **2018**, *2*, 351−367. (b) Hooshmand, S. E.; Heidari, B.; Sedghi, R.; Varma, R. S. Recent advances in the Suzuki-Miyaura cross-coupling reaction using efficient catalysts in eco-friendly media. *Green Chem.* **2019**, *21*, 381−405. (c) Guo, L.; Srimontree, W.; Zhu, C.; Maity, B.; Liu, X.; Cavallo, L.; Rueping, M. Nickel-catalyzed Suzuki-Miyaura cross-couplings of aldehydes. *Nat. Commun.* **2019**, *10*, 1957.

(49) Koshvandi, A. T. K.; Heravi, M. M.; Momeni, T. Current Applications of Suzuki−Miyaura Coupling Reaction in The Total Synthesis of Natural Products: An update. *Appl. Organomet. Chem.* **2018**, *32*, e4210.

(50) (a) Nielsen, S. F.; Peters, D.; Axelsson, O. The Suzuki reaction under solvent-free conditions. *Synth. Commun.* **2000**, *30*, 3501−3509. (b) Gribanov, P. S.; Chesnokov, G. A.; Dzhevakov, P. B.; Kirilenko, N. Y.; Rzhevskiy, S. A.; Ageshina, A. A.; Topchiy, M. A.; Bermeshev, M. V.; Asachenko, A. F.; Nechaev, M. S. Solvent-free Suzuki and Stille cross-coupling reactions of 4- and 5-halo-1,2,3-triazoles. *Mendeleev Commun.* **2019**, *29*, 147−149.

(51) Jiang, Z. J.; Li, Z. H.; Yu, J. B.; Su, W. K. Liquid-Assisted Grinding Accelerating: Suzuki-Miyaura Reaction of Aryl Chlorides under High-Speed Ball-Milling Conditions. *J. Org. Chem.* **2016**, *81*, 10049−10055.

(52) (A) Grätz, S.; Wolfrum, B.; Borchardt, L. Mechanochemical Suzuki polycondensation-from linear to hyperbranched polyphenylenes. *Green Chem.* **2017**, *19*, 2973−2979. (b) Vogt, C. G.; Grätz, S.; Lukin, S.; Halasz, I.; Etter, M.; Evans, J. D.; Borchardt, L. Direct Mechanocatalysis: Palladium as Milling Media and Catalyst in the Mechanochemical Suzuki Polymerization. *Angew. Chem., Int. Ed.* **2019**, *58* (52), 18942−18947.

(53) Seo, T.; Ishiyama, T.; Kubota, K.; Ito, H. Solid-state Suzuki-Miyaura cross-coupling reactions: Olefin-accelerated C-C coupling using mechanochemistry. *Chem. Sci.* **2019**, *10*, 8202−8210.

(54) Pentsak, E. O.; Ananikov, V. P. Pseudo-Solid-State Suzuki−Miyaura Reaction and the Role of Water Formed by Dehydration of Arylboronic Acids. *Eur. J. Org. Chem.* **2019**, *2019*, 4239−4247.

https://dx.doi.org/10.1021/acscatal.0c00142
ACS Catal. 2020, 10, 8344−8394

(55) Cao, Q.; Howard, J. L.; Wheatley, E.; Browne, D. L. Mechanochemical Activation of Zinc and Application to Negishi Cross-Coupling. *Angew. Chem., Int. Ed.* **2018**, *57*, 11339−11343.
(56) Haas, D.; Hammann, J. M.; Greiner, R.; Knochel, P. Recent Developments in Negishi Cross-Coupling Reactions. *ACS Catal.* **2016**, *6*, 1540−1552.
(57) (a) Polynski, M. V.; Pidko, E. A. Intermetallic species in the Negishi coupling and their involvement in inhibition pathways. *Catal. Sci. Technol.* **2019**, *9* (17), 4561−4572. Rocard, L.; Hudhomme, P. Recent developments in the Suzuki−Miyaura reaction using nitroarenes as electrophilic coupling reagents. *Catalysts* **2019**, *9*, 213.
(58) (a) Heck, K. F.; Nolley, J. P. Palladium-Catalyzed Vinylic Hydrogen Substitution Reactions with Aryl, Benzyl, and Styryl Halides. *J. Org. Chem.* **1972**, *37*, 2320−2322. (b) Beletskaya, I. P.; Cheprakov, A. V. Heck reaction as a sharpening stone of palladium catalysis. *Chem. Rev.* **2000**, *100*, 3009−3066. (c) Jadhav, S. N.; Rode, C. V. An efficient palladium catalyzed Mizoroki-Heck cross-coupling in water. *Green Chem.* **2017**, *19*, 5958−5970. (d) Biffis, A.; Centomo, P.; Del Zotto, A.; Zecca, M. Pd Metal Catalysts for Cross-Couplings and Related Reactions in the 21st Century: A Critical Review. *Chem. Rev.* **2018**, *118*, 2249−2295. (e) Shi, S.; Nawaz, K. S.; Zaman, M. K.; Sun, Z. Advances in enantioselective C-H activation/Mizoroki-Heck reaction and Suzuki reaction. *Catalysts* **2018**, *8*, 90. Oxtoby, L. J.; Gurak, J. A.; Wisniewski, S. R.; Eastgate, M. D.; Engle, K. M. Palladium-Catalyzed Reductive Heck Coupling of Alkenes. *Trends Chem.* **2019**, *1*, 572−587.
(59) (a) Kurandina, D.; Chuentragool, P.; Gevorgyan, V. Transition-Metal-Catalyzed Alkyl Heck-Type Reactions. *Synthesis* **2019**, *51*, 985−1005. (b) https://www.organic-chemistry.org/namedreactions/heck-reaction.shtm (accessed March 21, 2020).
(60) Tullberg, E.; Schacher, F.; Peters, D.; Frejd, T. Solvent-free Heck-Jeffery reactions under ball-milling conditions applied to the synthesis of unnatural amino acids precursors and indoles. *Synthesis* **2006**, 1183−1189.
(61) Margetić, D.; Štrukil, V. Chapter 2 - Carbon−Carbon Bond-Forming Reactions. *Mechanochemical Organic Synthesis*, 1st ed.; Elsevier, 2016; pp 55−139. DOI: 10.1016/B978-0-12-802184-2.00002-9.
(62) (a) Cyr, P.; Deng, S. T.; Hawkins, J. M.; Price, K. E. Flow heck reactions using extremely low loadings of phosphine-free palladium acetate. *Org. Lett.* **2013**, *15*, 4342−4345. (b) Humphrey, G. R.; Dalby, S. M.; Andreani, T.; Xiang, B.; Luzung, M. R.; Song, Z. J.; Shevlin, M.; Christensen, M.; Belyk, K. M.; Tschaen, D. M. Asymmetric synthesis of letermovir using a novel phase-Transfer-catalyzed aza-michael reaction. *Org. Process Res. Dev.* **2016**, *20*, 1097−1103. (c) Jedinák, L.; Zátopková, R.; Zemánková, H.; Šustková, A.; Cankař, P. The Suzuki-Miyaura Cross-Coupling Reaction of Halogenated Aminopyrazoles: Method Development, Scope, and Mechanism of Dehalogenation Side Reaction. *J. Org. Chem.* **2017**, *82*, 157−169.
(63) Yu, J.; Hong, Z.; Yang, X.; Jiang, Y.; Jiang, Z.; Su, W. Bromide-assisted chemoselective Heck reaction of 3-bromoindazoles under high-speed ball-milling conditions: Synthesis of axitinib. *Beilstein J. Org. Chem.* **2018**, *14*, 786−795.
(64) (a) Grela, K. Progress in metathesis chemistry II. *Beilstein J. Org. Chem.* **2015**, *11*, 1639−1640. (b) Sabatino, V.; Ward, T. R. Aqueous olefin metathesis: Recent developments and applications. *Beilstein J. Org. Chem.* **2019**, *15*, 445−468. (c) Müller, D. S.; Baslé, O.; Mauduit, M. A tutorial review of stereoretentive olefin metathesis based on ruthenium dithiolate catalysts. *Beilstein J. Org. Chem.* **2018**, *14*, 2999−3010.
(65) Balcar, H.; Čejka, J. SBA-15 as a support for effective olefin metathesis catalysts. *Catalysts* **2019**, *9*, 743.
(66) (a) Hoveyda, A. H.; Khan, R. K. M.; Torker, S.; Malcolmson, S. J. in *Handbook of Metathesis*, Vol. 2; Grubbs, R. H., Ed.; Wiley-VCH: Weinheim, 2015. (b) http://allthingsmetathesis.com/solvent-considerations-in-ruthenium-catalyzed-metathesis-reactions/ (accessed March 22, 2020).
(67) Groso, E. J.; Schindler, C. S. Recent Advances in the Application of Ring-Closing Metathesis for the Synthesis of Unsaturated Nitrogen Heterocycles. *Synthesis* **2019**, *51*, 1100−1114.
(68) Song, K.; Kim, K.; Hong, D.; Kim, J.; Heo, C. E.; Kim, H. I.; Hong, S. H. Highly active ruthenium metathesis catalysts enabling ring-opening metathesis polymerization of cyclopentadiene at low temperatures. *Nat. Commun.* **2019**, *10*, 1−9.
(69) (a) Pollini, J.; Pankau, W. M.; Gooßen, L. J. Isomerizing Olefin Metathesis. *Chem. - Eur. J.* **2019**, *25*, 7416−7425. (b) Timmer, B. J. J.; Ramström, O. Acid-Assisted Direct Olefin Metathesis of Unprotected Carbohydrates in Water. *Chem. - Eur. J.* **2019**, *25*, 14408−14413. (c) Mukherjee, N.; Marczyk, A.; Szczepaniak, G.; Sytniczuk, A.; Kajetanowicz, A.; Grela, K. A Gentler Touch: Synthesis of Modern Ruthenium Olefin Metathesis Catalysts Sustained by Mechanical Force. *ChemCatChem* **2019**, *11*, 5362−5369. (d) Quintin, F.; Pinaud, J.; Lamaty, F.; Bantreil, X. Mechanosynthesis of Noels-Type NHC-Ruthenium Complexes and Applications in Ring-Opening Metathesis Polymerization. *Organometallics* **2020**, *39*, 636.
(70) Do, J. L.; Mottillo, C.; Tan, D.; Štrukil, V.; Friščić, T. Mechanochemical ruthenium-catalyzed olefin metathesis. *J. Am. Chem. Soc.* **2015**, *137*, 2476−2479.
(71) Li, J. J. (Ed.). (2006). *Friedel-Crafts reaction BT - Name Reactions: A Collection of Detailed Reaction Mechanisms*. DOI: 10.1007/3-540-30031-7_107;. Gore, P. H. The Friedel-Crafts Acylation Reaction and its Application to Polycyclic Aromatic Hydrocarbons. *Chem. Rev.* **1955**, *55*, 229−281.
(72) (a) Olah, G. A.; Reddy, V. P.; Prakash, G. K. S. Friedel-Crafts Reactions. *Kirk-Othmer Encyclopedia of Chemical Technology*; Wiley: New York, 2000. DOI: 10.1002/0471238961.0618090515120108.a01 ;. (b) Sartori, G.; Maggi, R. *Advances in Friedel-Crafts Acylation Reactions: Catalytic and Green Processes*; CRC Press: Boca Raton, FL, 2009. DOI: 10.1201/9781420067934.
(73) Dud, M.; Briš, A.; Jušinski, I.; Gracin, D.; Margetić, D. Mechanochemical Friedel-Crafts acylations. *Beilstein J. Org. Chem.* **2019**, *15*, 1313−1320.
(74) Troschke, E.; Grätz, S.; Lübken, T.; Borchardt, L. Mechanochemical Friedel−Crafts Alkylation—A Sustainable Pathway Towards Porous Organic Polymers. *Angew. Chem., Int. Ed.* **2017**, *56*, 6859−6863.
(75) (a) Li, S. M. Prenylated indole derivatives from fungi: Structure diversity, biological activities, biosynthesis and chemoenzymatic synthesis. *Nat. Prod. Rep.* **2010**, *27*, 57−78. (b) Kochanowska-Karamyan, A. J.; Hamann, M. T. Marine indole alkaloids: Potential new drug leads for the control of depression and anxiety. *Chem. Rev.* **2010**, *110*, 4489−4497. (c) Ishikura, M.; Abe, T.; Choshi, T.; Hibino, S. Simple indole alkaloids and those with a no rearranged monoterpenoid unit. *Nat. Prod. Rep.* **2015**, *32*, 1389−1471.
(76) (a) Zheng, K.; Liu, X.; Feng, X. Recent Advances in Metal-Catalyzed Asymmetric 1,4-Conjugate Addition (ACA) of Non-organometallic Nucleophiles. *Chem. Rev.* **2018**, *118*, 7586−7656. (b) Bandini, M.; Umani-Ronchi, A. *Catalytic Asymmetric Friedel-Crafts Alkylations*; Wiley-VCH, Mörlenbach, 2009. DOI: 10.1002/9783527626977. (c) Bandini, M.; Eichholzer, A. Catalytic functionalization of Indoles in a new dimension. *Angew. Chem., Int. Ed.* **2009**, *48*, 9608−9644.
(77) (a) Liu, Y.; Shang, D.; Zhou, X.; Liu, X.; Feng, X. Enantioselective Friedel-Crafts alkylation of indoles with alkylidene malonates catalyzed by *N,N′*-dioxide-scandium(III) complexes: Asymmetric synthesis of *β*-carbolines. *Chem. - Eur. J.* **2009**, *15*, 2055−2058. (b) Chen, H.; Du, F.; Liu, L.; Li, J.; Zhao, Q.; Fu, B. Malonate-type bis(oxazoline) ligands with sp^2 hybridized bridge carbon: Synthesis and application in Friedel-Crafts alkylation and allylic alkylation. *Tetrahedron* **2011**, *67*, 9602−9608. (c) Desyatkin, V. G.; Anokhin, M. V.; Rodionov, V. O.; Beletskaya, I. P. Polystyrene-supported cu(II)-R-Box as recyclable catalyst in asymmetric Friedel−Crafts reaction. *Russ. J. Org. Chem.* **2016**, *52*, 1717−1727.
(78) Staleva, P.; Hernández, J. G.; Bolm, C. Mechanochemical Copper-Catalyzed Asymmetric Michael-Type Friedel−Crafts Alkyla-

https://dx.doi.org/10.1021/acscatal.0c00142
ACS Catal. 2020, 10, 8344−8394

tion of Indoles with Arylidene Malonates. *Chem. - Eur. J.* **2019**, *25*, 9202−9205.
(79) Franke, R.; Selent, D.; Börner, A. Applied hydroformylation. *Chem. Rev.* **2012**, *112*, 5675−5732.
(80) Cornils, B.; Herrmann, W. A.; Rasch, M. Otto Roelen, Pioneer in Industrial Homogeneous Catalysis. *Angew. Chem., Int. Ed. Engl.* **1994**, *33*, 2144−2163.
(81) (a) Fang, X.; Jackstell, R.; Franke, R.; Beller, M. Domino-Hydroformylation/Aldol Condensation Catalysis: Highly Selective Synthesis of α,β-Unsaturated Aldehydes from Olefins. *Chem. - Eur. J.* **2014**, *20*, 13210−13216. (b) Tan, G.; Wu, Y.; Shi, Y.; You, J. Syngas-Free Highly Regioselective Rhodium-Catalyzed Transfer Hydroformylation of Alkynes to α,β-Unsaturated Aldehydes. *Angew. Chem., Int. Ed.* **2019**, *58*, 7440−7444. (c) Peng, J. B.; Wu, F. P.; Wu, X. F. First-Row Transition-Metal-Catalyzed Carbonylative Transformations of Carbon Electrophiles. *Chem. Rev.* **2019**, *119*, 2090−2127.
(82) Cornils, B.; Börner, A.; Franke, R.; Zhang, B.; Wiebus, E.; Schmid, K. *Hydroformylation in Applied Homogeneous Catalysis with Organometallic Compounds: A Comprehensive Handbook in Four Volumes*, 3rd ed.; Cornils, B., Herrmann, W. A., Beller, M., Pacciello, R., Eds.; Wiley-VCH: Weinheim, Germany, 2017, pp 23−90.
(83) Leclercq, L.; Hapiot, F.; Tilloy, S.; Ramkisoensing, K.; Reek, J. N. H.; Van Leeuwen, P. W. N. M.; Monflier, E. Sulfonated xantphos ligand and methylated cyclodextrin: A winning combination for rhodium-catalyzed hydroformylation of higher olefins in aqueous medium. *Organometallics* **2005**, *24*, 2070−2075.
(84) Cousin, K.; Menuel, S.; Monflier, E.; Hapiot, F. Hydroformylation of Alkenes in a Planetary Ball Mill: From Additive-Controlled Reactivity to Supramolecular Control of Regioselectivity. *Angew. Chem., Int. Ed.* **2017**, *56*, 10564−10568.
(85) Bolm, C.; Mocci, R.; Schumacher, C.; Turberg, M.; Puccetti, F.; Hernández, J. G. Mechanochemical Activation of Iron Cyano Complexes: A Prebiotic Impact Scenario for the Synthesis of α-Amino Acid Derivatives. *Angew. Chem., Int. Ed.* **2018**, *57*, 2423−2426.
(86) Voronin, V. V.; Ledovskaya, M. S.; Bogachenkov, A. S.; Rodygin, K. S.; Ananikov, V. P. Acetylene in organic synthesis: recent progress and new uses. *Molecules* **2018**, *23*, 2442.
(87) https://www.sciencedirect.com/topics/chemistry/acetylene (accessed March 21, 2020).
(88) Rodygin, K. S.; Vikenteva, Y. A.; Ananikov, V. P. Calcium-Based Sustainable Chemical Technologies for Total Carbon Recycling. *ChemSusChem* **2019**, *12*, 1483−1516.
(89) Rodygin, K. S.; Werner, G.; Kucherov, F. A.; Ananikov, V. P. Calcium Carbide: A Unique Reagent for Organic Synthesis and Nanotechnology. *Chem. - Asian J.* **2016**, *11*, 965−976.
(90) Turberg, M.; Ardila-Fierro, K. J.; Bolm, C.; Hernández, J. G. Altering Copper-Catalyzed A3 Couplings by Mechanochemistry: One-Pot Synthesis of 1,4-Diamino-2-butynes from Aldehydes, Amines, and Calcium Carbide. *Angew. Chem., Int. Ed.* **2018**, *57*, 10718−10722.
(91) Ardila-Fierro, K. J.; Bolm, C.; Hernández, J. G. Mechanosynthesis of Odd-Numbered Tetraaryl[n]cumulenes. *Angew. Chem.* **2019**, *131*, 13079−13083.
(92) (a) Bariwal, J.; Van Der Eycken, E. C-N bond forming cross-coupling reactions: An overview. *Chem. Soc. Rev.* **2013**, *42*, 9283−9303. (b) Luo, J.; Wei, W. T. Recent Advances in the Construction of C−N Bonds Through Coupling Reactions between Carbon Radicals and Nitrogen Radicals. *Adv. Synth. Catal.* **2018**, *360*, 2076−2086. (c) Guo, W.; Zhao, M.; Tan, W.; Zheng, L.; Tao, K.; Fan, X. Developments towards synthesis of *N*-heterocycles from amidines: Via C-N/C-C bond formation. *Org. Chem. Front.* **2019**, *6*, 2120−2141. (d) Dayaker, G.; Tan, D.; Biggins, N.; Shelam, A.; Do, J.-L.; Katsenis, A.; Friscic, T. Catalytic room-temperature C-N coupling of amides andisocyanates using mechanochemistry. *ChemSusChem* **2020**, Accepted Article, DOI: 10.1002/cssc.201902576.
(93) Burke, A. J.; Marques, C. S.; Turner, N.; Hermann, G. J.; *Active Pharmaceutical Ingredients in Synthesis*; Wiley-VCH: Chennai (India), 2018.
(94) Wang, Q.; Su, Y.; Li, L.; Huang, H. Transition-metal catalysed C-N bond activation. *Chem. Soc. Rev.* **2016**, *45*, 1257−1272.
(95) (a) Yu, J. Q.; Shi, Z. J.; Eds. C−H Activation; *Topics in Current Chemistry*; Springer, 2010; Vol. *292*. Shin, K.; Kim, H.; Chang, S. Transition-metal-catalyzed C-N bond forming reactions using organic azides as the nitrogen source: A journey for the mild and versatile C-H amination. *Acc. Chem. Res.* **2015**, *48*, 1040−1052. (b) Wang, Q.; Su, Y.; Li, L.; Huang, H. Transition-metal catalysed C-N bond activation. *Chem. Soc. Rev.* **2016**, *45*, 1257−1272. Li, J. J. *C−H bond activation in organic synthesis*; CRC Press, 2017.
(96) (a) Ryu, J.; Kwak, J.; Shin, K.; Lee, D.; Chang, S. Ir(III)-catalyzed mild C-H amidation of arenes and alkenes: An efficient usage of acyl azides as the nitrogen source. *J. Am. Chem. Soc.* **2013**, *135*, 12861−12868. (b) Lee, D.; Kim, Y.; Chang, S. Iridium-catalyzed direct arene C-H bond amidation with sulfonyl- and aryl azides. *J. Org. Chem.* **2013**, *78*, 11102−11109.
(97) (a) Hermann, G. N.; Becker, P.; Bolm, C. Mechanochemical Iridium(III)-Catalyzed C-H Bond Amidation of Benzamides with Sulfonyl Azides under Solvent-Free Conditions in a Ball Mill. *Angew. Chem., Int. Ed.* **2016**, *55*, 3781−3784. (b) Hermann, G. N.; Bolm, C. Mechanochemical Rhodium(III)-Catalyzed C−H Bond Amidation of Arenes with Dioxazolones under Solventless Conditions in a Ball Mill. *ACS Catal.* **2017**, *7*, 4592−4596.
(98) Cheng, H.; Hernández, J. G.; Bolm, C. Mechanochemical Cobalt-Catalyzed C−H Bond Functionalizations by Ball Milling. *Adv. Synth. Catal.* **2018**, *360*, 1800−1804.
(99) (a) Zhu, R. Y.; Farmer, M. E.; Chen, Y. Q.; Yu, J. Q. A Simple and Versatile Amide Directing Group for C−H Functionalizations. *Angew. Chem., Int. Ed.* **2016**, *55*, 10578−10599. (b) Moselage, M.; Li, J.; Ackermann, L. Cobalt-Catalyzed C-H Activation. *ACS Catal.* **2016**, *6*, 498−525. (c) Della Ca, N.; Fontana, M.; Motti, E.; Catellani, M. Pd/Norbornene: A Winning Combination for Selective Aromatic Functionalization via C-H Bond Activation. *Acc. Chem. Res.* **2016**, *49*, 1389−1400. (d) Pichette Drapeau, M.; Gooßen, L. J. Carboxylic Acids as Directing Groups for C−H Bond Functionalization. *Chem. - Eur. J.* **2016**, *22*, 18654−18677. (e) Yamaguchi, J.; Muto, K.; Itami, K. Nickel-Catalyzed Aromatic C−H Functionalization. *Top. Curr. Chem.* **2016**, *374*, 55. (f) Gao, D. W.; Gu, Q.; Zheng, C.; You, S. L. Synthesis of Planar Chiral Ferrocenes via Transition-Metal-Catalyzed Direct C-H Bond Functionalization. *Acc. Chem. Res.* **2017**, *50*, 351−365.
(100) Cheng, H.; Hernández, J. G.; Bolm, C. Mechanochemical Ruthenium-Catalyzed Hydroarylations of Alkynes under Ball-Milling Conditions. *Org. Lett.* **2017**, *19*, 6284−6287.
(101) Hermann, G. N.; Unruh, M. T.; Jung, S. H.; Krings, M.; Bolm, C. Mechanochemical Rhodium(III)- and Gold(I)-Catalyzed C−H Bond Alkynylations of Indoles under Solventless Conditions in Mixer Mills. *Angew. Chem., Int. Ed.* **2018**, *57*, 10723−10727.
(102) (a) Cacchi, S.; Fabrizi, G. Synthesis and functionalization of indoles through palladium-catalyzed reactions. *Chem. Rev.* **2005**, *105*, 2873−2920. (b) Daly, S.; Hayden, K.; Malik, I.; Porch, N.; Tang, H.; Rogelj, S.; Frolova, L. V.; Lepthien, K.; Kornienko, A.; Magedov, I. V Unprecedented C-2 arylation of indole with diazonium salts: Syntheses of 2,3-disubstituted indoles and their antimicrobial activity. *Bioorg. Med. Chem. Lett.* **2011**, *21*, 4720−4723. (c) Kaushik, N. K.; Kaushik, N.; Attri, P.; Kumar, N.; Kim, C. H.; Verma, A. K.; Choi, E. Biomedical importance of indoles. *Molecules* **2013**, *18*, 6620−6662.
(103) (a) Lane, B. S.; Sames, D. Direct C-H bond arylation: Selective palladium-catalyzed C2-arylation of *N*-substituted indoles. *Org. Lett.* **2004**, *6*, 2897−2900. (b) Bressy, C.; Alberico, D.; Lautens, M. A route to annulated indoles via a palladium-catalyzed tandem alkylation/direct arylation reaction. *J. Am. Chem. Soc.* **2005**, *127*, 13148−13149. (c) Zhou, J.; Hu, P.; Zhang, M.; Huang, S.; Wang, M.; Su, W. A versatile catalyst for intermolecular direct arylation of Indoles with benzoic acids as arylating reagents. *Chem. - Eur. J.* **2010**, *16*, 5876−5881.

https://dx.doi.org/10.1021/acscatal.0c00142
ACS Catal. 2020, 10, 8344−8394

(104) Zhou, J.; Hu, P.; Zhang, M.; Huang, S.; Wang, M.; Su, W. A versatile catalyst for intermolecular direct arylation of Indoles with benzoic acids as arylating reagents. *Chem. - Eur. J.* **2010**, *16*, 5876−5881.
(105) Lebrasseur, N.; Larrosa, I. Room temperature and phosphine free palladium catalyzed direct C-2 arylation of indoles. *J. Am. Chem. Soc.* **2008**, *130*, 2926−2927.
(106) Das, D.; Bhutia, Z. T.; Chatterjee, A.; Banerjee, M. Mechanochemical Pd(II)-catalyzed direct and C-2-selective arylation of indoles. *J. Org. Chem.* **2019**, *84*, 10764−10774.
(107) Yu, J.; Zhang, C.; Yang, X.; Su, W. Decarboxylative acylation of: N -free indoles enabled by a catalytic amount of copper catalyst and liquid-assisted grinding. *Org. Biomol. Chem.* **2019**, *17*, 4446−4451.
(108) Hall, D. G. *Boronic Acids: Preparation and Applications in Organic synthesis, Medicine and Materials*, 2nd revised ed.; Wiley-VCH: Weinheim, 2011.
(109) Pang, Y.; Ishiyama, T.; Kubota, K.; Ito, H. (2019). Iridium(I)-Catalyzed C−H Borylation in Air by Using Mechanochemistry. *Chem. - Eur. J.* **2019**, *25*, 4654−4659.
(110) (a) Hartwig, J. F. Evolution of a fourth generation catalyst for the amination and thioetherification of aryl halides. *Acc. Chem. Res.* **2008**, *41*, 1534−1544. (b) Surry, D. S.; Buchwald, S. L. Biaryl phosphane ligands in palladium-catalyzed amination. *Angew. Chem., Int. Ed.* **2008**, *47*, 6338−6361. (c) Valente, C.; Pompeo, M.; Sayah, M.; Organ, M. G. Carbon-heteroatom coupling using Pd-PEPPSI complexes. *Org. Process Res. Dev.* **2014**, *18*, 180−190.
(111) (a) O'Brien, C. J.; Kantchev, E. A. B.; Valente, C.; Hadei, N.; Chass, G. A.; Lough, A.; Hopkinson, A. C.; Organ, M. G. Easily prepared air- and moisture-stable Pd-NHC (NHC = N-heterocyclic carbene) complexes: A reliable, user-friendly, highly active palladium precatalyst for the Suzuki-Miyaura reaction. *Chem. - Eur. J.* **2006**, *12* (18), 4743−4748. (b) Hoi, K. H.; Çalimsiz, S.; Froese, R. D. J.; Hopkinson, A. C.; Organ, M. G. Amination with Pd-NHC complexes: Rate and computational studies on the effects of the oxidative addition partner. *Chem. - Eur. J.* **2011**, *17*, 3086−3090. (c) Pompeo, M.; Farmer, J. L.; Froese, R. D. J.; Organ, M. G. Room-temperature amination of deactivated aniline and aryl halide partners with carbonate base using a Pd-PEPPSI-IPentCl-o-picoline catalyst. *Angew. Chem., Int. Ed.* **2014**, *53*, 3223−3226.
(112) Cao, Q.; Nicholson, W. I.; Jones, A. C.; Browne, D. L. Robust Buchwald-Hartwig amination enabled by ball-milling. *Org. Biomol. Chem.* **2019**, *17*, 1722−1726.
(113) Kubota, K.; Seo, T.; Koide, K.; Hasegawa, Y.; Ito, H. Olefin-accelerated solid-state C−N cross-coupling reactions using mechanochemistry. *Nat. Commun.* **2019**, *10*, 1−11.
(114) Zhu, X.; Li, Z.; Shu, Q.; Zhou, C.; Su, W. Mechanically Activated Solid-State Synthesis of Flavones by High-Speed Ball Milling. *Synth. Commun.* **2009**, *39*, 4199−4211.
(115) Haley, R. A.; Zellner, A. R.; Krause, J. A.; Guan, H.; Mack, J. Nickel Catalysis in a High Speed Ball Mill: A Recyclable Mechanochemical Method for Producing Substituted Cyclooctatetraene Compounds. *ACS Sustainable Chem. Eng.* **2016**, *4*, 2464−2469.
(116) Chen, L.; Leslie, D.; Coleman, M. G.; Mack, J. Recyclable heterogeneous metal foil-catalyzed cyclopropenation of alkynes and diazoacetates under solvent-free mechanochemical reaction conditions. *Chem. Sci.* **2018**, *9*, 4650−4661.
(117) Chelucci, G.; Porcheddu, A. Synthesis of Quinolines via a Metal-Catalyzed Dehydrogenative N-Heterocyclization. *Chem. Rec.* **2017**, *17*, 200−216.
(118) Tan, Y. J.; Wang, F. J.; Asirib, A. M.; Marwanib, H. M.; Zhang, Z. $FeCl_3$-Mediated One-Pot Cyclization−Aromatization of Anilines, Benzaldehydes, and Phenylacetylenes under Ball Milling: A New Alternative for the Synthesis of 2,4-Diphenylquinolines. *J. Chin. Chem. Soc.* **2018**, *65*, 65−73.
(119) Rinaldi, L.; Martina, K.; Baricco, F.; Rotolo, L.; Cravotto, G. Solvent-free copper-catalyzed azide-alkyne cycloaddition under mechanochemical activation. *Molecules* **2015**, *20*, 2837−2849.
(120) Tireli, M.; Maračić, S.; Lukin, S.; Kulcsár, M. J.; Žilić, D.; Cetina, M.; Halasz, I.; Raić-Malić, S.; Užarević, Krunoslav Solvent-free copper-catalyzed click chemistry for the synthesis of N-heterocyclic hybrids based on quinoline and 1, 2, 3-triazole. *Beilstein J. Org. Chem.* **2017**, *13*, 2352−2363.
(121) (a) Beejapur, H. A.; Zhang, Q.; Hu, K.; Zhu, L.; Wang, J.; Ye, Z. Tempo in chemical transformations: from homogeneous to heterogeneous. *ACS Catal.* **2019**, *9*, 2777−2830. (b) Denlinger, K. L.; Carr, P.; Waddell, D. C.; Mack, J. A Recyclable, Metal-Free Mechanochemical Approach for the Oxidation of Alcohols to Carboxylic Acids. *Molecules* **2020**, *25*, 364.
(122) Anelli, P. L.; Biffi, C.; Montanari, F.; Quici, S. Fast and selective oxidation of primary alcohols to aldehydes or to carboxylic acids and of secondary alcohols to ketones mediated by oxoammonium salts under two-phase conditions. *J. Org. Chem.* **1987**, *52*, 2559−2562.
(123) Hoover, J. M.; Ryland, B. L.; Stahl, S. S. Mechanism of copper(i)/tempo-catalyzed aerobic alcohol oxidation. *J. Am. Chem. Soc.* **2013**, *135*, 2357−2367.
(124) Porcheddu, A.; Colacino, E.; Cravotto, G.; Delogu, F.; De Luca, L. Mechanically induced oxidation of alcohols to aldehydes and ketones in ambient air: Revisiting TEMPO-assisted oxidations. *Beilstein J. Org. Chem.* **2017**, *13*, 2049−2055.
(125) Porcheddu, A.; Delogu, F.; De Luca, L.; Fattuoni, C.; Colacino, E. Metal-free mechanochemical oxidations in Ertalyte® jars. *Beilstein J. Org. Chem.* **2019**, *15*, 1786−1794.
(126) For full technical details about the Ertalyte®, see the following website: (a) https://www.aetnaplastics.com/products/d/PET (accessed March 21, 2020);. (b) https://www.alro.com/DIVPlastics/PlasticsProduct_Ertalyte.aspx (accessed March 21, 2020).
(127) Zhang, Z. Y.; Ji, D.; Mao, W.; Cui, Y.; Wang, Q.; Han, L.; Zhong, H.; Wei, Z.; Zhao, Y.; Nørgaard, K.; Li, T. Dry Chemistry of Ferrate(VI): A Solvent-Free Mechanochemical Way for Versatile Green Oxidation. *Angew. Chem., Int. Ed.* **2018**, *57*, 10949−10953.
(128) Sawama, Y.; Yasukawa, N.; Ban, K.; Goto, R.; Niikawa, M.; Monguchi, Y.; Itoh, M.; Sajiki, H. Stainless Steel-Mediated Hydrogen Generation from Alkanes and Diethyl Ether and Its Application for Arene Reduction. *Org. Lett.* **2018**, *20*, 2892−2896.
(129) Young, J. F.; Osborn, J. A.; Jardine, F. H.; Wilkinson, G. *Chem. Comm.* **1965**, 131−132. DOI: 10.1039/C19650000131.
(130) Osborn, J. A.; Jardine, F. H.; Young, J. F.; Wilkinson, G. *J. Chem. Soc. A* **1966**, 1711−1732.
(131) Schumacher, C.; Crawford, D. E.; Raguž, B.; Glaum, R.; James, S. L.; Bolm, C.; Hernández, J. G. Mechanochemical dehydrocoupling of dimethylamine borane and hydrogenation reactions using Wilkinson's catalyst. *Chem. Commun.* **2018**, *54*, 8355−8358.
(132) (a) https://phys.org/news/2018-05-solubility-problemmechanochemistry-solution.html (accessed March 21, 2020);. (b) Casco, M. E.; Kirchhoff, S.; Leistenschneider, D.; Rauche, M.; Brunner, E.; Borchardt, L. Mechanochemical Synthesis of N-Doped Porous Carbon at Room Temperature. *Nanoscale* **2019**, *11* (11), 4712−4718.
(133) Kubota, K.; Takahashi, R.; Ito, H. Mechanochemistry allows carrying out sensitive organometallic reactions in air: Glove-box-and-Schlenk-line-free synthesis of oxidative addition complexes from aryl halides and palladium(0). *Chem. Sci.* **2019**, *10*, 5837−5842.
(134) Bolm, C.; Hernández, J. G. Mechanochemistry of Gaseous Reactants. *Angew. Chem., Int. Ed.* **2019**, *58*, 3285−6899.
(135) Gordon, A. J.; Ford, R. F. *The Chemists Companion*; Wiley: New York, 1972.
(136) Shriver, D. F.; Drezdon, M. A. *The Manipulations of Air-Sensitive Compounds*, 2nd ed.; John Wiley & Sons: New York, 1986.
(137) Waddell, D. C.; Clark, T. D.; Mack, J. Conducting moisture sensitive reactions under mechanochemical conditions. *Tetrahedron Lett.* **2012**, *53*, 4510−4513.
(138) Experimental section about this reaction is very scarce, and the reader is referred to the original paper for more details.

(139) Harrowfield, J. M.; Hart, R. J.; Whitaker, C. R. Magnesium and Aromatics: Mechanically-Induced Grignard and McMurry Reactions. *Aust. J. Chem.* **2001**, *54*, 423−425.
(140) Speight, I. R.; Hanusa, T. P. Exploration of Mechanochemical Activation in Solid-State Fluoro-grignard Reactions. *Molecules* **2020**, *25*, 570.
(141) (a) Shu, Y.; Komatsu, M.; Zhang, Q.; Saito, F.; Sato, T. Mechanochemical Synthesis of Visible-Light Induced Photocatalyst with Nitrogen and Carbon Doping. *The Chinese Journal of Process Engineering* **2006**, *6*, 477−481. (b) Prier, C. K.; Rankic, D. A.; MacMillan, D. W. C. Visible Light Photoredox Catalysis with Transition Metal Complexes: Applications in Organic Synthesis. *Chem. Rev.* **2013**, *113*, 5322−5363. (c) Romero, N. A.; Nicewicz, D. A. Organic Photoredox Catalysis. *Chem. Rev.* **2016**, *116*, 10075−10166. (d) Skubi, K. L.; Blum, T. R.; Yoon, T. P. Dual Catalysis Strategies in Photochemical Synthesis. *Chem. Rev.* **2016**, *116*, 10035−10074. (e) Wang, C.-S.; Dixneuf, P. H.; Soulé, J.-F. Photoredox Catalysis for Building C−C Bonds from C(sp2)−H Bonds *Chem. Chem. Rev.* **2018**, *118*, 7532−7585. Stephenson, C.; Yoon, T.; MacMillan, D. W. C. *Visible Light Photocatalysis in Organic Chemistry*, 1st ed.; Wiley, 2018.
(142) Kubota, K.; Pang, Y.; Miura, A.; Ito, H. Redox Reactions of Small Organic Molecules Using Ball Milling and Piezoelectric Materials. *Science* **2019**, *366* (6472), 1500−1504.
(143) Yu, J.; Zhang, L.; Yan, G. Metal-Free, Visible Light-Induced Borylation of Aryldiazonium Salts: A Simple and Green Synthetic Route to Arylboronates. *Adv. Synth. Catal.* **2012**, *354*, 2625−2628.
(144) Hari, D. P.; Schroll, P.; König, B. Metal-Free, Visible-Light-Mediated Direct C−H Arylation of Heteroarenes with Aryl Diazonium Salts. *J. Am. Chem. Soc.* **2012**, *134*, 2958−2961.
(145) Move S1 in https://science.sciencemag.org/content/suppl/2019/12/18/366.6472.1500.DC1.
(146) https://www.chemistryworld.com/news/iupac-names-10-chemistry-innovations-that-will-change-the-world/3010335.article (accessed March 21, 2020).
(147) Eckert, R.; Felderhoff, M.; Schüth, F. Preferential Carbon Monoxide Oxidation over Copper-Based Catalysts under In Situ Ball Milling. *Angew. Chem., Int. Ed.* **2017**, *56*, 2445−2448.

https://dx.doi.org/10.1021/acscatal.0c00142
ACS Catal. 2020, 10, 8344−8394